



**HAL**  
open science

## Advanced cellulose composites; preparation and properties

Ragab Abouzeid

► **To cite this version:**

Ragab Abouzeid. Advanced cellulose composites; preparation and properties. Other. Université de Grenoble; HELWAN UNIVERSITY, 2012. English. NNT : 2012GRENI085 . tel-00947624

**HAL Id: tel-00947624**

**<https://theses.hal.science/tel-00947624>**

Submitted on 17 Feb 2014

**HAL** is a multi-disciplinary open access archive for the deposit and dissemination of scientific research documents, whether they are published or not. The documents may come from teaching and research institutions in France or abroad, or from public or private research centers.

L'archive ouverte pluridisciplinaire **HAL**, est destinée au dépôt et à la diffusion de documents scientifiques de niveau recherche, publiés ou non, émanant des établissements d'enseignement et de recherche français ou étrangers, des laboratoires publics ou privés.



UNIVERSITÉ DE  
GRENOBLE

## THÈSE

Pour obtenir le grade de

### DOCTEUR DE L'UNIVERSITÉ DE GRENOBLE

Spécialité : **Mécanique des fluides, Energétique, Procédés**  
Arrêté ministériel : le 6 janvier 2005 -7 août 2006

Et de

### DOCTEUR DE LA Faculte Des Sciences de L'Université de Helwan

Spécialité : **Chimie**

Présentée par

### « Ragab ABOUZEID »

Thèse dirigée par « **Alain DUFRESNE** » codirigée par  
« **Mohamed YOUSEF** »  
préparée au sein des **Laboratoire de Génie des Procédés  
Papetiers**  
dans l'**École Doctorale Ingénierie-Matériaux, Mécanique,  
Environnement, Energétique, Procédés, Production.**

Et du **Laboratoire des Chimie Organique**  
dans la **Faculté des Sciences de Helwan Université.**

## Composites haute performance à base de cellulose: Préparation et Propriétés.

Thèse soutenue publiquement le « **date de soutenance** »,  
devant le jury composé de :

**Monsieur, Aid, KHALIL**

Professeur, Faculté des Sciences de Helwan Université, Président.

**Monsieur, Magdi, NAOUM**

Professeur, Faculté des Sciences de Cairo Université, Rapporteur.

**Monsieur, Etienne FLEURY**

Professeur, INSA, Lyon, France. Rapporteur.

**Monsieur, Alain Dufresne**

Professeur, Institut Polytechnique de Grenoble, Membre.

**Monsieur, Mohamed Adel YOUSEF**

Professeur, Faculté des Sciences de Helwan Université, Membre.

**Mme, Nahla El-Wakil**

Professeur, Centre national de recherche, Egypte, Membre

**Monsieur, Ali Ali Sarhan**

Professeur, Faculté des Sciences de Mansora Université, Rapporteur.

*Université Joseph Fourier / Université Pierre Mendès France /  
Université Stendhal / Université de Savoie / Grenoble INP*



UNIVERSITÉ DE  
GRENOBLE



*Université Joseph Fourier / Université Pierre Mendès France /  
Université Stendhal / Université de Savoie / Grenoble INP*



## ACKNOWLEDGEMENT

First and foremost, I kneel meekly to ALLAH, thanking him for paving the way for me.

This work was carried out under joint supervision of collaboration between the International School of Paper and Print Media and Biomaterials (INP-Pagora), Grenoble, France and Helwan University, Faculty of Sciences, Egypt. I take this opportunity to thank the financial support for French government “Campus France” and Centre Français de Culture et de Coopération in Egypt.

I deeply thank my supervisor, Prof. Dr. Alain Dufresne, Grenoble Institute of Technology, Grenoble, France for his guidance, comments and constructive advices.

The author wishes to express his thanks and appreciation to Prof. Dr. Mohamed Adel Yousef Professor of Chemistry, Faculty of Science, Helwan University and Dr. Samya El-Sherbeny, Assistant Professor of Chemistry, Faculty of Science, Helwan University, for their encouragement and guidance during the course of this study.

Special and sincere thanks are due to Prof. Dr. Yehia Fahmy, Cellulose and Paper Department, National Research Center, for his supervision, suggestions, discussions, and support.

I am also indebted to my supervisor Prof. Dr. Nahla Abd El-Aziz El-Wakil for her continuous encouragement, endless help, favors and support.

I would like to offer my deep thanks to. Dr/ Ahmed Ali El-Gendy for his support and assistance.

I deeply express my gratitude to Professor Waleed El-Zawawy, Professor Naceur Belgacem, Professor Evelyne Mauret, Professor Mohamed Hassan, Professor Mohamed Elsakawy, Professor Samir Kamel, Dr/Ramzi Khiari and Dr/ Mohammed Krouit for their kind cooperation.

Special and sincere thanks are devoted to my colleagues and technical staff from the NRC and PAGORA for their friendship assistance and help during the course of this work.

I thank to all the persons that directly or indirectly contributed to the accomplishment of this work.

Thank you all of you!

Merci beaucoup à vous tous!

شكرا جزيلا



## Contents

List of Figures .....	vi
List of Tables.....	xii
List of abbreviations.....	xiv
Aim of Work.....	xvi
Abstract.....	xviii

### **Chapter 1. Introduction**

1.1. Cellulose.....	1
1.1.1. Hydrogen bonding.....	1
1.1.2. Polymorphism of cellulose.....	3
1.2. Natural sources of cellulose.....	5
1.2.1. Wood.....	5
1.2.1.1. Softwood.....	6
1.2.1.2. Hardwood.....	6
1.2. 2. Non-wood fibers.....	7
1.2.2.1 Sugarcane bagasse.....	11
1.3. Papermaking.....	13
1.3.1. Factors affecting paper properties.....	14
1.4. Chemical modification of cellulose.....	25
1.5. Liquid crystal.....	33

## Chapter 2. Experimental

2.1.	Materials and methods.....	45
2.1.1.	Analysis of pulp.....	46
2.1.1.1.	$\alpha$ -Cellulose content.....	46
2.1.1.2.	Pentosan content.....	46
2.1.1.3.	Lignin content.....	47
2.1.1.4.	Ash Content.....	49
2.1.1.5.	Morphological analysis by Morfi.....	49
2.1.1.6.	Water Retention Values (WRV) of pulp.....	50
2.1.2.	Preparation of soy protein Isolate (SPI).....	51
2.1.2.1.	Preparation of SPI binders.....	51
2.1.3.	Preparation and characterization of the paper sheets.....	52
2.1.3.1.	Preparation of handsheets.....	52
2.1.3.2.	Scanning Electron Microscopy.....	53
2.1.3.3.	Thickness and Grammage of handsheets.....	53
2.1.3.4.	Breaking length.....	53
2.1.3.5.	Tear Strength.....	54
2.1.3.6.	Burst Strength.....	54
2.1.3.7.	Brightness.....	55
2.1.3.8.	Opacity.....	55
2.1.3.9.	Determination of retention of fillers.....	56

2.1.4. Synthesis of alkoxybenzoyloxypropyl cellulose (ABPC-n) from HPC of DS 3 and 4-alkoxybenzoic acid derivatives.....	56
2.1.5. Preparation of dissolving bagasse pulp.....	56
2.1.5.1. Synthesis of alkoxybenzoyloxypropyl cellulose (ABPC-m) from partially substituted HPCB and 4-alkoxybenzoic acids derivatives.....	57
2.1.5.2. Synthesis of alkoxybenzoyloxypropyl cellulose (ABPC-m) from partially substituted HPCB and 4-alkoxybenzoic acids.....	58
2.1.6. Characterizations of HPC and its derivatives.....	59
2.1.6.1. FT-IR spectroscopic analysis.....	59
2.1.6.2. <sup>1</sup> H NMR Spectra.....	59
2.1.6.3. Differential Scanning Calorimetry.....	61
2.1.6.4. Polarized light Microscope.....	62
2.1.6.5. Refractive indices.....	63

### **Chapter 3. Results and Discussions**

3.1. Modification of soy protein.....	66
3.1.1. Influence of soy protein isolate denatured by urea and NaOH.....	67

3.1.2.	Influence of soy protein isolate denatured by urea, NaOH and acrylamide.....	70
3.1.3.	Effect of pH of SPI on the strength of paper sheets.....	76
3.2.	Influence of addition of kaolin to paper sheets loaded with SPI.....	79
3.3.	Liquid crystalline behavior of hydroxypropyl cellulose with esterified with 4-alkoxybenzoic acids.....	82
3.3.1.	Investigation of ABPC-n structure.....	82
3.3.1.1.	FT-IR spectroscopic analysis.....	82
3.3.1.2.	$^1\text{H}$ NMR spectra and determination of degree of substitution.....	86
3.3.2.	Phase behavior of ABPC-n.....	91
3.3.3.	Thermotropic liquid crystalline behavior.....	95
3.3.4.	Lyotropic liquid crystalline properties of ABPC-n.....	101
3.4.	Hydroxypropylation of dissolving bagasse pulp.....	106
3.4.1.	FT-IR spectroscopic analysis.....	107
3.4.2.	$^1\text{H}$ NMR analysis.....	108
3.4.3.	Thermal characterization of $\text{HPC}_B$ .....	109
3.4.4.	The lyotropic liquid crystal phase of $\text{HPC}_B$ .....	110
3.5.	Characterization of n-alkoxybenzoyloxypropyl cellulose (ABPC-m).....	112

---

3.5.1.	Thermotropic phase behavior of n- alkoxybenzoyloxypropyl ABPC-m.....	114
3.5.2.	Lyotropic liquid crystalline properties of ABPC-m.....	119
	<b>Chapter 4. Summary .....</b>	<b>124</b>
	<b>Chapter 5. French Summary.....</b>	<b>128</b>
	<b>Chapter 6. References.....</b>	<b>132</b>
	<b>Chapter 7. Arabic Summary.....</b>	<b>155</b>

**List of Figures**

<b>FIGURES</b>	<b>PAGE</b>
Figure (1) Structure of cellulose.....	1
Figure (2) Cellulose I and cellulose II.....	3
Figure (3) Schematic representation of cellulose transformation into its several polymorphs....	4
Figure (4) Consumption of non-wood pulp in paper production.....	8
Figure (5) Potential uses of bagasse.....	13
Figure (6) Chemical structure of starch: repeated glucose Units.....	20
Figure (7) The molecular structures of synthetic polymers.....	25
Figure (8) Schematic representation of the main types of cellulose chemical modification and some of the typical ensuing products...	26
Figure (9) The schematics of (a) crystal, (b) liquid crystal and (c) liquid.....	35
Figure (10) Thermotropic liquid crystalline transition....	36
Figure (11) Schematic representation of molecular arrangements in nematic phase.....	37

---

Figure (12) Schematic representations of molecular arrangements of the smectic-A and smectic-C phase.....	38
Figure (13) Schematic representation of cholesteric liquid crystalline phase.....	39
Figure (14) Chiral nematic phase; p refers to the chiral pitch.....	40
Figure (15) Lyotropic liquid crystalline transition.....	41
Figure (16) Structure of lyotropic liquid crystal. The red heads of surfactant molecules are in contact with water, whereas the tails are immersed in oil (blue): bilayer (left) and micelle (right).....	42
Figure (17) SEM images (a, c) cross section and surface morphology of paper sheet without SPI and (b, d) cross section and surface morphology of paper sheet with 2.5% SPI, respectively..	70
Figure (18) The effect of pH of SPI on the physical properties of paper sheets.....	78

Figure		
(19,A)	FTIR of a) HPC, b) ABPC-1, c) ABPC-2, d) ABPC-3, e) ABPC-4 and , f) ABPC-7...	84
Figure		
(19,B)	FTIR of a) HPC, b) ABPC-8, c) ABPC-10, d) ABPC-12 and e) ABPC 14.....	85
Figure (20)	Chemical structure of ABPC-n.....	86
Figure		
(21,A)	<sup>1</sup> H NMR spectra of HPC, ABPC-1, ABPC- 2 ABPC-3, ABPC-4 and ABPC-7.....	89
Figure		
(21,B)	<sup>1</sup> H NMR spectra of HPC, ABPC-8, ABPC- 10, ABPC-12, and ABPC-14.....	90
Figure (22)	DSC heating curves of ABPC-n.....	92
Figure (23)	DSC thermograms of ABPC-1, 2, 3 and 4 upon heating and cooling.....	94
Figure (24)	DSC thermograms and the observed PLM images for ABPC-7 on heating; a) 120 °C and b) 140 °C and on cooling c) 90.0 °C and d) 30.0 °C.....	96

---

Figure (25)	DSC thermograms and the observed PLM images for ABPC-8 on heating; a) 120 °C and on cooling b) 90.0 °C and c) 30.0 °C....	97
Figure(26)	DSC thermograms and the observed PLM images for ABPC-10 on heating; a) 120.0 °C, and on cooling b) 110.0 °C, c) 80.0 °C and d) 50 °C.....	98
Figure(27)	DSC thermograms and the observed PLM images for ABPC-12 on heating; a) 85.0 °C, and on cooling b) 85.0 °C and c) 65.0 °C.....	99
Figure (28)	DSC thermograms and the observed PLM images for ABPC-14 on heating; a) 70.0 °C, and on cooling b) 90.0 °C and c) 60.0 °C.....	100
Figure (29)	Plot of the mean refractive index vs. concentration for a) ABPC-2, b) ABPC-4, c) ABPC-8, d) ABPC-10, e) ABPC-12 and f) ABPC-14.....	102
Figure (30)	PLM images of a) ABPC-2, b) ABPC-4, c) ABPC-8, d) ABPC-12, e) ABPC-10 and f) ABPC-14 in 60 wt % DMA at room temperature.....	103

---

Figure (31) Dependence of the birefringence on the number of the methylene groups of ABPC-n.....	106
Figure (32) FTIR spectra of (A) bagasse pulp (cellulose) and (B) its Hydroxypropyl derivatives (HPC <sub>B</sub> ).....	108
Figure (33) <sup>1</sup> H NMR spectra of HPC <sub>B</sub> .....	109
Figure (34) DSC heating/cooling curves of HPC <sub>B</sub> , and PLM image (a) of HPC at 180°C.....	110
Figure (35) PLM image of HPC solution in DMSO (60 wt %) at room temperature.....	111
Figure (36) FTIR spectra of HPC, ABPC-2, ABPC-10 and ABPC-12.....	113
Figure (37) <sup>1</sup> H NMR spectra of HPC, ABPC-2, ABPC-10 and ABPC-12.....	114
Figure (38) DSC heating curves of ABPC-2, ABPC-10 and ABPC-12.....	115
Figure (39) DSC thermograms and the observed PLM images for ABPC-10 on heating; a) 125.0 °C, and on cooling b) 120.0 °C and c) 75.0 °C.....	117

---

Figure (40) DSC heating curves of ABPC- <i>m</i> DSC thermograms and the observed PLM images for ABPC-12 on heating; a) 100.0 °C, and on cooling b) 95.0 °C and c) 70 °C.....	119
Figure (41) Plot of the mean refractive index vs. concentration for a) HPC <sub>B</sub> , b) ABPC-2, c) ABPC-10 and d) ABPC-12.....	121
Figure (42) PLM images of a) ABPC-2, b) ABPC-10 and c) ABPC-12 in 60 wt % DMA at room temperature.....	123

**List of Tables**

<b>TABLES</b>	<b>PAGE</b>
Table(1) Unit cell dimensions of the four main types of cellulose polymorphs, as published by Krässig.....	4
Table(2) Typical composition for hardwoods and softwoods.....	7
Table(3) Physical and chemical properties of some non-woods used for papermaking.....	10
Table(4) Composition of Commercial Soy Proteins.....	22
Table(5) Effect of beating on fibre morphology and WRV of bagasse pulp.....	66
Table(6) Influence of soy protein isolate denatured by urea and NaOH.....	69
Table(7) Influence of soy protein isolate denatured by urea, NaOH and 1.5% Acrylamide (SPI2).....	73
Table(8) Influence of soy protein isolate denatured by urea, NaOH and 2.5% Acrylamide (SPI3).....	74

---

Table(9)	Influence of soy protein isolate denatured by urea, NaOH and 5% Acrylamide (SPI4).....	75
Table(10)	The effect of pH of SPI on the physical properties of paper sheets.....	78
Table(11)	Influence of addition of kaolin together with the soy protein isolate on the paper properties.....	80
Table(12)	Retention value of kaolin by bagasse pulp in absence of binder and with 2.5% SPI <sub>4</sub> .....	81
Table(13)	<sup>1</sup> H NMR data for ABPC-n.....	88
Table(14)	Thermal Properties ABPC-n.....	93
Table(15)	Optical Properties of ABPC-n.....	107
Table(17)	Thermal properties of ABPC-m.....	116
Table(18)	Optical Properties of ABPC-m.....	122

## **List of Abbreviations**

CNCs	Nanocrystals
MCC	Microcrystalline cellulose
SCB	Sugarcane bagasse
WRV	Water retention value
GCC	Ground calcium carbonate
PCC	Precipitated calcium carbonate
SPI	Soy protein isolate
SPC	Soy protein concentrate
SF	Soy flour
UF	Ureaformaldehyde
MF	Melamine-formaldehyde
PAE	Poly(amideamine) epichlorohydrin resins
C-PAM	Cationic poly (acrylamides)
PVAm	Polyvinylamine
DMSO	Dimethyl sulfoxide
DMF	Dimethylformamide
DMA	N,N-Dimethylacetamide
LC	Liquid crystals
HPC	Hydroxypropyl cellulose
CEC	Cyanoethylcellulose
EC	Ethylcellulose
MC	Methylcellulose
HEC	Hydroxyethylcellulose

---

HPMC	Hydroxypropylmethylcellulose
CMHEC	Carboxymethylhydroxyethylcellulose
DS	Degree of substitution
MS	Moles of substitution
°SR	Schopper riegler degree
TsCL	Para-toluenesulfonylchloride
THF	Tetrahydrofuran
DSC	Differential scanning calorimetry
T <sub>g</sub>	Glass transition temperature
T <sub>c</sub>	Clearing temperature
T <sub>m</sub>	Melting temperature
PLM	Polarized light microscope

### **Aim of work**

The general aim of the present work is to utilize local Egyptian bagasse pulp in both conventional and non-conventional applications. The conventional application is devoted to papermaking, and the second is dedicated to the preparation of advanced cellulosic derivatives having liquid crystalline properties.

Many problems in traditional paper industry, such as environmental pollution, low production efficiency and high energy consumption exist. Nowadays, energy and environment become two main bottlenecks in the development of paper industry. The excessive use of petroleum-based binders will accelerate the deterioration of environment. So, there is a need to develop eco-friendly polymeric materials using renewable resources such as soy protein isolate (SPI) in paper industry as petroleum resources are finite and are becoming limited. The process of modification of SPI comprises three types; the first is denaturation using urea/NaOH, the second is addition of Acrylamide to denatured SPI and the third is studying the effect of pH of SPI on protein adsorption. Finally addition of kaolin with denatured SPI and studying the role of SPI as a retention aid of Kaolin will be studied. For all the previously mentioned

modifications, evaluation of the mechanical and physical properties of the paper sheet loaded with SPI will be investigated.

Cellulose derivatives prepared by substituting part or all of the hydroxyl groups showed a wide variation of their characteristics from industrial point of view. The variation of the properties is expectedly dependant, to large extent, on the degree of substitution (DS). Literature survey, concerning 4-alkoxybenzoyloxypropyl cellulose, showed that no studies have been conducted regarding its preparation and characterization. A series of 4-alkoxybenzoyloxypropyl cellulose samples will be synthesized via the esterification of hydroxypropyl cellulose (HPC) of DS 3 with 4-alkoxybenzoic acid bearing 1, 2, 3, 4, 7, 8, 10, 12 and 14 carbon atoms in the side chain. On the other hand, partially substituted HPC prepared from dissolving bagasse pulp through hydroxypropylation will be performed. Further, esterification of the partially substituted HPC and 4-alkoxybenzoic acids, bearing 2, 10 and 12 carbon atoms in the side chain will be carried out. The liquid crystalline (LC) phases and transitions behaviors of the HPC and its derivatives will be investigated using polarized light microscopy (PLM) and differential scanning calorimetry (DSC), respectively.

**Abstract**

The present study deals with utilization of Egyptian bagasse in both conventional and non-conventional fields. The conventional application is devoted to papermaking, where bagasse pulp is the most appropriate pulp for this purpose due to the suitability of fiber length and high cellulose and hemicellulose contents. The non-conventional application is dedicated to the preparation of cellulosic derivatives having liquid crystalline properties.

The first approach deals with using modified soy protein isolate (SPI) as binder for cellulosic fibers in paper composites. Modification of SPI was carried out through i) denaturation with urea and NaOH. ii) addition of acrylamide to the denatured SPI. iii) changing pH of SPI. These types of modification were used to improve the adhesion properties of SPI. Pronounced mechanical and physical properties of paper sheets filled with 0.5, 2.5 or 5% denatured SPI was obtained upon using 2.5%. The optimum condition of SPI addition was used in ii and iii modifications. The additional effect of acrylamide on SPI was pronounced where the mechanical and physical properties were enhanced. Correlation between the mechanical and physical properties of paper sheets with the pH of SPI was studied. The used pHs were 3, 5, 7 and 10. The results showed that the maximum breaking length was obtained

at the isoelectric point of SPI at pH 5 (at the isoelectric point (IEP) the number of positive and negative charges on the polyion is the same, giving a net charge of zero) and it began to decrease when the pH is increased to pH 10. Both the burst index and the tear index showed parallel trends.

In the second approach, a series of 4-alkoxybenzoyloxypropyl cellulose (ABPC-*n*) samples were synthesized via the esterification of hydroxypropyl cellulose (HPC) with 4-alkoxybenzoic acid bearing alkoxy chain with different lengths. On the other hand, cellulose was isolated in pure form from Egyptian bagasse pulp. Hydroxypropylation was then conducted on the isolated cellulose. 4-alkoxybenzoyloxypropyl cellulose (ABPC-*m*) samples were synthesized via the esterification of the latter product with the same acid, bearing 2, 10 and 12 carbon atoms in the side chain and characterized.

The molecular structure of both esters (ABPC-*n* and ABPC-*m*) was confirmed by Fourier transform infrared (FT-IR) and <sup>1</sup>H NMR spectroscopy. The liquid crystalline (LC) phases and transition behaviors were investigated using polarized light microscopy (PLM), and differential scanning calorimetry (DSC), respectively. The lyotropic behavior of the derivatives was investigated in DMA solutions using PLM and

the critical concentration was firstly determined via refractive index measurements.

**Key Words:** Bagasse, cellulose, soy protein, paper composite, mechanical properties, physical properties, 4-alkyloxybenzoic acids, hydroxypropyl cellulose, thermotropic and lyotropic phase behavior.

## Chapter 1. Introduction

### 1.1. Cellulose

Cellulose is a polysaccharide common in all plant materials. It was first discovered and isolated by Anselme Payen and since then has been studied for over 150 years (Atalla 1999, French *et al.* 2004, O'Sullivan 1997, Salmon and Hudson 1997). Cellulose is also present in some fungi, bacteria, algae, and tunicates. It consists of repeating monomer units of  $\beta$ -D-anhydroglucopyranose rings linked by  $\beta$ -1, 4-linkages forming a linear chain. Each monomer unit contains three hydroxyl functions which are of interest for chemical modification. Each cellulose chain has a reducing end and non-reducing one, which gives it directionality. The reducing end ring can be opened to an aldehyde group at the C-1 position (see Figure 1) (Kontturi *et al.* 2006).

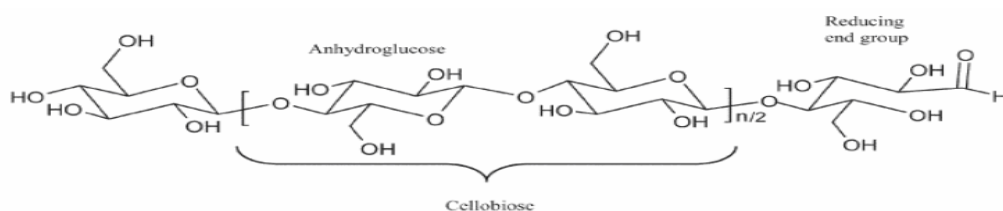


Figure (1): Cellulose structure (Kontturi *et al.* 2006).

#### 1.1.1. Hydrogen bonding

There are intramolecular hydrogen bonds within an individual chain between the ring oxygen and C-3 hydroxyl

group, and between the C-2 and C-6 hydroxyl groups. This hydrogen bonding also contributes to the chain's linearity. Individual cellulose chains are usually tightly packed together forming microfibrillar units making up a fiber by this strong intra- and intermolecular hydrogen bonds making up the crystalline or ordered domains. There can also be more loosely packed domains of microfibrils which form the amorphous or disordered regions. In the case of intermolecular hydrogen bonds between cellulose molecules in crystalline regions, it is of a very complex nature.

Depending on the native source and treatment of cellulose, the hydrogen bonding network and molecular orientation can be completely different. These differences give rise to the polymorphism of cellulose. So far, cellulose has been identified to exist in four different forms depending on native origin and treatment, cellulose I ( $\alpha$  and  $\beta$ ), II, III, and IV. Differences in crystal structure of these polymorphs are usually determined by X-ray diffraction and each gives a different diffraction pattern.

Cellulose I ( $\alpha$  and  $\beta$ ) is the native form and depending on its origin, exists in different ratios. For example, tunicates, wood, cotton and ramie fibers have primarily  $I_\beta$  form, while some algae and bacterial cellulose have primarily  $I_\alpha$  (French *et al.* 2004). The differences between these two polymorphs lie within the crystal structure and hydrogen bonding pattern, although both have cellulose chains aligned in parallel.  $I_\alpha$  has a triclinic unit cell with

one cellulose chain per unit cell, whereas  $I_\beta$  has a monoclinic unit cell with two chains per unit cell and actually it is the more stable form between the two.  $I_\alpha$  can be annealed to produce  $I_\beta$ , but it cannot be reversed.

### 1.1.2. Polymorphism of cellulose

When native cellulose I ( $\alpha$  and  $\beta$ ) is treated with alkali or dissolved in a suitable solvent and regenerated, the polymorph is converted to cellulose II (Atalla 1999, French *et al.* 2004, O'Sullivan 1997, Salmon and Hudson 1997). The structure of cellulose II differs from I in that the chains in II are in an anti-parallel arrangement where reducing and non-reducing end groups alternate in a microfibril, yielding a more stable structural arrangement. Thus, it has been found that cellulose II cannot be converted back to cellulose I. It is also important to note that the crystal densities of cellulose II and cellulose  $I_\beta$  are almost identical. Shown in Figure 2 is the major supramolecular distinction between cellulose I and cellulose II (Kontturi *et al.* 2006).

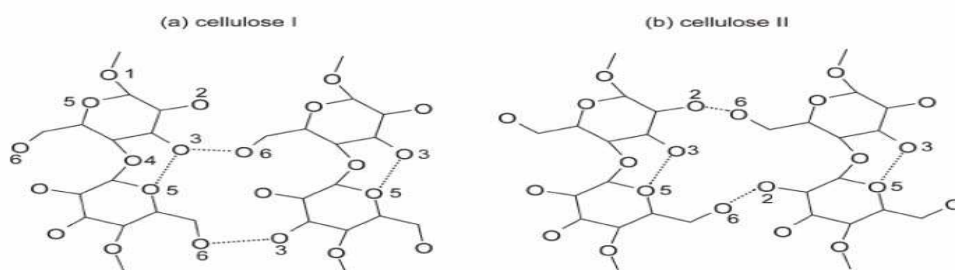
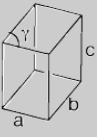


Figure (2): (a) Cellulose I and (b) cellulose II (Kontturi *et al.* 2006).

If cellulose I ( $\alpha$  and  $\beta$ ) or cellulose II is treated with amines or liquid ammonia and then removed, cellulose III (either III<sub>I</sub> or III<sub>II</sub>) is formed (Atalla 1999, French *et al.* 2004, O'Sullivan 1997, Salmon and Hudson 1997). Polymorph IV can be obtained by heating cellulose III up to 260 °C in glycerol. A summary of possible cellulose polymorph transformations is shown in Figure 3 and their unit cell dimensions are given in Table 1.

Table (1): Unit cell dimensions of the four main types of cellulose polymorphs, as published by Krässig 1993.

Unit cell	a-axis (Å)	b-axis (Å)	c-axis (Å)	$\gamma$ (°)	Polymorph
	7.85	8.17	10.34	96.4	Cellulose I
	9.08	7.92	10.34	117.3	Cellulose II
	9.9	7.74	10.3	122	Cellulose III
	7.9	8.11	10.3	90	Cellulose IV

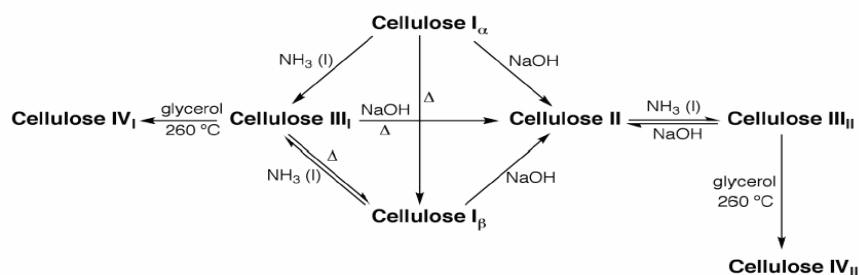


Figure (3): Schematic representation of cellulose transformation into its several polymorphs (Klemm *et al.* 2002).

In order to separate and obtain all of the highly crystalline domains of cellulose from the amorphous regions, workers have employed different types of acid hydrolysis (French *et al.* 2004, Sturcova *et al.* 2004, De Souza *et al.* 2004, Hamad 2006).

Some variables in this process are the type of acid used, time, and temperature. For example, if one employs sulfuric acid hydrolysis, a more stable aqueous suspension of crystalline cellulose will be obtained because of anionic sulfate groups present on the surface. There are a few types of products made of mainly of crystalline cellulose, namely cellulose nanocrystals (CNCs) or whiskers and microcrystalline cellulose (MCC). CNCs are usually produced by either sulfuric acid or hydrochloric acid hydrolysis which hydrolyzes cellulose chains in amorphous regions, leaving rod or whisker-like crystals that the acid has not penetrated. MCC is usually derived from pulverized wood pulp hydrolyzed with hydrochloric acid to produce a colloidal cellulose powder. Some current uses for MCC are for fillers in foods and for tableting in pharmaceuticals (French *et al.* 2004).

## **1.2. Natural sources of cellulose**

Cellulose can be derived from a variety of sources such as woods, annual plants, microbes, and animals. These include seed fiber (cotton), wood fibers (hardwoods and softwoods), bast fibers (flax, hemp, jute, ramie), grasses (bagasse, bamboo), algae (*Valonica ventricosa*), and bacteria (*Acetobacter xylinum*) (Nevell and Zeronian 1985).

### **1.2.1. Wood**

Wood is one of the world's most important resources, as raw material for industries, for construction and as fuel. Forests

cover an estimated 3,952 million hectares or 30 percent of the total land area (Rowell 2004). There is a very wide selection of species of trees, each having its own characteristics. Two basic groups of fibers are those from softwood (gymnosperms) species, such as pines, firs, and cedars, and hardwood (angiosperms) species, such as maples, oaks, poplars, and elms.

#### **1.2.1.1. Softwoods**

Softwoods consist of tracheids (90-95%) with approximate dimensions of 1.4-6.0 mm  $\times$  20-50  $\mu$ m, running in the axial direction of the stem. The tracheids' function is to support the tree and transport liquid within the tree. The other significant species of cells in softwoods are the ray parenchyma cells (5-10%) which are much smaller (0.01-0.16 mm  $\times$  2-50  $\mu$ m) and arranged radially, taking care of storage of reserve food supplies. The most important morphological characteristics of softwood fibers are fiber length (3-7mm), which contributes to their tendency to flocculate when suspended in water, fiber width or diameter (20-50  $\mu$ m), and fiber wall thickness (3-7  $\mu$ m) (Fengel and Wegener 1983).

#### **1.2.1.2. Hardwoods**

Hardwoods have a greater variety of cell types in contrast to the tracheid as the main cell in softwoods. The hardwood consists of 36-70 % fibers (fibers form the basic tissue of the support system), 20-55 % vessel elements (handle the liquid

transport), and storage functions by longitudinal and ray parenchyma cells. In addition, hardwoods, compared to softwoods, have fibers that are shorter (1-2 mm) and narrower (10-40  $\mu\text{m}$ ) and rays that are more variable in width (Scott 1996).

Wood fibers are composed of three major components, cellulose, hemicelluloses and lignin. These compositions change with different wood species, wood age, location, and wood morphology. The typical compositions of softwood and hardwood are shown in Table 2 (Fengel and Wegener 1979).

Table (2): Typical composition for hardwoods and softwoods.

Parameters	Hardwoods	Softwoods
Cellulose	45 $\pm$ 2 %	42 $\pm$ 2 %
Hemicellulose	30 $\pm$ 5 %	27 $\pm$ 2 %
Lignin	20 $\pm$ 4 %	28 $\pm$ 3 %
Extractives	5 $\pm$ 3 %	3 $\pm$ 2 %

### 1.2.2. Non-wood fibers

There is a growing interest in the use of non-wood fibers, such as annual plants and agricultural residues, as a raw material for pulp and paper and cellulose derivatives applications. According to their origin, non-wood fibers are divided into three main types: (1) agricultural by-products; (2) industrial crops; and (3) naturally growing plants (Rowell and Cook, 1998; Svenningsen *et al.*, 1999). *Agricultural by-products* are the

secondary products of the principal crops (usually cereals and grains) and are characterized by low raw material price and moderate quality, such as rice straw and wheat straw (Navaee-Ardeh *et al.* 2004; Deniz *et al.* 2004). **Industrial crops**, such as hemp, sugarcane and kenaf, can produce high quality pulps with high expense cost of raw materials. However, the source of the pulp is limited and these materials come from crops planted specifically to yield fiber (Kaldor *et al.* 1990; Zomers *et al.* 1995). **Naturally growing plants** are also used for the production of high quality pulps, such as bamboo and some grass fibers e.g. reed and sabai grass (Walsh, 1998; Poudyal, 1999; Shatalov and Pereira, 2002; Salmela *et al.* 2008).

Non-wood fibers account for less than 10% of the total pulp and paper production worldwide (Waranyou 2010). This is made up of 44% straw, 18% bagasse, 14% reeds, 13% bamboo and 11% others (Figure 4). The production of non-wood pulp mainly takes place in countries with shortage of wood, such as China, India and Egypt (Oinonen and Koskivirta, 1999).

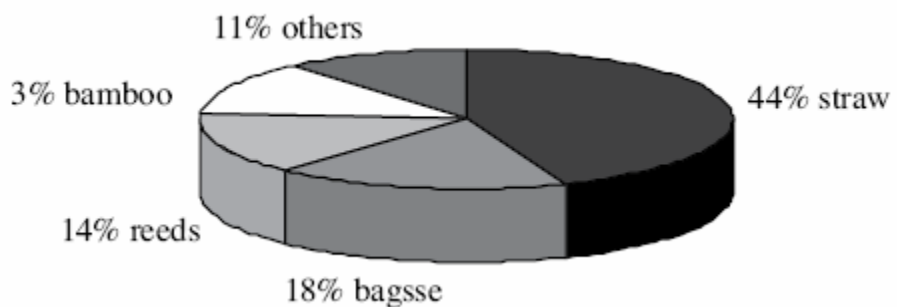


Figure (4): Consumption of non-wood pulp in paper production.

The chemical compositions of non-wood materials have tremendous variations in chemical and physical properties compared to wood fibers (Gümüüşkaya and Usta, 2002; Rezayati-Charani *et al.* 2006). They vary according to the non-wood species and the local conditions, such as soil and climate (Bicho *et al.* 1999; Jacobs *et al.* 1999). The non-wood materials generally have higher silicon, nutrient and hemicellulose contents than wood (Hurter, 1988). Some parts of the non-fibrous materials may be removed by the treatment of the raw material that has a positive influence on the ash content and consequently on the pulp and paper properties. Table 3 shows average results of the chemical and physical analyses of some non-wood fibers (Hurter, 1988; Chen *et al.* 1987; Rodríguez *et al.* 2008).

The utilization of non-wood fibers is an ethically sound way to produce pulp and paper compared to the clear-cutting of rain forests or primeval forests. The benefits of non-wood plants as a fiber resource are their fast annual growth and the smaller amount of lignin that binds their fibers together. Another advantage is that non-wood pulp can be produced at low temperatures with lower chemical charges. In addition, smaller mill sizes can be economically possible, giving a simplified process. Non-wood pulps are also more easily refined. Moreover, non-food applications can give additional income to the farmer

from food crops or cattle production (Rousu et al. 2002; Kissinger et al. 2007; Rodríguez et al. 2008).

Table (3): Physical and chemical properties of some non-woods used for papermaking.

Properties	Unit	Rice straw	Wheat straw	Bagasse	Reed grass	Bamboo	Jute	Hemp (bast)	Kenaf (bast)
Avg. fiber length	mm	1.41	1.48	1.70	1.5	1.36-4.03	2.5	20	2.74
Avg. diameter	µm	8	13	20	20	8-30	18	22	20
L/D ratio		175:1	110:1	85:1	75:1	135-175:1	139:1	1000:1	135:1
Alpha cellulose	%	28-36	29-35	32-44	45	26-43	61	55-65	31-39
Lignin	%	12-16	16-21	19-24	22	21-31	11.5	2-4	15-18
Pentosan	%	23-28	26-32	27-32	20	15-26	24	4-7	21-23
HWS	%	7.3	12.27	4.4	5.4	4.8	3.7	20.5	5.0
ABS	%	0.56	4.01	1.7	6.4	2.3	2.4	2.6	2.1
SS	%	57.7	43.58	33.9	34.8	24.9	28.5	-	28.4
Ash	%	15-20	4-9	1.5-5	3	1.7-5	1.6	5-7	2-5
Silica	%	9-14	3-7	0.7-3	2	1.5-3	<1	<1	-

HWS: hot water solubility, ABS: alcohol benzene solubility, SS: 1% sodium hydroxide solubility

Non-wood fibers are used for all kinds of paper. Writing and printing grades produced from bleached non-wood fibers are quite common. Some non-wood fibers are also used for packaging. This reflects the substantially increased use of non-wood raw materials, from 12,000 tons in 2003 to 850,000 tons in 2006 (FAO, 2009; López et al. 2010).

### **1.2.2.1. Sugarcane bagasse (SCB)**

The most important non-wood raw material in Egypt, Brazil, China etc. is sugarcane bagasse (SCB) as a secondary by-product of sugarcane extraction factories. It is used in the manufacture of pressed fibrous woods, paper pulp and as fuel. Bagasse represents 30-32 % of the sugar cane plant (Barnes, 1980). In Egypt, more than 33 million tons of crop residues are produced annually; sugarcane bagasse represents 3 million tons of these residues (Agriculture Economic and Statistics Institute, 2009). SCB has proved to be the easiest non-wood raw materials to collect transport and process. Processes with efficient systems for recovery of chemicals and heat are available to make various types of pulp and several grades of paper from bagasse. In general,  $5.4 \times 10^8$  dry tons of sugarcane is processed annually throughout the world and 1 ton of sugarcane generates 280 kg of bagasse. Structurally, the sugarcane stalk consists of two parts, an inner pith containing most of the sucrose and an outer rind with lignocellulosic fibers. During sugar processing, the sugarcane stalk is crushed to extract sucrose (Boopathy 2004). This procedure produces a large volume of residue, the bagasse, which contains both crushed rind and pith fibers. Bagasse is a fibrous residue that remains after crushing the stalks, and contains short fibers. Basically, it is a waste product that causes mills to acquire additional disposal costs. It consists of water, fibers, and small

amounts of soluble solids. Percent contribution of each of these components varies according to the variety, maturity, method of harvesting, and the efficiency of the crushing plant.

***The potential uses of bagasse:*** In sugarcane factory, bagasse is normally burnt as a fuel to produce steam and renewable electricity. Despite its 50% moisture content, bagasse has a high calorific value, 9.9 MJ/kg and has properties suitable for a range of highly value-added renewable products such as pulp and paper products, polymers, building materials and renewable fuels (Figure 5). Researchers have investigated bagasse lignin and cellulose as resources for renewable polymeric materials (Doherty, *et al.* 2007; Park, *et al.* 2008). Income from bagasse based polymers may grow substantially in the medium-term because consumer demand for plastics produced from renewable and sustainable resources is likely to increase.

Currently, there is much research on the uses of bagasse in synthesis of celluloseic derivatives. Cellulose acetate (Rodrigues Filho *et al.* 2000), methylcellulose (Viera *et al.* 2004) and carboxymethylcellulose (Morais and Campana 1999) were successfully prepared from cellulose extracted from bagasse. The relatively high cellulose content in bagasse, about 40 to 55%, makes it possible to use this residue in the production of cellulosic derivatives (Goldemberg *et al.* 2008; Aguiar, 2010).

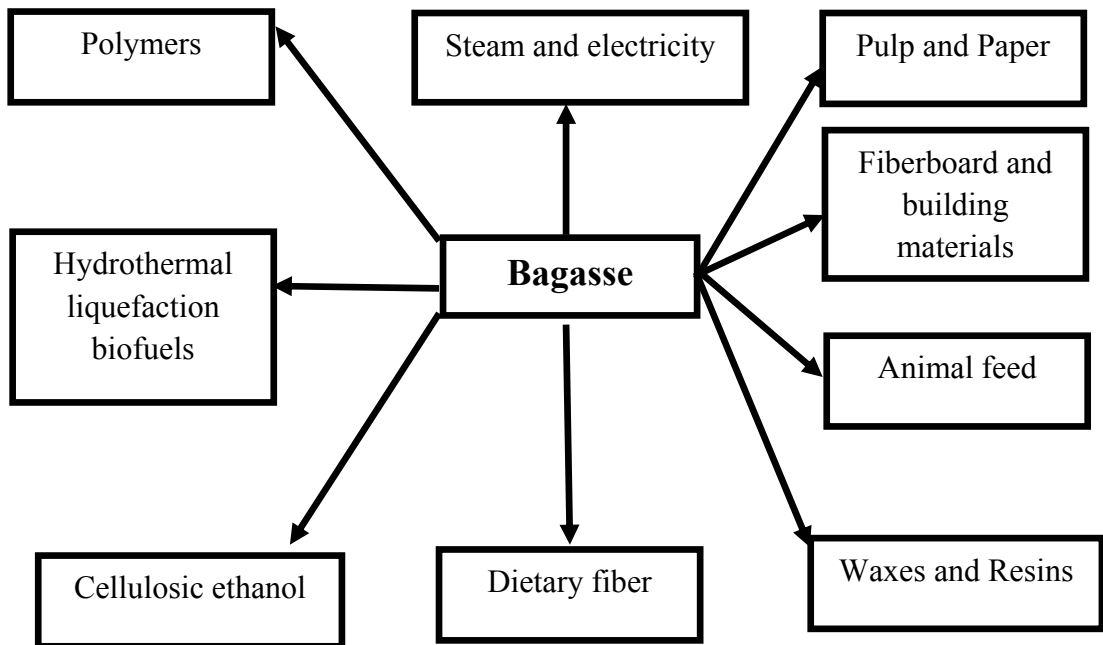


Figure (5): Potential uses of bagasse.

### 1.3. Papermaking

Paper manufacture spans a very wide range of science and technology (Roberts 1996). The formation of paper is a continuous filtration process in which cellulosic fibers are formed into a network, which is then pressed and dried. The important chemistry involved in this process is, firstly, the retention of colloidal material during the filtration and, secondly, the modifications of fiber and sheet properties so as to widen the scope for the use of paper and board products. The chemistry of paper manufacture can be considered to fall into two distinct areas, namely paper formation and finishing.

The total global consumption from papermaking was projected to increase from 316 million tons in 1999 and 351 million tons in 2005 to about 425 million tons by 2010 (Waranyou 2010). Progress in pulp and paper technology has overcome most of the related environmental problems. The environmental problems have brought forth the cleaner technology now involved in papermaking. Non-wood materials have replaced traditional wood raw materials with less polluting cooking.

### **1.3.1. Factors affecting paper properties**

#### ***- Fiber length***

The properties of paper are dependent on the structural characteristics of the fibers that compose the sheet. Fiber length is one of the most important characteristics of papermaking fibers. Long fibers are more strongly held in the network than short fibers.

#### ***- Beating and water retention value***

The term beating refers to the mechanical treatment of chemical pulp to make it suitable for papermaking. Chemical pulp practically is never converted to paper without first being subjected to beating. Beating is an important process step since this type of pulp can be said to have no papermaking properties until modified by the mechanical action of a beater.

Beating increases the bonding ability of fibers so that most paper strength properties improve. However, certain paper properties, e.g. optical parameters, decrease during beating. Tear strength typically first increases, reaching a maximum and then decrease (Seth and Page 1975). Beating has several structural effects on fibers: fines production, external fibrillation, internal fibrillation (swelling), fiber straightening (or curling) and fiber cutting (Page, 1989; Ebeling, 1980). Among the effects, the internal fibrillation of fibers plays a major role in the development of paper strength, because it improves the flexibility and collapsibility of fibers, which are essential for inter-fiber bonding and aspect which seems to be gaining more attention.

The Water Retention Value, (WRV) (g water/g pulp), primarily quantifies the inner fibrillation of the fibers and thus the swelling of the fibers. The amount of water it is able to hold gives a measure of the degree of swelling. The WRV increases with increased beating. It gives a hint of the paper webs performance in the press section. The higher the WRV the more difficult it is to press out water from the paper web.

#### ***- Effect of fines***

Fines contribute to consolidation of sheet, interfiber bonding and to wet web strength. Interfiber bonds can be strengthened by adding strength chemicals and fines (Joseph 1982). As they have large specific area and their capacity

to adsorb polymers is therefore higher than that for whole fibers (Patricia 2006). Presence of fines has a positive effect on tensile strength and light scattering. On the other hand they have a negative effect on density, where low density is better (Minna 2007).

### ***- Effect of additives***

Additives play an important role in papermaking. In fact, almost all types of paper contain one or more added non-fibrous substance. These additives modify sheet properties in order that paper meets the specific requirements for its intended use (Fardous *et al.* 1997; Lenorad and Coughlin, 1984; Maher, 1985; Halpern, 1975). In general, the use of these additives is determined by economic considerations, i.e., whether it is more economical to use expensive raw materials or even more expensive binders, which, however, need only to be used in small amounts to produce the desired strengths. An optimum level of retention can reduce the costs of the chemicals.

The most common additives are classified into three main types: sizing agents, binders and filling materials. The objective of sizing is to retard the penetration of water or ink into the pores of paper and their spreading on the paper surfaces (Casey, 1961; Mobarak, 1968; Reichel, 1990). The binders represent the second main class of additives used in papermaking. Their main function

as can be anticipated from their name is promotion of fiber bonding, i.e. to increase the number of interfiber bonding and hence paper strength. These substances are usually hydrophilic compounds such as starches, vegetable gums, synthetic hydrophilic or water-soluble materials and resin emulsions or lattices. The third main class of additives is represented by the filling or loading the web to increase the opacity and brightness of the paper, and to some extent the smoothness and finishing of the paper which are important properties especially in printing papers.

### ***-Fillers***

Fillers can generally be divided into two groups, inorganic fillers and organic ones. The dominant fillers used in papermaking are inorganic fillers. Organic fillers are two main types, hollow micro-spheres and porous fillers, and they are suitable only for special applications because of high price (Mollaahmad 2008). In addition to the traditional fillers in micrometers, the use of nanofillers in papermaking has become very hot topic (Koivunen *et al.* 2009). The most common inorganic fillers used in papermaking are ground calcium carbonate (GCC), kaolin, and precipitated calcium carbonate (PCC). Talc and TiO<sub>2</sub> are commonly used as well.

*Kaolin* is a pigment that is commonly used in papermaking. The popularity of kaolin can be explained by its low price, good availability and its relatively white color. Kaolin meets most of the filling requirements (except high refractive index) and hence is admirably suited for filling. This accounts for the large quantities consumed in the manufacture of magazine paper, book paper and other printing papers. Kaolin is found in natural deposits and can be processed in various ways to give a variety of different qualities. The cheaper grades are fractionated by air after drying and milling and these clays are commonly used as fillers. The better grades are water washed in order to obtain a better color and finer particle size (Casey 1982).

#### ***- Strength additives***

Binders or adhesives are classified according to their effect on paper sheets. It is possible to distinguish between three basic types of paper strength. The initial wet strength is the strength of the paper in the wet state before drying. It greatly influences the operational characteristics of the paper machine. The dry strength which the paper possesses in the finished state is responsible for a trouble-free running in further processing steps, e. g. in a printing press or packaging machine. Finally the wet strength describes the strength of the paper after it has been wet (Franz and Sheldon 1991).

Dry strength additives are usually water soluble, hydrophilic natural and synthetic polymers. The commercially most important are cationic starch, natural vegetable gums, and acrylamide polymers. There are also others which are used in specialized applications, these are unmodified and anionically modified starches, proteins, soluble cellulose derivatives such as carboxymethyl cellulose, dual-purpose wet end dry- strength resins and polyvinyl alcohol's, latexes and other polymers. The strength additives can be divided into two types: natural and synthetic polymers.

#### ***- Natural polymers***

***Starch*** is a biodegradable, renewable and inexpensive polymer. Additionally, it is one of the most abundant polymers in the world (Tiefenbacher 1997). Starch is found in a wide variety of naturally grown products, including rice, maize (corn), potato, tapioca and beans. Starch is made up of a repeated glucose chain, which can be found in Figure 6. The gelatinization of starch occurs when the starch granules swell and cross-link (Chen, *et al.* 1999). In the presence of excess water, a three dimensional matrix of swollen gelatinized starch granules forms, increasing the stiffness of the starch (Nagano *et al.* 2008). This thickening activity allows starch to be used as a resin.

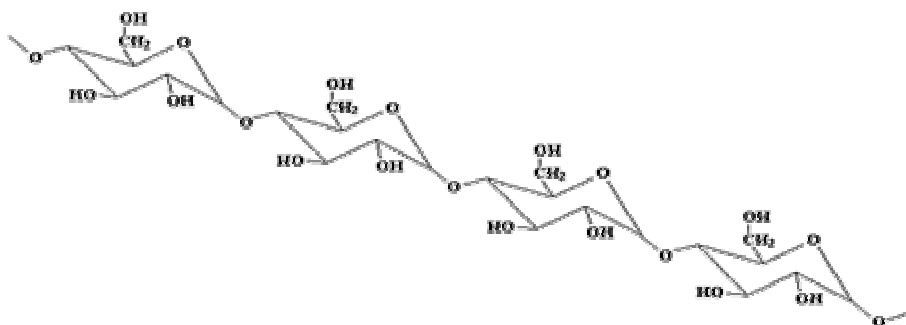


Figure (6): Chemical Structure of Starch: Repeated Glucose Units (<http://pslc.ws/macrogcss/starch.html>).

### **- Soy proteins**

The studies on soy proteins and their applications in industrial products, such as adhesives for wood and paper, binders in coatings and paints and as emulsifiers in colloidal rubber products were carried out extensively during early part of the twentieth century and are well documented (Endres 2001; Moure *et al.*, 2006; Park *et al.*, 2002). However, the availability of oil at a lower cost and biochemical inertness of petroleum-based products proved disastrous for the industrial use of soy protein. It is only after a lapse of almost 50 years that the significance of eco-friendly materials has been realized and once again, the polymer scientists are looking at biopolymers. There is a need to develop eco-friendly polymeric materials using renewable resources. Paper industry needs environment-friendly adhesives

from renewable resources because petroleum resources are finite and are becoming limited, whereas the demand for adhesives is increasing (Qiang *et al.* 2011). Soy protein is extracted from soy beans and is available worldwide. Although in the United States soy beans have mainly been used to feed animals, soy protein has good film-forming ability and has been used for sustainable films (Yamamoto, 2006).

Soy protein is commercially available in three forms: soy protein isolate (SPI), soy protein concentrate (SPC) and soy flour (SF). The compositions of these forms can be found in Table 4. SPI has the highest percentage of protein, and therefore has the best mechanical properties. For this reason, SPI was used as the soy protein binder in this work.

Soy proteins have different functional properties, which result from its amino acid composition, its structure, and its interaction with other proteins and substances present such as water, lipids and cellulose (Ghorpade *et al.* 1995). Due to the high availability and excellent mechanical properties of soy protein isolate, it has become a popular choice for resins in paper composites. Various studies have been performed using SPI as the resin of choice (Ghorpade, *et al.* 1995).

Table (4): Composition of Commercial Soy Proteins (Yamamoto, 2006).

Soy proteins	SPI	SPC	SF
Protein, %	90	68-72	46-53
Fat (acid hydrolysis), %	4-5	3-4	3-19
Ash, %	5-6	5-6	-
Dietary Fiber, %	-	19-20	16-18
Carbohydrates, %	-	-	26-30
Moisture, %	6	6-9	8-9

In a native protein, the majority of polar and non polar groups are unavailable due to the internal bonds resulting from Van der Waals forces, hydrogen bonds and hydrophobic interactions. As a result of these bonds, a simple paste of protein is a poor adhesive and a chemical change is required to break the internal bonds and uncoil or disperse the polar protein molecules. Dispersion and unfolding of protein are enhanced by hydrolysis or by increasing the pH to about 11 or higher (Lambuth 1977).

Modifications of soy protein have introduced new cross-links in the protein structure, in addition to the naturally occurring ones (Singh, 1991). Improvements in cross-linking have been shown to improve the mechanical properties in SPI because of the increased linkage between the molecules of SPI (Ghorpade, *et al.* 1995). Modification of soy protein for functionality

improvements has been carried out via physical means such as heat treatment (Renkema and van Vliet, 2004) and application of pressure (Torrezan *et al.* 2007) or via chemical means such as acidification (Tay *et al.* 2005), addition of salts (Puppo and Añón, 1999) and by the Maillard reaction inducing cross-linking (Md Yasir *et al.* 2007b). SPI might be chemically modified by reaction with acrylamide or methacrylamide group to provide sites for crosslinking. These groups are hydrophobic and help prevent swelling of container film in water.

There are three types of modification used in this work to improve the adhesion properties of SPI i) denaturation with urea and NaOH ii) addition of acrylamide to the denatured SPI iii) changing pH of SPI. Urea is one of the chemical denaturation agents that unfold the secondary helical structure of protein. Urea has oxygen and hydrogen atoms that interact effectively with the hydroxyl groups of the soy protein, a reaction that may break down the hydrogen bonding in the protein body and, consequently, unfold the protein complex. The major effect of urea on soy protein globulins is dissociation of high molecular weight protein into sub units. Alkali denaturation by NaOH, is the most commonly used process to increase the adhesive strength and water resistance of soy protein. NaOH hydrolyzes the protein molecules which cause decrease in the molecular weight of the protein, increase in the free amino and carboxylic free end groups

and consequently increases its solubility and destroys the globulin structure of the protein (Huang and Sun 2000; Mo *et al.* 2001).

### **- *Synthetic polymers***

Synthetic polymers as strength additives that are used in papermaking include polyacrylamide (PAM), polyvinylamine (PVAm), and different wet strength resins: urea-formaldehyde (UF), melamine-formaldehyde (MF), and polyamideamine epichlorohydrin (PAE) resins (Petri 2009). Cationic polyacrylamides (C-PAM) are prepared by radical copolymerization of an acrylamide monomer with a cationic charge carrying co-monomer (Figure 7). The polymers can be prepared with different molecular weights and charge densities depending on the use (strength, retention). Synthetic polyampholytes and polyelectrolyte complexes of polyacrylamides and other polyelectrolytes have also been shown as potential strength additives. Polyvinylamine is a linear amine functional polymer (Figure 7) known to improve both the wet and dry strength of paper. Wet strength resins are chemically reactive condensation products of urea-formaldehyde, melamine-formaldehyde, and polyamideamine epichlorohydrin (Figure 7), that gives wet strength to paper after drying and curing (Petri 2009).

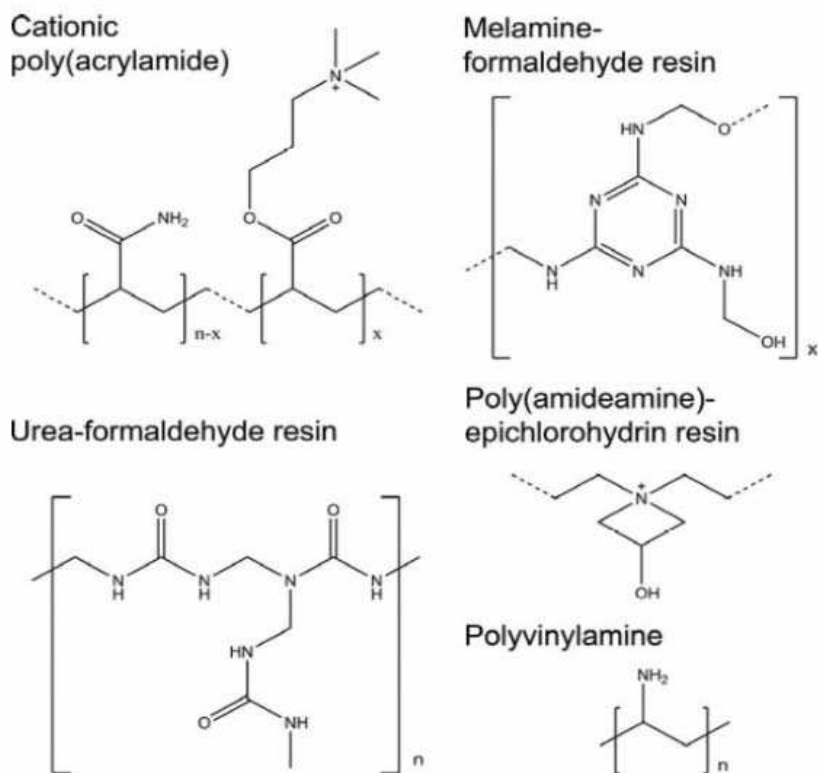


Figure (7): The molecular structures of synthetic polymers (Petri 2009).

#### 1.4. Chemical modification of cellulose

Cellulose derivatives constitute a very important and promising domain, representing value-added products derived from the chemical modification of a low-cost naturally available raw material. The chemical modification of cellulose is a common approach whose actors are its hydroxyl groups. Accordingly, it is typically carried out under the well-known classical reactions of these moieties, specifically esterification, etherification and oxidation reactions, as depicted in Figure 8.

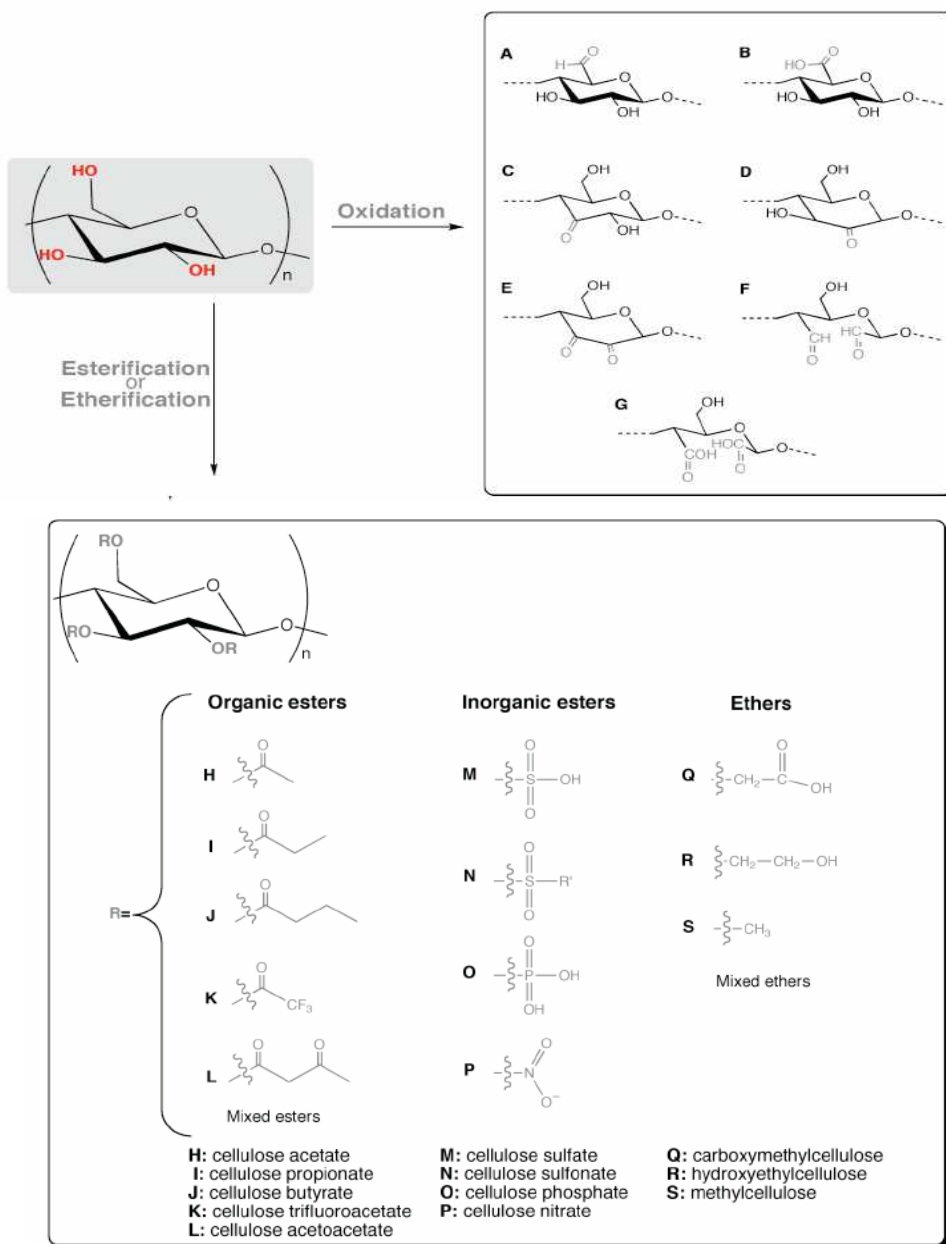


Figure (8): Schematic representation of the main types of cellulose chemical modification and some of the typical ensuing products (Klemm et al. 1998).

Esterification is usually accomplished by reacting cellulose with an appropriate acid anhydride or acid chloride (Klemm, *et al.* 2005; Klemm, *et al.* 1998). Cellulose etherification can be carried

out by three main routes, namely i) by the Williamson ether synthesis with alkyl halides in the presence of a strong base, ii) with alkylene oxides in a weakly basic medium, or iii) by Michael addition of acrylic or related unsaturated compounds, such as acrylonitrile (Klemm, *et al.* 1998).

The esterification and etherification reactions can also serve as starting point for other more elaborated strategies, such as crosslinking and grafting polymerization; the former one is usually carried out by employing bifunctional modification reagents (Klemm, *et al.* 1998) The latter can consist, on the one hand, of the grafting of short side chains onto the cellulose backbone performed, for example, during etherification with alkylene oxides via addition of more than one alkylene oxide unit or, on the other hand, of a grafting-from process, for instance, by radical polymerization of vinyl compounds after the creation of a radical site at the cellulose chain (Klemm, *et al.* 2005; Klemm, *et al.* 1998).

The oxidation of the cellulose hydroxyl groups can occur at the C-6 position first to give an aldehyde group and then the corresponding carboxylic counterpart (Figure 8 , A and B). If this reaction takes place at C-2 and/or C-3 positions, it generates ketones (Figure 8, C to E) or, in the case of bond scission between C-2 and C-3, the corresponding dialdehyde (Figure 8, F) may be oxidized in turn to the diacid moieties

(Figure 8, G) (Klemm, *et al.* 1998). The preference towards a certain type of oxidation depends substantially on the nature of the oxidant, but usually both carbonyl and carboxylic functions are produced in varying proportions (Klemm, *et al.* 1998).

The supramolecular arrangement of cellulose, in terms of crystallinity or fibrillar architecture, strongly influences its properties. In addition to the solubility, this structural aspect plays an important role in determining the rate and often also the course of a chemical reaction, especially in the case of heterogeneous systems, thus influencing the extent and distribution of substituents and the product solubility.

For instance, a high supramolecular order of the cellulose chains, synonymous of lower accessibility of the hydroxyl groups due to the large amount of interfibrillar hydrogen-bonding, generally hinders the progress of chemical reactions (Klemm, *et al.* 1998). This problem can be easily overcome however, and thus the reaction rate is enhanced, by changing the nature of the medium, i.e., from heterogeneous to homogeneous (Klemm, *et al.* 1998).

***The heterogeneous modification*** of cellulose is usually carried out in a medium where the polysaccharide is insoluble, where the reaction products could dissolve gradually into it (Klemm, *et al.* 2005). Contrary to the homogeneous modifications, with these types of conditions, the

supramolecular order and fibrillar architecture of the cellulose substrate largely determine the extent and rate of the chemical transformation. Thus, depending on the type of reaction, the medium, the degree of steric hindrance with the reagent, the sample morphology and reaction parameters, heterogeneous cellulose modifications can proceed within a wide spectrum of situations, from a surface-limited transformation to an in-depth or quasi-homogeneous bulk reaction (Klemm, *et al.* 1998).

The non-uniform character of the macromolecular ordering in native cellulose, due to the presence of the crystalline and amorphous regions, frequently leads to reactions that, depending on the conditions, can be limited to the latter regions or at least can proceed much faster in these disordered domains as compared with those of high order, as already mentioned. As a result, frequently the modification extent of cellulose in heterogeneous conditions can be significantly increased by lowering the supramolecular order and/or by loosening the interfibrillar bonding via an appropriate pretreatment. This pretreatment can either results in the complete destruction of the supramolecular order by dissolution and subsequent reprecipitation of the sample in a more amorphous form (only suitable for laboratory-scale studies), or in cellulose activation using liquids of high swelling power, such as water, aqueous alkali or dimethyl sulfoxide (DMSO),

which may also be employed as the reaction medium (Klemm, *et al.* 1998). These liquids promote a loosening of the cellulose supramolecular structure, while usually preserving the original solid state of the sample (Klemm, *et al.* 1998).

*In homogeneous reaction* conditions, cellulose is dissolved in an appropriate medium and consequently all the OH moieties are equally available for reaction, thus leading to a bulk modification (Klemm, *et al.* 1998 and Liebert, 2010).

This kind of modification implies the destruction of the microfibrillar integrity of the cellulose fibers, i.e., the hydrogen-bonding between the cellulose microfibrils, which deeply affects their supramolecular structure. As a consequence, the products obtained generally possess properties totally different from those of the perfect cellulose fibers, including physical and mechanical properties, constituting materials with thoroughly novel features. Homogeneous modifications have represented an important aspect of cellulose research for many years, because more uniform products can be obtained, compared to reactions conducted in heterogeneous conditions.

Cellulose dissolution can be attained by (i) physical interactions with the solvent or (ii) chemical reaction with the solvent leading to covalent bond formation (Heinze, and Petzold, 2008). Accordingly cellulose solvents can be subdivided

into derivatizing and non-derivatizing, and both categories include aqueous and non-aqueous media (Heinze, and Liebert, 2001; Liebert, 2010; Heinze, and Koschella, 2005). The term “derivatizing solvents” refers to all solvents and solvent systems in which the dissolution of cellulose occurs together with the formation of a labile ether, ester, or acetal derivative, called intermediate. This means that the intermediates should be easily decompose to regenerate cellulose by changing the medium (e.g. non-aqueous to aqueous) or its pH. N,N-dimethylformamide DMF/N<sub>2</sub>O<sub>4</sub> is an example of a derivatizing system, whose intermediate is cellulose nitrite (Klemm, *et al.* 1998).

On the other hand, the non-derivatizing category comprises solvents or solvent systems, such as cadoxen (common denomination for cadmium ethylenediamine) and N,N-dimethylacetamide (DMA/LiCl system), which are able to dissolve cellulose only by intermolecular interactions (Edgar *et al.* 2001). Additionally, more recently, much attention has been focused on a new class of solvents, the ionic liquids, also known as “green solvents” due to their essential features, such as negligible volatility, i.e. the absence of one of the main problems associated with the use of common organic solvents (Pinkert *et al.* 2009).

### ***- Applications of cellulose derivatives***

Cellulose derivatives, being of natural origin, have diverse physicochemical properties and are revered for their large scale use mainly as additives of fine/special chemicals in textile, pharmaceutical, cosmetic, food, and packaging industries (Balser *et al.* 1986; Barndt 1986). Cellulose and some derivatives form liquid crystals (LC) and represent excellent materials for basic studies on this subject. A variety of different structures are forming thermotropic and lyotropic LC phases, which exhibit unusual behavior (Bhadani *et al.* 1983; Tseng *et al.* 1982).

Despite the large variety of cellulose derivatives that have been made, there is a continuous expansion in the worldwide market of cellulose ethers because of their availability, economic efficiency, easy handling, low toxicity, and great variety of types. Combined effects of flow control, stabilization, water retention, film formation, etc. provided by cellulose ethers are not generally obtainable by the use of fully synthetic polymers. Cellulose ethers such as carboxymethyl cellulose (CMC), hydroxypropyl cellulose (HPC), ethylcellulose (EC), methylcellulose (MC), hydroxyethylcellulose (HEC), hydroxypropylmethylcellulose (HPMC), carboxymethylhydroxyethylcellulose (CMHEC), etc. have gained their position in the market due to their multifunctional properties.

### ***1.5. Liquid crystal***

As we know, there are three basic states of matter, solid, liquid, and gaseous states. These states of matter can be transformed into each other at appropriate conditions. In the solid state (generally meaning the crystalline state), the building blocks, such as atoms, or molecules, or clusters of molecules are packed closely and regularly, forming a crystal lattice. The physical properties of crystals are basically anisotropic. The crystals have a constant melting temperature (except for amorphous solids). As the temperature of matter increases the thermal movement of atoms or molecules becomes so severe that the crystal lattice is dissolved and fluidity appears. At this temperature, matter does not have a regular shape and anisotropic properties any more. It becomes a liquid. In the liquid state, the atoms or molecules are no longer arranged in a regular order, but they are still bonded to each other tightly, though not in the tightest packing. Increasing the temperature further up beyond the melting point, matter is transformed to the gaseous state. In the gaseous state, no short-range order exists. The interaction between the constituent molecules is extremely weak. Due to thermal excitation the molecules fill the container uniformly and hence the gas no longer has a flat surface. Generally, as the temperature increases progressively, matter at first appears in the form of a crystal solid, and then a liquid and finally the gaseous state.

As the understanding about the states of matter became deeper, people had found that in addition to the above mentioned well-known three states, there exists other state of matter in nature such as liquid crystal state. The liquid crystal state is a kind of state whose order is between the crystal solid and isotropic liquid states. In the crystal state, there is a long range order in position and orientation, while in the liquid state there is no long range ordering in either of them. Figure 9 is a comparison of the crystal (a), the liquid crystal (b) and the liquid (c) states.

Liquid crystals are also called mesogens and various intermediate phases in which they could exist are termed mesophases or mesomorphic phases. LCs are anisotropic materials whose flow properties strongly depend on their structures and molecular orientation. The mesomorphic phases appear as a more or less viscous fluid which can be identified visually by their characteristic turbidity or by optical birefringence. Whereas LCs exhibit a degree of macroscopic orientational order that is found between the boundaries of crystalline solid state and isotropic, ordinary liquid state, the properties of LCs are intermediate between those of an isotropic liquid and those of a crystalline solid.

Many organic compounds, including macromolecules, would possibly form liquid crystals when they are heated above their melting temperatures. The well-known and widely studied liquid crystals are thermotropic and lyotropic (Priestley 1974; Meier, *et al.* 1975; Hans and Rolf 1980). Thermotropic liquid crystals are of interest both from the standpoint of basic research and also for applications in electro-optic displays, temperature and pressure sensors (Meier, *et al.* 1975). Lyotropic liquid crystals, on the other hand, are of great interest biologically and appear to play an important role in living systems (Meier, *et al.* 1975). Depending on temperature, pressure, constitutes, concentration, substitutes, and so on, mesogens can exhibit rich mesophases, including nematic (N), smectic (S) and cholesteric (Ch), Priestley 1974; Meier, Sackmann *et al.* 1975; Hans and Rolf 1980; Finkelmann 1987; Leadbetter 1987).

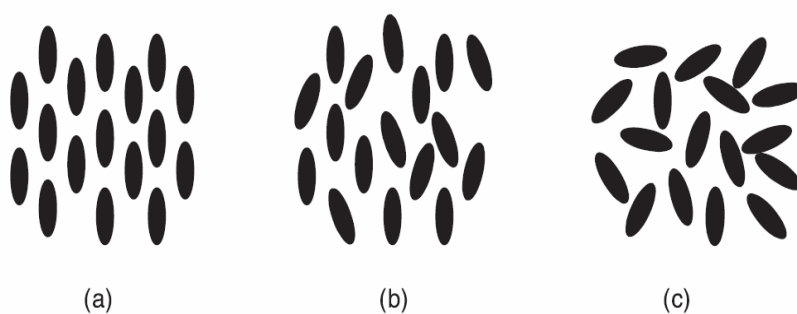


Figure 9: The schematics of (a) crystal, (b) liquid crystal and (c) liquid.

### - *Thermotropic Liquid Crystals*

A mesogen is thermotropic if the order of its components is determined or changed by temperature (Priestley 1974; Hans and Rolf 1980; Pavel, *et al.* 2002). If temperature is too high, the rise in energy and therefore in motion of the components will induce a phase change: the LC will become an isotropic liquid. If, on the contrary, temperature is too low to support a thermotropic LC phase, the LC will become a crystal. The liquid crystallinity of thermotropic LC appears only in a particular temperature range, as schematically shown in Figure 10. Smectic, nematic and cholesteric are the three main types of thermotropic LC phases (Pavel, *et al.* 2002).

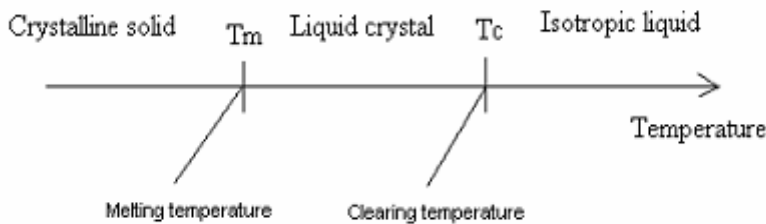


Figure (10): Thermotropic liquid crystalline transition (Pavel, *et al.* 2002).

### *I-Nematic Liquid Crystals*

One of the most common LC phases is the nematic phase, where the molecules have no positional order, but they have long-range orientational order. Thus, the molecules flow and their center of mass positions are randomly distributed as in a liquid,

but they all point in the same direction (within each domain). Most nematics are uniaxial: they have one axis that is longer and preferred. Some liquid crystals are biaxial nematics, meaning that in addition to orienting their long axis, they also orient along a secondary axis (Cladis and Kleman 1972; Cladis 1974; Priestley 1974) as seen in Figure 11.



Nematic phase

Figure (11): Schematic representation of molecular arrangements in nematic phase.

## ***II-Smectic Liquid Crystals***

The smectic phases are found at lower temperatures than the nematic. The smectics are thus positionally ordered along one direction. There are many different smectic phases, all characterized by different types and degrees of positional and orientational order. In the smectic A phase, the molecules are oriented along the layer normal, while in the smectic C phase they are tilted away from the layer normal. These phases are liquid-

like within the layers. Schematic of alignment in the smectic phases is shown in Figure 12.

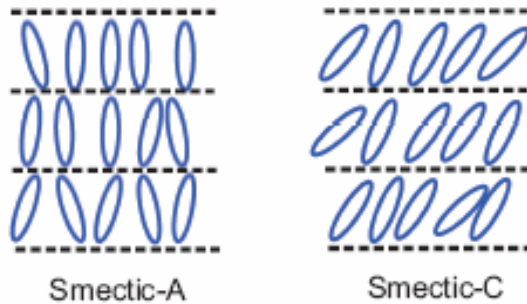


Figure (12): Schematic structure of the molecular arrangement of the smectic-*A* and smectic-*C* phase.

### ***III-Chiral phases***

The chiral nematic phase or called cholesteric phase exhibits chirality (handedness). This phase is often called the cholesteric phase because it was first observed for cholesterol derivatives. Only chiral molecules (i.e. those that lack inversion symmetry) can give rise to such a phase. This phase exhibits a twisting of the molecules perpendicular to the director, with the molecular axis parallel to the director. The finite twist angle between adjacent molecules is due to their asymmetric packing, which results in longer-range chiral order. In the smectic C\* phase (an asterisk denotes a chiral phase), the molecules have positional ordering in a layered structure (as in the other smectic phases), with the molecules tilted by a finite angle with respect to

the layer normal. The cholesteric phase is characterized by layers of nematic molecules where each layer is twisted with respect to the ones above and below it. As a succession of layers is passed through, the director turns through  $360^\circ$  (as shown in Figure 13) and the thickness of such a period represents a pitch length of the helix.

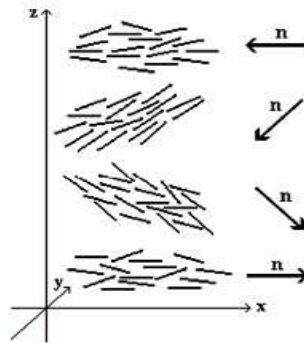


Figure (13): Schematic representation of cholesteric liquid crystalline phase.

An important characteristic of the cholesteric mesophase is the pitch. The chiral pitch,  $p$ , refers to the distance over which the LC molecules undergo a full  $360^\circ$  twist (but note that the structure of the chiral nematic phase repeats itself every half-pitch, since in this phase directors at  $0^\circ$  and  $\pm 180^\circ$  are equivalent). The pitch,  $p$ , typically changes when the temperature is altered or when other molecules are added to the LC host (an achiral LC host material will form a chiral phase if doped with a chiral material), allowing the pitch of a given material to be tuned accordingly (Hou *et al.* 2000).

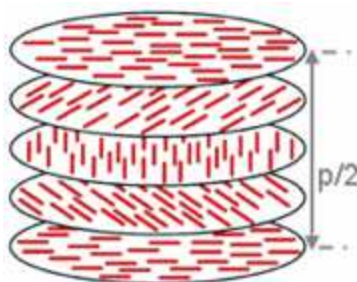


Figure (14): Chiral nematic phase;  $p$  refers to the chiral pitch.

### ***- Lyotropic liquid crystals***

There is a class of materials that exhibit liquid crystal behavior only when being in solution. Liquid crystalline phases formed in such solutions are said to be lyotropic (Priestley 1974; Hans and Rolf 1980). A lyotropic LC consists of two or more components that exhibit liquid-crystalline properties in appropriate concentrations. Lyotropic liquid crystalline transition process is presented in Figure 15.

In lyotropic phases, solvent molecules fill the space around the compounds to provide fluidity to the system. In contrast to thermotropic LCs, the lyotropics have another degree of freedom of concentration that enables them to induce a variety of different phases. A compound, which has two immiscible hydrophilic and hydrophobic parts within the same molecule, is called an amphiphilic molecule.

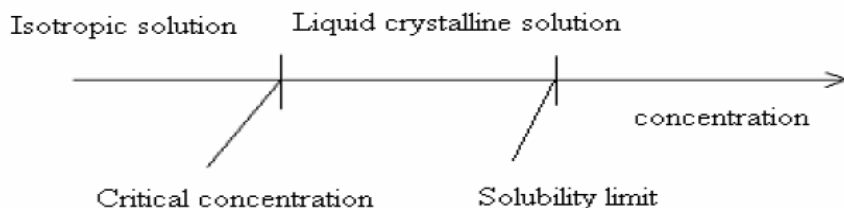


Figure (15): Lyotropic liquid crystalline transition. (Pavel, 2002).

Many amphiphilic molecules show lyotropic liquid-crystalline phase sequences depending on the volume balances between the hydrophilic part and hydrophobic part. These structures are formed through the micro-phase segregation of two incompatible components on a nanometer scale. Soap is an everyday example of a lyotropic liquid crystal (Finkelmann 1987). The content of water or other solvent molecules changes the self-assembled structures. At very low amphiphilic molecule concentration, the molecules will be dispersed randomly without any ordering. At slightly higher (but still low) concentrations, amphiphilic molecules will spontaneously assemble into micelles or vesicles. This is done so as to hide the hydrophobic tail of the amphiphilic molecule inside the micelle core, exposing a hydrophilic (water-soluble) surface to aqueous solution. These spherical objects do not order themselves in solution, however. At higher concentrations, the assemblies will become ordered. A typical phase is a hexagonal columnar phase, where the amphiphilic molecules form long cylinders (again with a hydrophilic surface) that arrange themselves into a roughly

hexagonal lattice. This is called the middle soap phase. At still higher concentrations, a lamellar phase (neat soap phase) may form, wherein extended sheets of amphiphilic molecules are separated by thin layers of water. For some systems, a cubic (also called viscous isotropic) phase may exist between the hexagonal and lamellar phases, wherein spheres are formed that create a dense cubic lattice. These spheres may also be connected to one another, forming a bicontinuous cubic phase.

The objects created by amphiphilic molecules are usually spherical (as in the case of micelles), but may also be disc-like (bicelles), rod-like, or biaxial (all three micelle axes are distinct). These anisotropic self-assembled nano-structures can then order themselves in much the same way as thermotropic liquid crystals do, forming large-scale versions of all the thermotropic phases (such as a nematic phase of rod-shaped micelles) (see Figure 16).

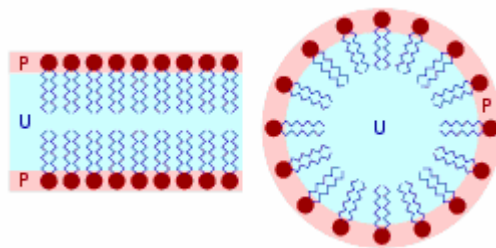


Figure (16): Structure of lyotropic liquid crystal. The red heads of surfactant molecules are in contact with water, whereas the tails are immersed in oil (blue): bilayer (left) and micelle (right).

### ***- Hydroxypropyl cellulose as liquid crystalline polymer***

Hydroxypropyl cellulose is an ether of cellulose in which some of the hydroxyl groups in the repeating glucose units have been hydroxypropylated forming  $-OCH_2CH(OH)CH_3$  groups using propylene oxide. The average number of substituted hydroxyl groups per glucose unit is referred to as the degree of substitution (DS). Complete substitution would provide a DS of 3. Because the hydroxypropyl group added contains a hydroxyl group, this can also be etherified during preparation of HPC. When this occurs, the number of moles of hydroxypropyl groups per glucose ring, moles of substitution (MS), can be higher than 3.

In the past 20 years interest has focused on the study of the liquid-crystalline characteristics of cellulose and its derivatives since Werbowyj and Gray (1976) found a cholesteric liquid-crystalline phase in concentrated aqueous solutions of HPC. HPC itself (Shimamura *et al.* 1981), HPC derivatives (Gray 1983), and other fully substituted cellulose derivatives (Yamagishi *et al.* 1988; 1989; 1990; 1991) with flexible side chains have been reported to melt readily, forming thermotropic liquid crystalline mesophases. HPC is able to form both lyotropic and thermotropic mesophases (Shimamura *et al.* 1981; Zugenmaier *et al.* 1989).

### - *Alkoxybenzoic acids*

4-Alkoxybenzoic acids are well-known for their mesomorphic behavior (Bryan, et al. 1980; Bryan and Hartley 1980; Babkov, *et al.* 1995; Kato, *et al.* 1995; Nelida, 2004). The compounds with a short terminal alkyl chain exhibit a nematic phase, and those with intermediate chain lengths show both a nematic and a smectic C phase; whereas compounds with very long alkyl chains show a smectic C phase only (Liesbet *et al.* 2003). Recent investigations have shown that the 4-alkoxybenzoic acids have interesting structural and physical properties (Manuel *et al.* 2010; Fukumasa *et al.* 1993; Song *et al.* 2003). These compounds tend to form extremely stable liquid crystals as a result of their ability to form hydrogen bonded cyclic dimers, thereby enabling the exhibition of a nematic liquid crystal phase and with the higher homologous also showing a smectic phase.

## **Chapter 2. Experimental**

### **2.1. Materials and methods**

- i.** Bleached bagasse pulp was supplied from Quena Paper Industry Company, Egypt. The pulp was beaten according to TAPPI Standard (TAPPI T 200 sp-2006) and the Schopper Riegler degree ( $^{\circ}\text{SR}$ ) is 40.
- ii.** Defatted soy flour of composition: protein 48.5 %, carbohydrate 35.1%, oil 0.98% and ash 5.63%, was purchased from Agriculture Center of Research, Egypt.
- iii.** Egyptian upgraded kaolin (Farch El-Gozlan) was prepared on pilot scale at CMRDI, El-Tebeen, Egypt.
- iv.** Acrylamide, hydrochloric acid, potassium hydroxide, urea and sodium hydroxide (Aldrich) were laboratory grade chemicals.
- v.** Hydroxypropylcellulose (HPC) (Aldrich,  $M_w = 100,000 \text{ g}\cdot\text{mol}^{-1}$ ) was dried under vacuum at  $50^{\circ}\text{C}$  for about 48h before use.
- vi.** Para-toluenesulfonylchloride (TsCL), anhydrous pyridine, dimethyl acetamide (DMA), tetrahydrofuran (THF), methanol, acetone, isopropanol and 4-Alkoxybenzoic acid ( $\text{C}_n\text{H}_{2n+1}\text{OC}_6\text{H}_4\text{CO}_2\text{H}$ ,  $n= 1, 2, 3, 4, 5, 7, 8, 10, 12$  and  $14$ ) were all purchased from Aldrich and used as received.

### **2.1.1. Analysis of pulps**

#### **2.1.1.1. $\alpha$ -cellulose content (Moore and Janson, 1967)**

$\alpha$ -cellulose content was determined as follows: about 3g of the pulp (exactly weighed) were put into porcelain beaker (250ml). Then 25 ml of 17.5% NaOH solution were added, and after leaving to swell for 4 minutes (time exactly measured from the last drop), the pulp was pressed with glass rod for 3 minutes. After pressing, another 25 ml of NaOH were added and mixed thoroughly till one gets a homogeneous paste (mixing for about 1 minute). The beaker was then covered and left for 35 minutes, at 20 °C, then 100ml of distilled water was added and quickly filtered under suction using a sintered glass funnel (G2 of 5 cm diameter). The filtrate was poured on the paste twice before washing with distilled water. After washing with distilled water till neutrality, 100 ml of 10 % acetic acid of were added drop-wise for washing followed by distilled water. The temperature must be kept constant at 20°C during the whole experiment. The  $\alpha$ -cellulose content was estimated gravimetrically after drying in oven at 105°C till constant weight.

#### **2.1.1.2. Pentosan content (Moore and Janson, 1967)**

Pentosan constitutes the major part of hemicelluloses fraction of the raw material. The procedure was carried out as follows: exactly weighed pulp material (2g) was placed in the

reaction vessel (500 ml round flask) together with 75 ml of distilled water and some glass beads. 75 ml of 40% hydrobromic acid were added to the reaction vessel and heating was controlled to obtain 50 ml filtrate within 15 minutes after which another 50 ml of distilled water were added. The process was repeated 8 times and a total of 400 ml of the distillate obtained were transferred to a 500 ml measuring flask and completed to the mark with distilled water. 50 ml of the latter solution were cooled to 12°C and 2 ml of hydrochloric acid (13%), 10 ml ammonium molybdate (25 g/L) and 20 ml of 0.05 N bromide-bromate solutions were successively added. After exactly four minutes of the appearance of the yellow color, about 10 ml of 10% potassium iodide solution were added. The mixture was allowed to stand for 5 minutes and the titration was carried out immediately against 0.05 N sodium thiosulphate solution using starch as indicator. The pentosan content was calculated according to the following equation:

$$\text{Pentosan \%} = \frac{\text{volume (ml) of bromide-bromate} - \text{volume (ml) of thiosulphat}}{\text{Weight of dry sample}} \times 3.3$$

### 2.1.1.3. Lignin content

Two general methods are in common use for such estimation. In the first, direct method according to the Institution of Papermaking, Appleton Wisconsin 428 (1951),

the non-ligninic components of the sample are extracted in concentrated sulfuric acid, or concentrated hydrochloric acid, or a mixture of them. The undissolved lignin is then determined. The results obtained are greatly affected by the working conditions such as acid concentration, time of treatment and temperature. Therefore, these conditions must be maintained constant through the whole estimation.

The second, indirect, method depends upon the estimation of chemical groups, such as the methoxyl group, in the lignin molecule, or the estimation of the amount of halogen consumed by lignin under specific conditions.

In this work the direct method was applied. An exact weight of the air dried sample (about 1 gram) was treated with 15 ml of 72% sulfuric acid for 24 hours at room temperature. The material was then transferred into a one liter flask, diluted with 560 ml of distilled water, and boiled under reflux for four hours. The lignin was filtered on a previously weighed dry ashless filter paper, and then washed with hot distilled water till neutrality. The filter paper and lignin were transferred to a weighed porcelain crucible and dried in an oven at 105 °C till constant weight.

For ash correction, the contents of the crucible were ignited at 400°C for 30 minutes and then at 85 °C for further

45 minutes. The weight of the ash was subtracted to give the weight of the pure lignin. The lignin content is calculated from:

$$\text{Lignin \%} = \frac{\text{Weight of lignin} - \text{Weight of its ash}}{\text{Weight of moisture free material}} \times 100$$

#### **2.1.1.4. Ash content**

The ash content was estimated by igniting an exactly weighed sample in muffle furnace for 30 minutes at 400°C, then for 45 minutes at 850°C and then gravimetrically estimated (Tappi standard 211-om 2007). The percentage of ash was calculated from:

$$\text{Ash \%} = \frac{\text{Weight of ash}}{\text{Weight of dry sample}} \times 100$$

#### **2.1.1.5. Morphological analysis by Morfi**

The Morfi is a laboratory device developed by Grenoble INP -Pagora and Paper Technical Center (PTC). It uses a technique of image analysis to determine the main morphological parameters of fibers suspended in water. This technique allows obtaining the following: the average fiber length (mm), the average fiber width ( $\mu\text{m}$ ), the coarseness, and the percent of macrofibril and fine elements. This measurement

depends on the suspension of 1.2 grams of dry pulp into 4 liters of water. Then, one liter of the suspension prepared is fed into the vat of the device so that a quantity of 300 mg dry fiber is analyzed. Four measurements were performed for each test and the average was taken.

#### **2.1.1.6. Water Retention Value of pulp**

Water Retention Value (WRV) is an empirical measure of the capacity of a test pad of fiber to hold water. A test pad consisting of pulp fiber is formed by dewatering a pulp suspension on a wire screen. The test pad is centrifuged under a specific centrifugal force for a specified time, weighed then dried and weighed again. The WRV is calculated from the wet mass of the centrifuged test pad and the dry mass of the test pad.

A laboratory hand-sheet former with 150 mesh wire plate was used to dewater the sample. Over the wire was placed a rubber frame of three compartments of equal areas ( $\sim 33 \text{ cm}^2$  each). 500 ml of the pulp slurry (equivalent to 1 g oven dry basis pulp weight) was measured and poured in the cylinder of the hand-sheet former, previously half filled with water, and the level of the water was to rise up to the mark. The sample was agitated gently and drained. The pulp samples from each of the compartment were picked up and put into the centrifugation tube having three small holes with sieves at the

bottom; the samples were centrifuged with centrifugal force of 3000g for 15 min at 20°C (according to Silvy's method 1968). After centrifugation, the pulp samples were transferred in a tared weighing bottle and immediately weighed on a precision balance to the nearest 0.1 mg. The weighing bottle with the pulp were dried in an oven to constant weight at 105°C. The WRV was calculated as follows:

$$\text{WRV} = \frac{M_1 - M_2}{M_2} \times 100$$

where  $M_1$  is weight of test bad after centrifugation (wet) and  $M_2$  weight of test bad after drying.

### **2.1.2. Preparation of soy protein Isolate (SPI)**

100 g of defatted soy flour was suspended in 700 ml distilled water and stirred for 30 min. The pH of the mixture was then adjusted to 9.0 with 0.2N NaOH and stirred for 2 hrs. The slurry was centrifuged to separate the insoluble portion. The pH of the remaining solution was adjusted to 4.5 by addition of hydrochloric acid to precipitate soy protein which was then washed with distilled water to remove undesirable carbohydrates such as a raffinose and stachyose. The isolated soy protein was air dried.

### **2.1.2.1. Preparation of SPI binders**

Soy protein isolate was added into distilled water and stirred mechanically for 20 min to prepare 15% slurry. The SPI thus prepared was modified using urea and sodium hydroxide, in which urea was added to give a final urea concentrations of 3M and 3% sodium hydroxide was added (with respect to SPI) to the mixture with stirring for 20 min to have a viscous solution. Modified SPI was added to the paper sheets in 0.5, 2.5 and 5% with respect to dry pulp. Different acrylamide contents relative to SPI (1.5, 2.5 and 5) were added to the mixture with stirring for 20 min. The obtained products were homogenous and stable at pH 9. The prepared mixtures were denoted as:

SPI<sub>1</sub> (SPI + Urea + NaOH), SPI<sub>2</sub> (SPI + Urea + NaOH + 1.5% Acrylamide), SPI<sub>3</sub> (SPI + Urea + NaOH + 2.5% Acrylamide), and SPI<sub>4</sub> (SPI + Urea + NaOH + 5% Acrylamide).

### **2.1.3. Preparation and characterization of the paper sheets**

#### **2.1.3.1. Preparation of handsheets**

The conventional hand-sheets of a basis weight of 60 g/m<sup>2</sup> were prepared on a Rapid Khöten sheet former following the standard method ISO 5269-2. The beaten pulp is used at a concentration of 2 g/L. One liter of this fiber suspension is poured into the cylinder of the apparatus to handsheets. This volume is then diluted by 5-7 L of water. After a stirring phase (air injection avoids aeration) the suspension is filtrated on a

wire. After pressing, the wet sheet is collected on blotting paper, protected between two sheets and dried under vacuum at 80°C for 10 minutes; each sample is represented by ten handsheets. The handsheets were conditioned at least for 48h before testing at 23±1°C and 50±2% relative humidity according to the Tappi standard 502 cm-2007.

### **2.1.3.2. Scanning electron microscopy**

The bagasse handsheets have been observed using scanning electron microscopy (a Zeiss ULTRA55 Scanning Electron Microscope (SEM) with an acceleration voltage of 15 kV). Surface and cross section were studied. Each sample was coated with gold/palladium alloy before observation.

### **2.1.3.3. Thickness and grammage of handsheets**

The thickness was measured using the MI 20 micrometer of Adamel Lhomargy according to ISO-534-1976. Then the grammage (basis weight) of the handsheets was determined according to the standard ISO 536-1976. Weight of each test sample was taken separately on a precision balance with an accuracy of 0.1mg and grammage was calculated as follows:

$$G = 4m/\pi d^2$$

where G is the grammage of paper in g/m<sup>2</sup>, m is the mass of handsheet in grams and d its diameter (0.2 m).

#### **2.1.3.4. Breaking length**

The breaking length is the length of strip of paper required to break the strip under its own weight. The breaking length in Km is obtained using the following relationship:

$$\text{Breaking Length in meter} = \frac{\text{Tensile Strength (g)}}{\text{Basis Weigh of paper(g/m}^2\text{) x Width at break (m)}}$$

Breaking length is a function of tensile strength and thickness. Tensile tests were performed with an SE 064 Lorentzen & Wettre tensile apparatus. The tensile strength was estimated using a strip of 15mm diameter (cut from the test handsheets) and placed between two clamps span by 10 cm and the cross head speed was fixed at 10mm/min.

#### **2.1.3.5. Tear strength**

The test was carried out on a test piece of 65×50 mm dimension, cut from the test sheet using Adamel Lhomargy tearing strength tester according to ISO 1974-1990. Tearing index (ID) is expressed in  $\text{mN.m}^2.\text{g}^{-1}$  and calculated as follows:

$$\text{ID} = (\text{D}/\text{W}) \times 100$$

where D is the tearing resistance (mN) and W is the grammage ( $\text{g/m}^2$ ).

### **2.1.3.6. Burst strength**

Burst strength was carried out using Adamel Lhomargy burst tester, according to ISO 2758-1983. The burst index (IE) was expressed in  $\text{kPa}\cdot\text{m}^2\cdot\text{g}^{-1}$  and calculated as follows:

$$\text{IE} = P/W$$

where P is the pressure at the time of burst (kPa) and W is the grammage ( $\text{g}/\text{m}^2$ ).

### **2.1.3.7. Brightness**

Brightness measurement is based on reflectance by white or near-white paper at single wavelength of 457 nm. The measure is done on a sample thickness enough to be opaque, often represented by several layers of simply folded sheet of samples. The apparatus used in this work for measuring the brightness was a spectrophotometer Touch COLOR Technidyne.

### **2.1.3.8. Opacity**

The Opacity of paper is often of interest, particularly for printing papers. It may be determined by:

1. Measuring the reflectance of a single sheet of paper at a certain wavelength (usually 457 nm) when held on a non-reflective black background.
2. Measuring the reflectance of a single sheet of paper when held on a standard white background.

The opacity is the ratio of the two reflectance values, expressed as a percentage. The opacity of the handsheets was measured using a spectrophotometer Touch COLOR Technidyne.

#### **2.1.3.9. Determination of retention of fillers**

The retention of fillers was calculated according to the following equation:

$$\text{Filler Retention Value \%} = \frac{\text{Retained Filler}}{\text{Added amount of filler}} \times 100$$

#### **2.1.4. Synthesis of alkoxybenzoyloxypropyl cellulose (ABPC-n) from HPC of DS 3 and 4-alkoxybenzoic acids**

2.0 g of HPC (16.14 mmol based on average number of hydroxypropyl unit in the glucose unit) were stirred in 100 ml DMA. 4-alkoxybenzoic acid, pyridine and TsCl (6 molar equivalent) were added and stirred at 80 °C for 24 hrs. The reaction mixture was then poured into cold methanol whereby the derivatives were separated as a white sticky mass. For purification, the filtered precipitate was dissolved in acetone, and then reprecipitated with cold methanol to get rid of all unreacted acid and other by-products. The derivatives were purified at least four times by dissolutions and reprecipitation, and the product was finally dried under vacuum at 60°C. The

derivatives were denoted as the ABPC- $n$  where  $n$  refers to the number of carbon atoms in the alkoxy chain.

### 2.1.5. Preparation of dissolving bagasse pulp

- Hydrolysis of bleached bagasse pulp was performed by adding 25 ml 2 M HCl per gram pulp in Erlenmeyer flask, the solution was refluxed for 20 min. and finally washed with distilled water until acid-free.
- Hemicellulose was degraded from the pulp by stirring with 10% KOH (liquor ratio 20:1) at room temperature for 20 hrs, followed by washing with distilled water until the filtrate tested was neutral. The extraction was repeated twice (Sun *et al.* 2001).
- The average degree of polymerization of bagasse and dissolving bagasse pulps was determined by measuring the intrinsic viscosity  $[\eta]$  ( $\text{cm}^3 \cdot \text{g}^{-1}$ ) using NFT 12-005 method. The average degree of polymerization ( $\overline{DP}_v$ ) of pulp was calculated using Mark-Houwink equation:

$$[\eta] = k (\overline{DP}_v)^\alpha$$

The constants  $K$  and  $\alpha$  selected are those which correspond to the polymer solution (cupraethylenediamine (CED) /cellulose) at 25 °C:  $K = 7.5 \times 10^{-3}$  and  $\alpha = 1$ .

- The dissolving pulp prepared was characterized and was found to be  $\alpha$ -cellulose (94%), Lignin (0.8%), hemicellulose (3%), ash (2.2 %) and  $\overline{DP}_v$  (550).

#### **2.1.5.1. Synthesis of partially substituted hydroxypropyl cellulose (HPC<sub>B</sub>)**

The reaction was carried out via alkalization and etherification of cellulose under heterogeneous conditions. Aqueous NaOH (22% w/v) was added to finely pulverized cellulose (1.0 g) in isopropanol (10 mL) at ambient temperature, with continuous stirring for 1 hr in closed vessel. Alkali cellulose was squeezed to remove the excess alkali till weight gain of 150% then transferred to a 250 mL three-necked round-bottom flask, fitted with condenser and nitrogen inlet. Ice-cold water was circulated in the condenser throughout the reaction. Propylene oxide (17 mol/anhydroglucose unit) and isopropanol (50 mL) were added to alkali cellulose and the reaction was allowed to proceed at 60°C for 6 hrs. After neutralizing the excess alkali with acetic acid, the synthesized hydroxypropyl cellulose sample was dissolved in water and precipitated in acetone, filtered, and washed with acetone. The purification was repeated three times and the product was dried at 60°C in vacuum oven.

### **2.1.5.2. Synthesis of alkoxybenzoyloxypropyl cellulose (ABPC-*m*) from partially substituted HPC<sub>B</sub> and 4-alkoxybenzoic acids**

Alkoxybenzoyloxypropyl cellulose was synthesized from partially substituted HPC and alkoxybenzoic acids as previously mentioned in section (2.1.4.) and the derivatives were denoted as ABPC-*m* where *m* referred to the number of carbon atom in the acid side chain (*m*= 2, 10, and 12).

### **2.1.6. Characterizations of HPC and its derivatives**

#### **2.1.6.1. FT-IR analysis**

FT-IR spectra were recorded, in KBr disc, on a JASCO 300-E Fourier transform infrared spectrometer.

#### **2.1.6.2. <sup>1</sup>H NMR spectra**

<sup>1</sup>H NMR spectra were recorded in deuterated dimethylsulfoxide (DMSO) using tetramethylsilane (TMS) as reference, on Varian UNITY400 spectrometer 5mm id-pfg- (inverse detection – pulse field gradient) probe. The DS of HPC and its derivatives were determined by <sup>1</sup>H NMR spectroscopy.

#### ***Calculation of the degree of substitution of HPC<sub>B</sub> using <sup>1</sup>H NMR***

The degree of substitution of HPC is defined as the number of the grafted hydroxypropyl groups per anhydroglucose units of cellulose.

For all the mathematical formulas set out below, the following abbreviations have been adopted:

$DS_{HPC}$  = Degree of substitution of hydroxypropyl groups per anhydroglucose unit of cellulose

$I_{CH_3}$  = Integration corresponding to the terminal protons of HPC and  $I_g$  = Integration corresponding to protons of anhydroglucose units of cellulose.

$$DS_{HPC} = \frac{\text{Number of chains}}{\text{Number of anhydroglucose units}} \quad \text{Eq.1}$$

The number of hydroxypropyl groups is equal to the integration of hydrogen corresponding to terminal protons ( $I_{CH_3}$ ) of the HPC ( $CH_3$  terminal) divided by 3. We can write the equation as follow:

$$\text{Number chains} = \frac{I_{CH_3}}{3} \quad \text{Eq.2}$$

The number of glucose units is equal to the integration of the sugar protons divided by the number of hydrogen atoms that are not substituted by hydroxypropyl chains. There are 10 hydrogen atoms in carbohydrate units, hence:

$$\text{Number of anhydroglucose units} = \frac{I_g}{10 - DS_{HPC}} \quad \text{Eq.3}$$

From Eq. 1, 2 and 3

$$DS_{HPC} = \frac{I_{CH_3}(10 - DS_{HPC})}{3I_g} \quad \text{Eq.4}$$

From Eq. 4

$$DS_{HPC} = \frac{10 I_{CH_3}}{3I_g + I_{CH_3}} \quad \text{Eq.5}$$

### *Calculation of the degree of substitution of ABPC-n and ABPC-m using <sup>1</sup>H NMR*

Equation 5 was modified to calculate the DS of HPC derivatives as follow.

$$DS = \frac{x I_{CH_3}}{3I_g + I_{CH_3}} \quad \text{Eq.6}$$

where x is the number of hydrogen atoms in the glucose unit bearing the calculated number of hydroxypropyl groups.

#### **2.1.6.3. Differential scanning calorimetry**

Differential scanning calorimetry (DSC) is a technique for measuring the energy necessary to establish a nearly zero temperature difference between the substance under

investigation and an inert reference (Schick and Hohne 1991), as the two specimens are subjected to identical temperature regimes in an environment, heated or cooled, at a controlled rate. DSC can be used to measure a number of characteristic properties of a material such as melting point, temperature of crystallization, and glass transition temperature ( $T_g$ ). For the present work, the analysis of DSC thermograms allowed to obtain the phase transition for the samples under investigation (Huang and Zhu 1990; Russell *et al.* 1995; Kihara *et al.* 2001). A matter transition between solid and liquid exhibits through a third phase, mesophase, which displays properties of both phases. Using DSC, it is possible to estimate the small energy changes that occur as the transition from the solid to a liquid crystal and from a liquid crystal to an isotropic liquid.

Differential scanning calorimetric was conducted on powder samples (around 8 mg) using DSC Q100 TA Instruments, USA, placed in a standard aluminum pan. All thermograms were carried out at a heating rate  $5\text{ }^{\circ}\text{C min}^{-1}$  and cooling rate  $20\text{ }^{\circ}\text{C min}^{-1}$  in an inert atmosphere of nitrogen and the transition temperatures were detected.

#### **2.1.8.4. Polarized light microscope (PLM)**

Polarized optical microscopy (THMS600 polarized-light microscope equipped with hot stage) is the most familiar tool for the study of the morphology of materials (Fayolle *et al.*

1979; Lovinger *et al.* 1994; Magagnini *et al.* 1999). Analyzer is placed between the specimen stage and the eyepiece, and it is rotated to the crossed position (zero light transmission) before inserting the specimen. This equipment is useful for a quick observation. After equipping with a camera, it is convenient to record observations in high resolution. PLM is equipped with a hot stage and temperature programmer. To investigate the lyotropic properties, samples were kept in the DMA (60 wt %) for at least one week before measurement using PLM.

#### 2.1.6.5. Refractive indices

Solutions of HPC and its derivatives (ABPC-*n* and ABPC-*m*) having concentrations 20, 30, 40, 50 and 60 wt% were prepared by mixing with the solvent (DMA) and kept for about one week at room temperature before use.

Measurements of refractive indices were performed on an Abbe 60 refractometer attached to an ultrathermostat and recorded at 25 °C. The average refractive index ( $n$ ) is calculated by the equation 7.

$$n^2 = \frac{(n_e^2 + 2n_o^2)}{3} \quad \text{Eq.7}$$

where  $n_e$ ,  $n_o$  are extraordinary and ordinary refractive indices respectively. f

### **Chapter 3. Results and Discussions**

The chemical composition of the bagasse pulp was determined and it was shown that it exhibits about 67.7%  $\alpha$ -cellulose. This high content, when compared with other lignocellulosic, (Antunes *et al.* 2000; Cordeiro *et al.* 2004; Jimenez *et al.* 1992; 1993; 2006; 2008; Fiserova *et al.* 2006; Barba *et al.* 2002; Sarwar *et al.* 2006; Gominho *et al.* 2001; Jimenez and Lopez 1990), renders bagasse a competitive potential source of cellulose, especially for papermaking applications. Moreover, its significant content in hemicelluloses (30%) constitutes another positive feature, as this component may play a plasticizing role, thus increasing the inter-fiber bonding in the ensuing paper sheets.

Soy protein isolate (SPI) was used as a binder for cellulosic fibers in paper composites. Denaturation of the SPI was performed via two methods, urea/NaOH and urea/NaOH/acrylamide. Since the net charge on SPI can be changed by varying the pH of the aqueous medium, so correlating the mechanical and physical properties of paper sheets with the pH of SPI was studied.

The effect of combination of SPI with kaolin on the retention of kaolin was estimated. The strength properties of paper as well as optical properties of the prepared sheets under all these conditions were investigated.

The water retention value (WRV) was determined for unbeaten (22 °SR) and beaten (40 °SR) pulps and were found to be 125.5 and 168 %, respectively. These values are relatively higher than those of hardwood and softwood pulps (Silvy *et al.* 1968), which generally vary between 90 and 100%. This variation is attributed to the high hemicellulose content in bagasse pulp which plays the important role in the enhancement of hydration, as it was already observed for other lignocellulosics (Antunes *et al.* 2000; Cordeiro *et al.* 2004; Abrantes *et al.* 2007; Dutt *et al.* 2008; Chia *et al.* 2008; Jimenez *et al.* 1993; Eugenio *et al.* 2006; Khristova *et al.* 2006; Fiserova *et al.* 2006; Barba *et al.* 2002; Shatalov *et al.* 2001).

At the same time the increase in WRV after beating may be ascribed to the internal fibrillation, a widening of the small internal pores and delaminations, which has been called "swelling" that occurs concurrently with the development of external fibrils; this also serve to hold additional water.

The morphology of fibers of bagasse pulp for unbeaten and beaten pulps illustrates the main fiber parameters e.g. the average length (mm), the average width ( $\mu\text{m}$ ), the coarseness (mg/m), the macrofibril content (%) and the proportion of fine elements (%). The results are tabulated in Table 5.

Table (5): Effect of beating on fiber morphology and WRV of bagasse pulp.

Pulp	Fiber length (mm)	Fiber width ( $\mu\text{m}$ )	Coarseness (mg/m)	Macrofibrils (%)	Fine elements (%)	WRV
Unbeaten pulp	1.02	28.2	0.0952	0.722	20	125.5
Beaten pulp	0.909	28.3	0.119	0.763	21	168

### 3.1. Modification of soy protein

Improvement of functional properties of protein by altering its molecular structure or conformation through physical, chemical or enzymatic agents at the secondary, tertiary and quaternary levels has been well documented in the literature (Feeney and Whitaker, 1977; 1985). The modification of soy proteins has been carried out to develop adhesives (Market opportunity summary, 2000) for the larger wood-composite market or for agro-composites based on renewable resources.

Denaturing and disulfide bond cleavage of proteins are expected to enhance the adhesive performance and water resistance by unfolding the protein molecules and increasing the interaction with cellulose (Kinsella, 1979; Kalapathy *et al.*, 1997). The decrease in viscosity enhances the flow of glues

and its penetration as well as spreading and foaming necessary for adhesives.

NaOH affects the SPI by partial hydrolysis of the long protein chains. This dissociation improves the dispersion of SPI molecules in water. Addition of urea leads to swelling of the protein aggregates and breaking of the hydrogen bonds, resulting in formation of low molecular weight units. Thus modification of the SPI with NaOH and urea can increase the contact area between the binder and the cellulose substrate, and hence improves the mechanical properties of paper sheets prepared using SPI binder.

### **3.1.1. Influence of soy protein isolate denatured by urea and NaOH on paper sheets properties**

Three concentrations of the denatured soy protein isolate (SPI) with urea and NaOH were used to determine the optimum conditions to be used in the following experiments, namely 0.5, 2.5 and 5%. The mechanical and physical properties of the paper sheets filled with SPI are tabulated in Table 6. Addition of increased amounts of protein led to an increase in all paper strength properties. However, loading with 2.5% SPI showed pronounced improvement. This improvement is due to increased interaction between OH groups of cellulose and the available groups of protein (COOH, NH<sub>2</sub>, SH and CONH<sub>2</sub>). Adsorption of SPI on the

surface of cellulose fibers generates more bonding sites which are stronger than the original inter-fiber bonding. So, these additional bonding sites enhance the overall bonding strength. Interfiber bonding is generally described by the formation of hydrogen bonds during consolidation and drying process of paper web. Also soy protein filled the voids between cellulose fibres. This is confirmed by the scanning electron microscope (SEM) images, cross section and surface morphology, of the paper sheets loaded with 2.5% SPI in Figure 17. However, 5% SPI addition accompanied by slight increase over that of 2.5%.

Loading of paper sheets with SPI resulted in an increase in the opacity and slight increase in brightness. The improvement in opacity is attributed to difference in refractive indices of the many interfaces involved namely cellulose/air, cellulose/protein, etc. which are responsible for light scattering (Yehia *et al.* 2010).

Table (6): Influence of soy protein isolate denatured by urea and NaOH.

Paper properties	Binder SPI <sub>1</sub> %			
	0%	0.5 %	2.5 %	5 %
Breaking length (Km)	5.23	6.29	6.45	6.46
% Increase in Breaking length	-	20.26	23.35	23.51
Burst Index (Kpa.m <sup>2</sup> /g)	3.36	4.33	4.91	4.95
% Increase in Burst Index	-	28.86	46.1	47.32
Tear Index (mN.m <sup>2</sup> /g)	4.75	5.41	6.29	6.31
% Increase in Tear Index	-	13.89	32.40	32.84
Brightness %	74	74	73.9	73.8
Opacity%	82.6	86.8	86.9	88.5
Ash%	0.64	0.68	0.74	0.8

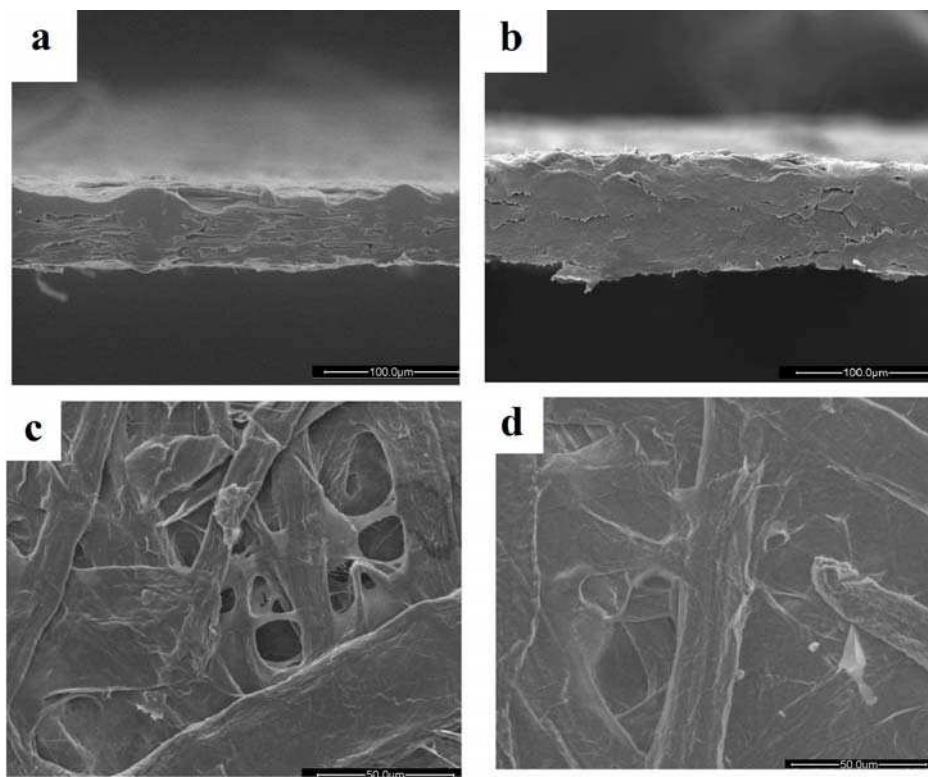


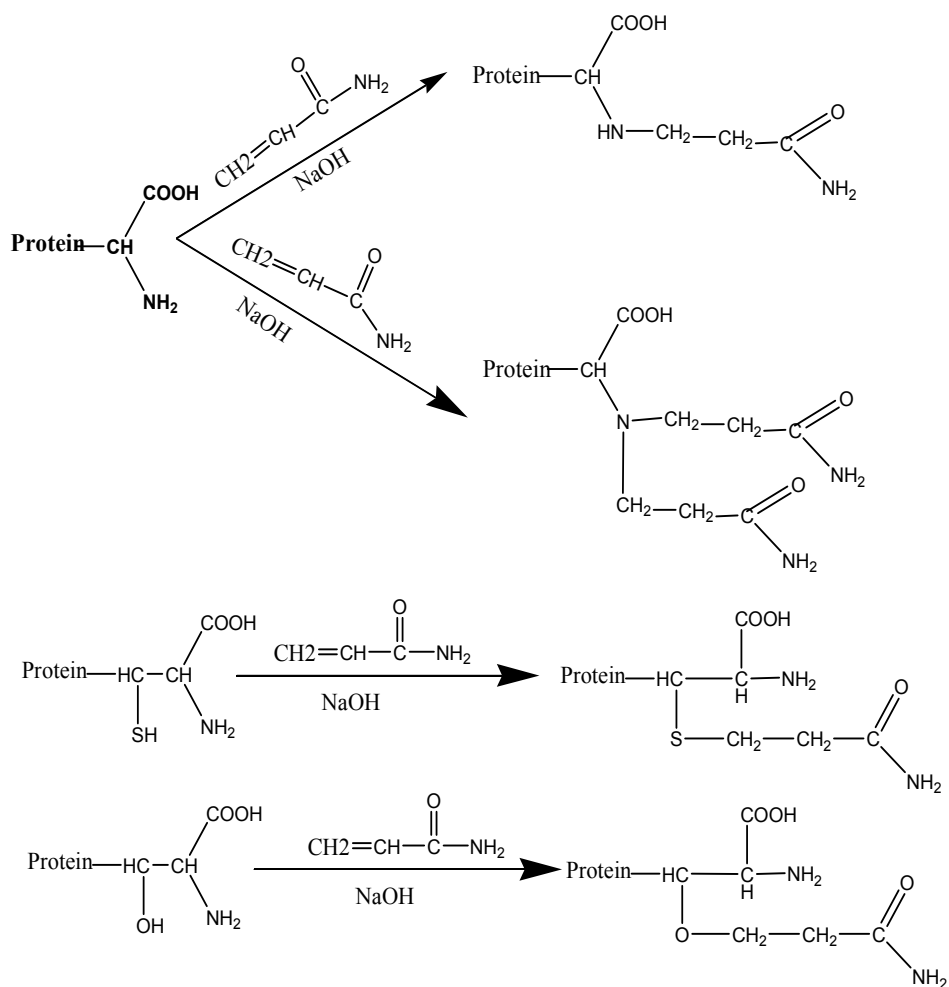
Figure (17): SEM images (a, c) cross section and surface morphology of paper sheet without SPI and (b, d) cross section and surface morphology of paper sheet with 2.5% SPI, respectively.

### **3.1.2. Influence of SPI denatured by urea, NaOH and acrylamide**

The previous experiment showed that loading paper sheets with 2.5% SPI denatured with urea and NaOH induced pronounced changes in mechanical and physical properties. SPI was used in combination with acrylamide and the resultant sheets were evaluated. The acrylamide contents used were 1.5, 2.5 and 5% and the samples were denoted as SPI<sub>2</sub>, SPI<sub>3</sub> and SPI<sub>4</sub>, respectively. Tables 7, 8 and 9 show the physical and

optical properties of paper sheets loaded with SPI<sub>2</sub>, SPI<sub>3</sub> and SPI<sub>4</sub>, respectively. The addition of increasing amounts of modified protein from 1.5 to 5% resulted in a significant increase of all strength properties as well as opacity, compared to those without acrylamide.

Scheme 1 represents theoretically possible protein derivatives that can result from reactions of proteins with acrylamide. From the diagram it is clear that nucleophilic addition proceeds through reaction between the conjugated double bond in acrylamide and active functional groups such as SH,  $\alpha$ NH<sub>2</sub> and OH in the protein. Theoretically, for each modified SPI molecule, two or more amide groups can be incorporated into the protein molecule as shown in Scheme 1. These added amide groups effect extensive unfolding of the protein molecule, and this improves the interaction between SPI and cellulose.



Scheme (1): The theoretical possible reactions between protein molecules and acrylamide.

Table (7) Influence of soy protein isolate denatured by urea, NaOH and 1.5% acrylamide (SPI<sub>2</sub>).

Paper properties	Binder SPI <sub>2</sub>			
	0%	0.5 %	2.5 %	5 %
Breaking length (Km)	5.23	6.15	6.56	6.5
% Increase in Breaking length	-	18.23	25.43	24.28
Burst Index (Kpa.m <sup>2</sup> /g)	3.36	4.22	4.66	6.23
% Increase in Burst Index	-	30.52	38.69	85.41
Tear Index (mN.m <sup>2</sup> /g)	4.75	5.75	6.62	6.79
% Increase in Tear Index	-	21.05	39.36	42.94
Brightness%	74	73.9	73.8	73.8
Opacity%	82.6	86	86.8	87
Ash%	0.64	0.66	0.67	0.75

Table (8): Influence of soy protein isolate denatured by urea, NaOH and 2.5% acrylamide (SPI<sub>3</sub>).

Paper properties	Binder SPI <sub>3</sub>			
	0%	0.5 %	2.5 %	5 %
Breaking length (Km)	5.23	6.16	6.5	6.51
% Increase in Breaking length	-	22.51	24.28	24.47
Burst Index (Kpa.m <sup>2</sup> /g)	3.36	4.15	4.64	4.91
% Increase in Burst Index	-	23.51	38.1	46.13
Tear Index (mN.m <sup>2</sup> /g)	4.41	5.41	6.32	6.47
% Increase in Tear Index	-	22.67	43.31	46.71
Brightness %	74	73.82	73.9	73.8
Opacity %	82.6	87	89.9	94
Ash %	0.64	0.71	0.73	0.79

Table (9): Influence of soy protein isolate denatured by urea, NaOH and 5% acrylamide (SPI<sub>4</sub>).

Paper properties	Binder SPI <sub>4</sub>			
	0	0.5 %	2.5 %	5 %
Breaking length (Km)	5.23	6.29	6.62	6.51
% Increase in Breaking length	-	20.00	26.57	24.47
Burst Index (Kpa.m <sup>2</sup> /g)	3.36	4.25	4.59	4.66
% Increase in Burst Index	-	26.48	36.63	38.69
Tear Index (mN.m <sup>2</sup> /g)	4.75	5.75	6.32	6
% Increase in Tear Index	-	21.05	33.05	26.31
Brightness %	74	73.9	73.8	73.8
Opacity %	82.6	88.2	89.8	92
Ash %	0.64	0.67	0.72	0.86

### **3.1.3. Effect of pH of SPI on the paper sheets properties.**

Soy proteins are composed mainly of  $\alpha$ -amino acids. These amino acids may be neutral such as glycine, basic (containing one or more additional amines) such as lysine, or acidic (containing one or more additional acid groups) such as aspartic acid; also, they may contain alcohol or thio functional groups. Under appropriate conditions the acidic and basic groups in soy protein dissociate in aqueous solution producing ionic groups and the respective counter ions. The effect of pH is critical in the functional properties and applications of soy proteins. If the amino acid groups on the soy protein chain are acids or bases, the net charge can be changed by varying the pH of the aqueous medium.

At high alkalinity (pH 10) the acidic groups are greater than the basic groups and the net charge is negative. On the contrary, at low acidity (pH 3) the basic groups are greater than the acidic groups and the net charge is positive. At the isoelectric point (IEP) the number of positive and negative charges on the polyion is the same, giving a net charge of zero. For soy protein the IEP is obtained at pH 5.

The effect of pH of SPI on the mechanical and physical properties of paper sheet has been studied and the results are shown in Table 10 and Figure 18. It is clear from the results that the maximum breaking length was obtained at the

isoelectric point at pH 5 and comparable results were also obtained at pH 7, and then it began to decrease when the pH increased to pH 10. Both the burst index and the tear index showed the parallel trends.

This improvement of the paper properties at isoelectric point is due to an increase in the protein adsorption onto the cellulose surface where in this case the adsorbing species exhibit the lowest repulsion in solution. Concurrently, bulk solubility at IEP is very low due to increased coagulation among neighboring proteins.

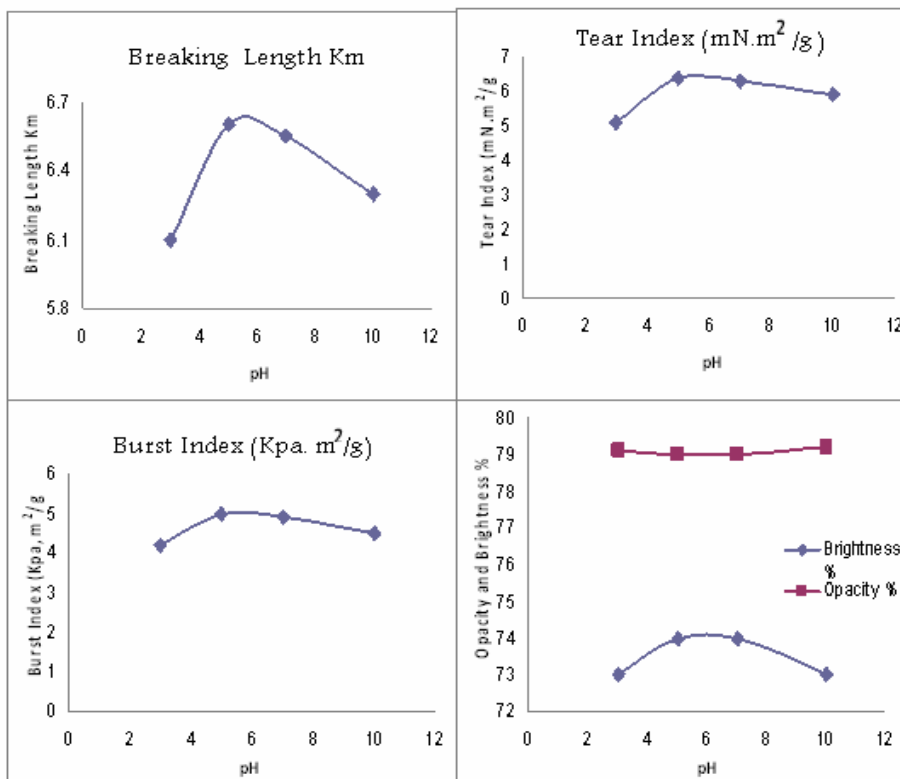


Figure (18): The effect of pH of the SPI on the physical properties of paper sheets.

Table (10): The effect of pH of the SPI on the physical properties of paper sheets.

Paper properties	pH			
	3	5	7	10
Breaking length Km	6.1	6.6	6.5	6.3
Burst Index (Kpa.m <sup>2</sup> /g)	4.2	5.0	4.9	4.5
Tear Index (mN.m <sup>2</sup> /g)	5.1	6.4	6.2	5.9
Brightness %	73.0	74.0	74.0	73.0
Opacity%	79.1	79.0	79.0	79.2

### **3.2. Influence of addition of kaolin to paper sheets loaded with SPI**

Generally fillers are incorporated into paper sheets to improve their optical and printing properties. However, some drawbacks or problems are usually associated with the use of fillers. Firstly, suspended filler particles in water are not easily retained into the formed paper sheet, because they are often too small to be mechanically entrapped. Secondly, both filler particles and fibers are negatively charged so they repel each other. Thirdly, filler particles prevent fiber-to-fiber bonding and the tensile strength of the filled paper is decreased (Alinec *et al.* 1990).

Table 11 shows the effect of addition of 2.5% denatured soy protein isolate (SPI<sub>4</sub>) and kaolin (5%, 10 and 15% based on dry pulp). From the table, it is clear that all the mechanical properties (breaking length, burst, and tear strength) were enhanced due to the addition of 2.5% SPI<sub>4</sub> without kaolin and further increase in filler content deteriorates the properties of paper sheet. On the other hand, increasing kaolin content increased the opacity and did not affect the brightness greatly.

Table (11): Influence of addition of kaolin together with the soy protein isolate on the paper properties.

Paper properties	0%filler 0%Binder	2.5% Binder SPI <sub>4</sub>			
		0%filler	5%filler	10% filler	15% filler
Breaking length Km	5.23	6.62	6.47	6.21	6.19
% Increase in Breaking length	-	26.58	23.7	18.7	18.3
Burst Index (Kpa.m <sup>2</sup> /g)	3.36	4.29	3.63	3.61	3.60
% Increase in Burst Index	-	27.6	8	7.4	7.1
Tear Index (mN.m <sup>2</sup> /g)	4.75	6.32	5.76	5.43	5.35
% Increase in Tear Index	-	33	21.2	14.3	12.6
Brightness %	74	77.8	77.5	77.21	77.1
Opacity %	82.6	89.8	87.3	91.2	94
Ash %	0.64	0.72	1.76	2.01	2.81

Retention of kaolin in paper sheets with and without soy protein binder was determined and the results are shown in Table 12. From this Table it is clear that the retention values increased as the added amount of kaolin increased. The maximum retention value was 21% for sheets filled with 15% kaolin in absence of the binder where as it was 37.2% for sheet filled with 15% kaolin using 2.5% SPI<sub>4</sub>. It is evident that the denatured soy protein acts as retention aid.

Table (12): Retention value of kaolin by bagasse pulp in absence of binder and with 2.5% SPI<sub>4</sub>.

Added amount of Kaolin g/100g pulp (%)	5	10	15
Retention value in absence of binder (%)	15.6	17.1	21
Retention value in presence of 2.5% SPI <sub>4</sub> (%)	32.5	35.4	37.2

### **3.3. Liquid crystalline behavior of hydroxypropyl cellulose esterified with 4-alkoxybenzoic acids**

In this work, the degree of substitution (DS) is referred to as the degree of esterification of hydroxyl groups per repeating unit of HPC. DS is usually determined either from elemental analysis, IR spectroscopy, or  $^1\text{H}$  NMR. In this contribution, DS was determined by  $^1\text{H}$  NMR (Ritcey *et al.* 1988). The substituted hydroxyl groups of the HPC were found to be 1.6-2.4 on average. Generally the long alkyl/alkoxy chains add flexibility to the rigid core structure that tends to be exhibited. Additionally the alkyl/alkoxy chains are believed to be responsible for stabilizing the molecular orientation necessary for liquid crystal phase generation (Collings, 1990), and the overall chain structure becomes semi-rigid; therefore, thermotropic or lyotropic cholesteric LC phases may be developed in bulk with certain temperature range (thermotropic) or in highly concentrated solutions (lyotropic) (Huang *et al.* 2007).

#### **3.3.1. Investigation of alkoxybenzoyloxypropyl cellulose (ABPC-*n*) structure**

##### **3.3.1.1. FT-IR spectroscopic analysis**

The progress of esterification with benzoic acid bearing different alkoxy chains ABPC-*n* was assessed by FT-IR spectroscopy. Figure 19 (A) represents the FT-IR spectra of HPC, ABPC-1, ABPC-2 ABPC-3, ABPC-4 and ABPC-7. Figure 19 (B)

represents the FT-IR spectra of HPC, ABPC-8, ABPC-10, ABPC-12 and ABPC-14. The FT-IR spectrum of HPC shows a broad peak at  $3463\text{ cm}^{-1}$  assigned to the O-H stretching vibration. The peak detected at  $2935\text{ cm}^{-1}$  is assigned to C-H asymmetric stretching vibration. On esterification, a pronounced decrease in the broadening of the OH absorption band is detected as a result of substitution.

The success of the esterification with the 4-alkoxybenzoic acid was clearly confirmed by the appearance of new carbonyl ester bands, stretching modes in the range of  $1750$  to  $1770\text{ cm}^{-1}$  for ABPC-*n* and the peaks observed in the range of  $1255$  to  $1265\text{ cm}^{-1}$  are assigned to C-O stretching vibrations of ester groups. Moreover, the occurrence of new absorptions in the range of  $650$ - $800\text{ cm}^{-1}$  is due to bending vibrations of the aromatic ring (Ar).

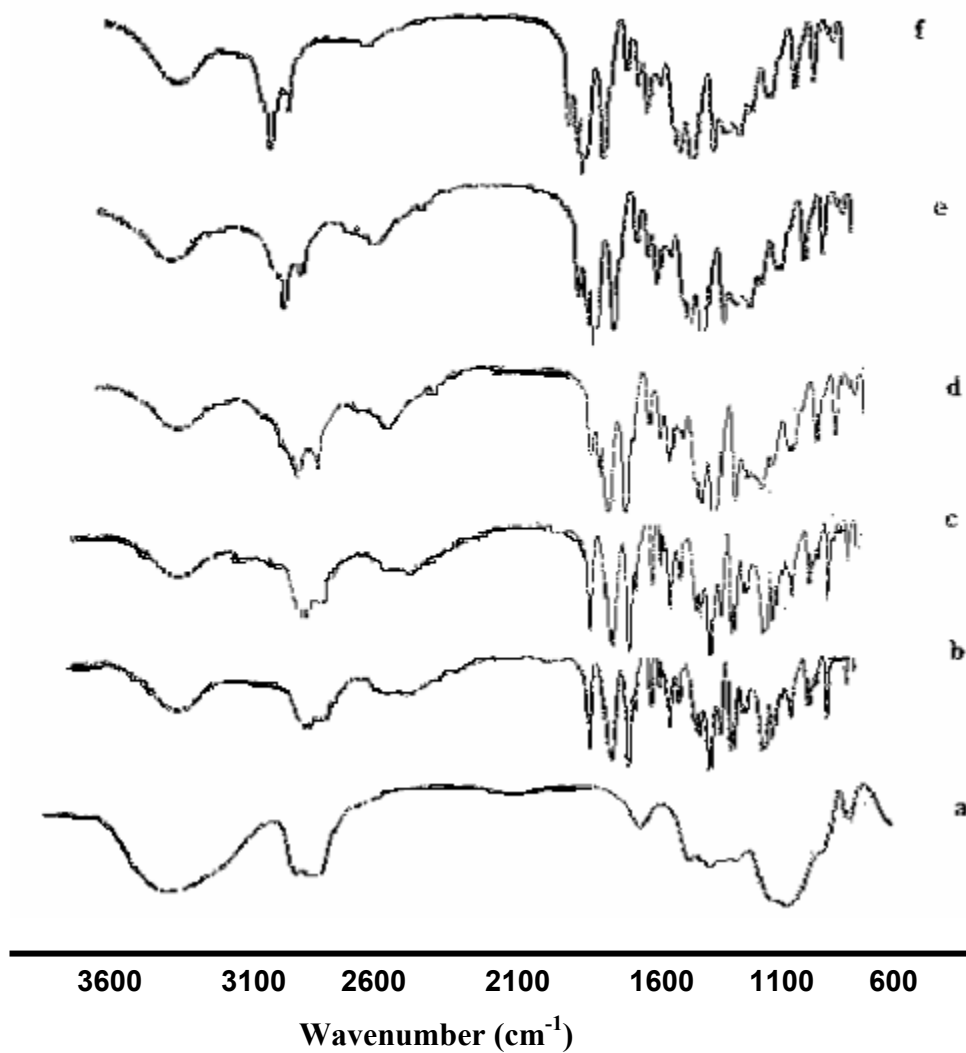


Figure (19, A): FTIR of a) HPC, b) ABPC-1, c) ABPC-2, d) ABPC-3, e) ABPC-4 and f) ABPC-7.

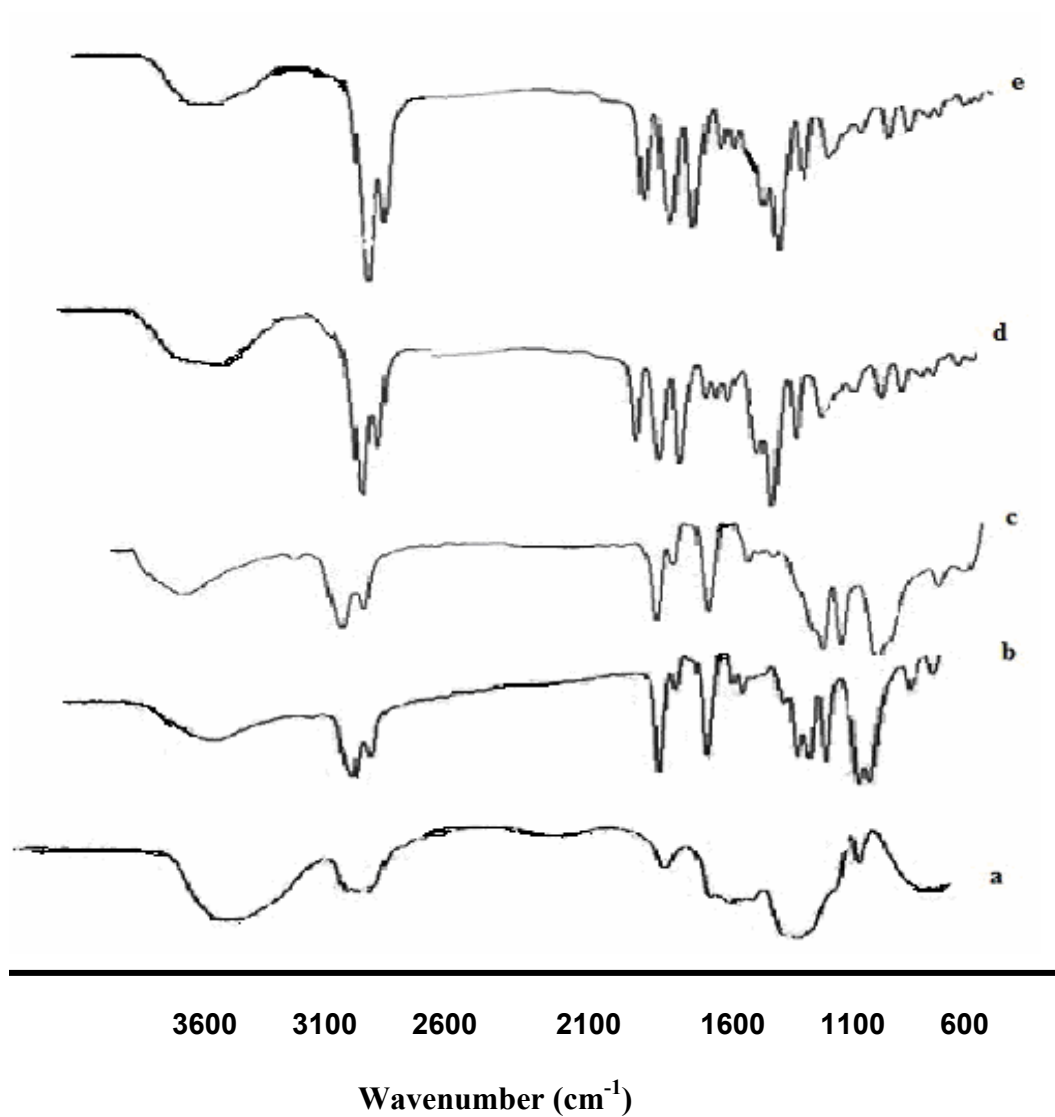


Figure (19, B): FTIR of a) HPC, b) ABPC-8, c) ABPC-10, d) ABPC-12 and e) ABPC-14.



Figure 21 (A) represents the  $^1\text{H}$  NMR spectra of HPC, ABPC-1, ABPC-2, ABPC-3, ABPC-4 and ABPC-7. Figure 21 (B) represents the  $^1\text{H}$  NMR spectra of HPC, ABPC-8, ABPC-10, ABPC-12 and ABPC-14. All the data of  $^1\text{H}$  NMR spectra are tabulated in Table 13.

For the HPC spectrum, the signals of the proton of the terminal methyl group were detected at 1.2 ppm and all the other protons in anhydroglucose unit were merged in the broad multiplets from 3.1 to 4.2 ppm. After derivatization of the HPC with different 4-alkoxybenzoic acids, the spectra of the derivatives exhibited common signals at 7.96 and 6.98 ppm for the aromatic protons, and in the of range 3.98-4.05 ppm for the methylene protons  $\text{O}-\underline{\text{CH}_2}-(\text{CH}_2)_{n-2}\text{CH}_3$ . The signals of methylene protons, denoted in the Table 13 and Figure 20 as (n-2), appear in the range 1.3-1.75 ppm. The terminal  $-\text{CH}_3$  appear at 3.24 for ABPC-2. The signal is shifted to lower absorption as alkoxy chain length increases and reaches to 0.87 ppm for ABPC-14.

The spectra were also used to determine the DS for substituted samples by the method described by Ritcey et al. 1988, and the results are collected in Table 14.

Table (13):  $^1\text{H}$  NMR data for ABPC-*n*.

Atom	$\delta$ (ppm)									
	HPC	n=1	n=2	n=3	n=4	n=7	n=8	n=10	n=12	n=14
11	-	7.95	7.961	7.963	7.963	7.964	7.964	7.964	7.966	7.96
10	-	6.981	6.982	6.983	6.985	6.985	6.984	6.986	6.991	6.992
8	3.72	5.21	5.21	5.20	5.192	5.191	5.190	5.190	5.185	5.182
1	5.56	5.025	5.02	5.02	5.021	5.02	5.02	5.020	5.020	5.021
2	4.2-3.1	4,5 -3,3	4,5 -3,3	4,5 -3,3	4,5 -3,3	4,5 -3,3	4,5 -3,3	4,5 -3,3	4,5 -3,3	4,5 -3,3
3										
4										
5										
6										
12	-	-	3.98	3.98	3.94	4.050	4.051	4.051	4.052	4.053
7	3.64	3.83	3.83	3.84	3.845	3.85	3.85	3.850	3.850	3.85
9	1.21	1.300	1.300	1.300	1.300	1.300	1.300	1.300	1.300	1.300
n-2	-	-	-	1.75	1.75-1.33	1.75-1.33	1.75-1.33	1,78 -1,33	1,78 - 1,31	1.78-1.31
13	-	3.240	1.330	1.060	0.960	0.910	0.880	0.865	0.866	0.868



Figure (21, A):  $^1\text{H}$  NMR spectra of HPC, ABPC-1, ABPC-2, ABPC-3, ABPC-4 and ABPC-7.

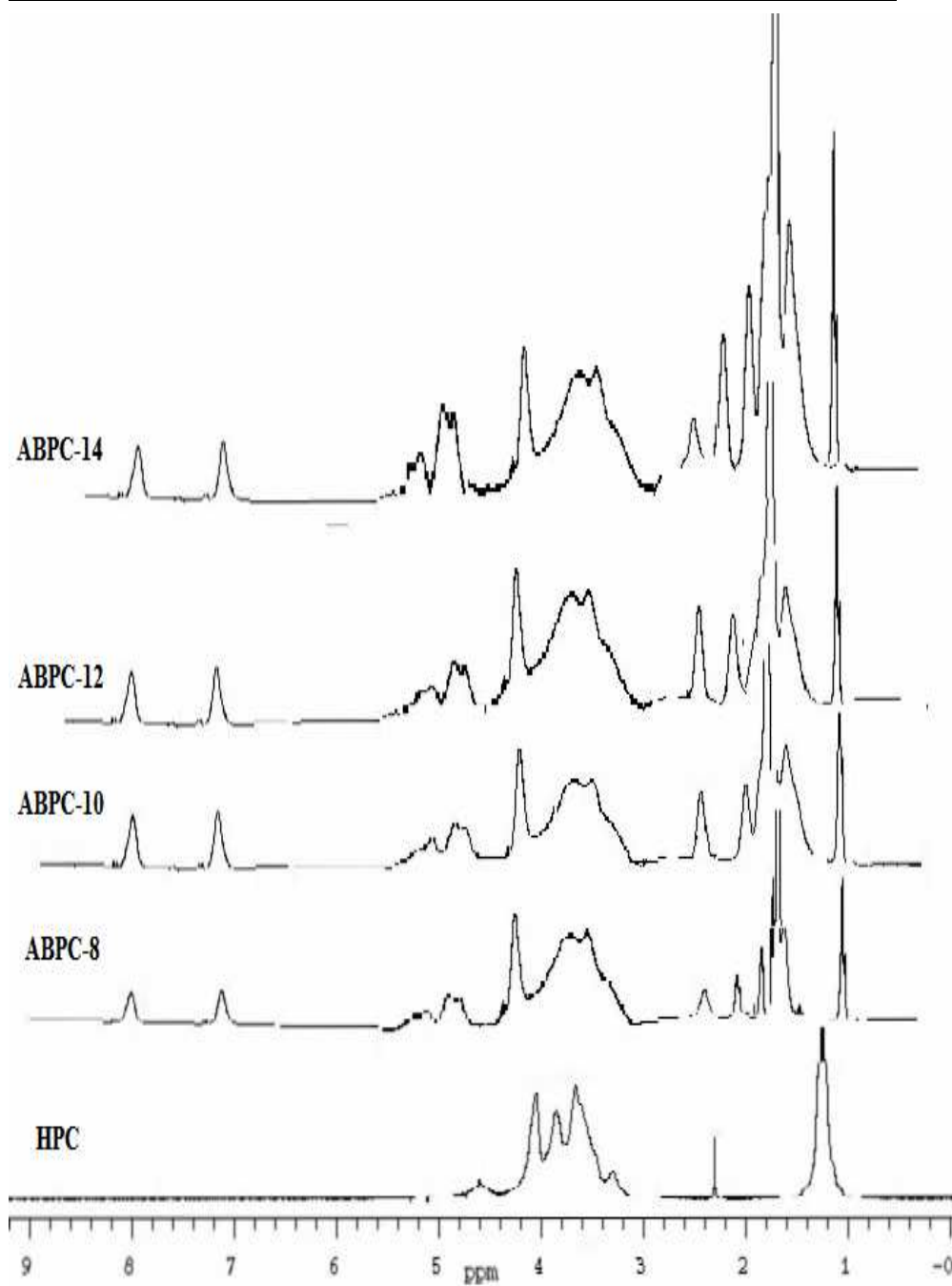


Figure (21, B):  $^1\text{H}$  NMR spectra of HPC, ABPC-8, ABPC-10, ABPC-12, and ABPC-14.

### 3.3.2. Phase behavior of ABPC-*n*.

Figure 22 shows the DSC heating thermograms for ABPC-*n* series. Melting ( $T_m$ ), glass transition ( $T_g$ ), and clearing ( $T_c$ ) temperatures and their corresponding enthalpies ( $\Delta H$ ) are listed in Table 14. The  $T_g$  of HPC was found to be 15°C. Upon heating HPC becomes soft and then melts leading to the formation of a mesophase at approximately 130°C and becomes isotropic at about 195°C. These results are in accordance with Charlet et al. (1987) and Rutt *et al.* (1991). As can be seen from Table 14, modification of HPC by 4-alkoxybenzoic acid led to variation in all transition temperatures ( $T_m$ ,  $T_c$ , and  $T_g$ ). The  $T_g$  values of ABPC-*n* were found to decrease as the length of alkoxy chain increased. A pronounced decrease in  $T_g$  was observed on increasing the number of methylene units in the alkoxy side chain whereas a slight decrease was observed on the substitutions of HPC with alkoxy groups bearing 8, 10, 12 and 14. Also this decrease is observed for  $T_m$  and  $T_c$  for all the derivatives.

$T_c - T_g$  of the LC phase becomes narrower with an increase in the alkoxy chain length. The same observation was found in the mesomorphic range ( $T_c - T_m$ ) where this range decreases on increasing the alkoxy chain length. The prepared derivatives were white sticky and were found to be soluble in THF, DMA, and DMSO. Based on all the previously mentioned changes upon

derivatization it can be concluded that not only the backbones but also the side chains are involved in the formation and modification of the LC phases and their transitions and this indicates that esterification of HPC with alkoxy benzoic acid may improve the processability of the final product. These observations of the thermal properties of ABPC-*n* indicate that the methylene units in the side chains not only serve as “diluent” but are also involved in these phase transitions by providing contributions to the enthalpy of LC-isotropic transitions (Huang *et al.* 2007).

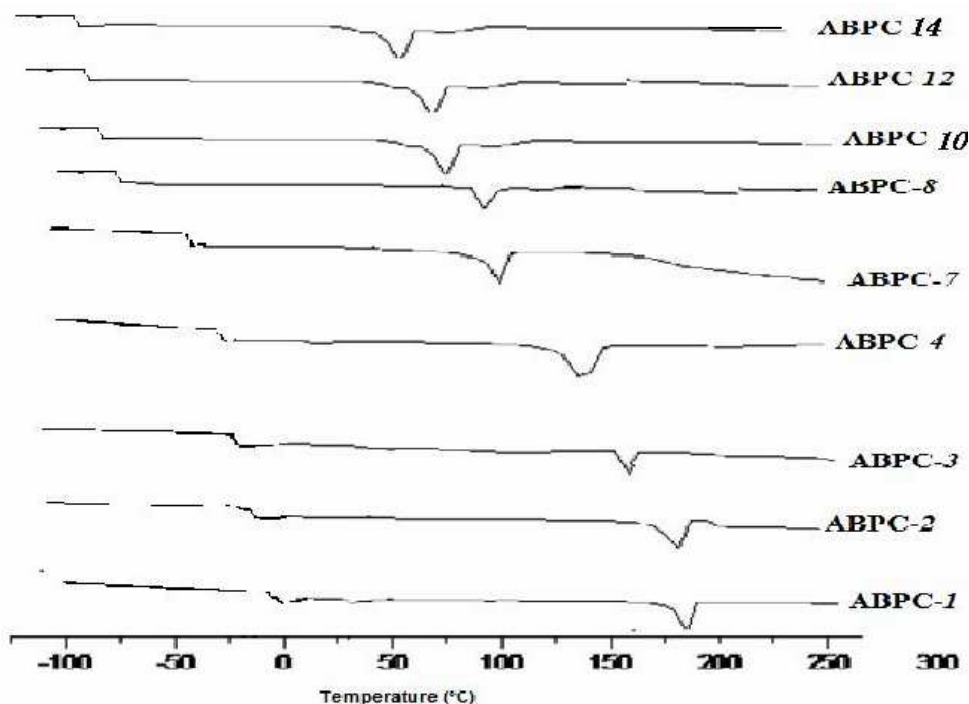


Figure (22): DSC heating curves of ABPC-*n*.

Table (14): Thermal Properties ABPC-*n*.

ABPC- <i>n</i>	DS	$T_g$ (°C)	$T_m$ (°C)	$\Delta H_m$ (J/g)	$T_c$ (°C)	$\Delta H_c$ (J/g)	$\Delta T$ (°C) $T_c - T_m$	$\Delta T$ (°C) $T_c - T_g$
ABPC-1	2.4	-1	182	184.7	-	-	-	-
ABPC-2	2.3	-13	178	131.1	-	-	-	-
ABPC-3	2.3	-16	155	118.1	-	-	-	-
ABPC-4	2.0	-29	147	112.0	-	-	-	-
ABPC-7	2.1	-40	101	109.1	152	6.2	51	112
ABPC-8	2.0	-70	100	89.0	149	6.6	49	79
ABPC-10	2.0	-70	90	86.6	120	5.2	30	50
ABPC-12	2.0	-70	72	78.8	100	2.8	28	30
ABPC-14	1.6	-75	62	70.5	100	2.6	25	12

Figure 23 represents the heating and cooling cycles of the DSC thermograms for the derivatives ABPC-1, 2, 3 and 4 the figure shows, for each derivative, an endothermic and an exothermic peaks during heating and cooling cycles, respectively. Direct melting of the solid phase to isotropic liquid phase at 182 °C, 178 °C, 155 °C and 174 °C respectively. Vice versa was therefore observed on cooling. Under polarized optical microscope (PLM), crystal changed to dark region isotropic during heating run. These observations indicate non-mesogenic character of these derivatives. On the other hand, the derivatives ABPC-7, 8, 10, 12 and 14 exhibited LC phase on heating, while upon cooling additional phases are observed before recrystallization and after the formation of LC phase as well be discussed in details in section 3.3.3. Conversely ABPC-8 shows only one phase upon cooling before recrystallization.

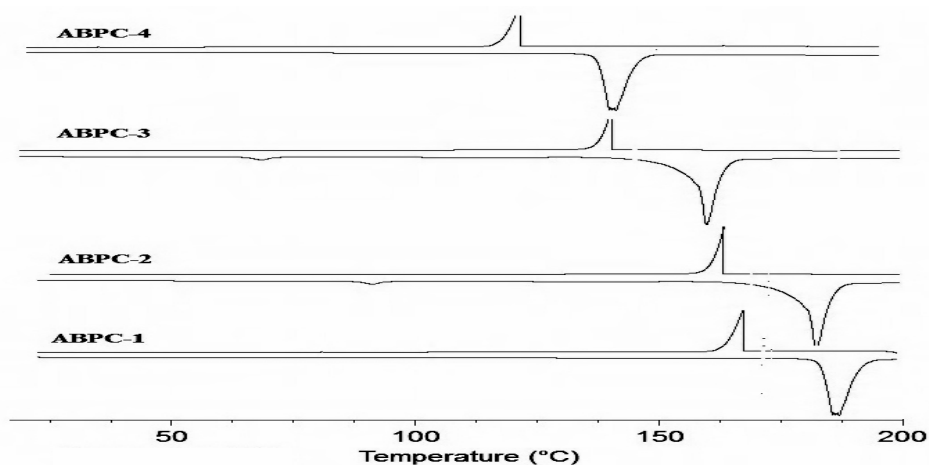


Figure (23): DSC thermograms of ABPC-1, 2, 3 and 4 on heating and cooling.

### 3.3.3. Thermotropic liquid crystalline behavior of higher ABPC-*n* derivatives.

DSC heating and cooling cycles and PLM textures of the higher derivatives (ABPC-7, 8, 10, 12 and 14) are illustrated in Figures 24, 25, 26, 27 and 28, respectively.

Figure 24 illustrates the DSC heating and cooling cycles of the sample ABPC-7 and its corresponding morphologies upon heating and cooling. The endothermic peak appeared at 101 °C, corresponding to the melting point, and is attributed to the change from the crystal structure to droplet nematic phase (Figure 24 (a)). The calculated enthalpy was 65.5 J/g. and the mesomorphic range ( $T_c$ - $T_m$ ) of nematic phase is about 49 °C. The nematic phase loses its birefringence and was transformed to an isotropic phase starting at 150 °C. On cooling, the thermogram showed that the droplet nematic phase (Figure 24 (b)) grew from the isotropic one in a broad range from 140 °C to 90 °C, when the temperature was reduced to 90 °C, the mesophase changed to the smectic phase (Figure 24 (c)) in a narrow range and the crystallization transition starts at 70 °C.

The DSC heating and cooling scans and the morphologies of ABPC-8 are presented in Figure 25. The endotherm at 100 °C, with an enthalpy of 38.3 J/g, is considered to be due to the change from crystallized form to droplet nematic phase, as the textures are displayed in Figure 25 (a) and the mesomorphic range is 50

°C. On cooling, the thermogram showed one transition phase (nematic) in a broad range (Figure 25 (b)) that started at 125 °C, and solidified at 40 °C.

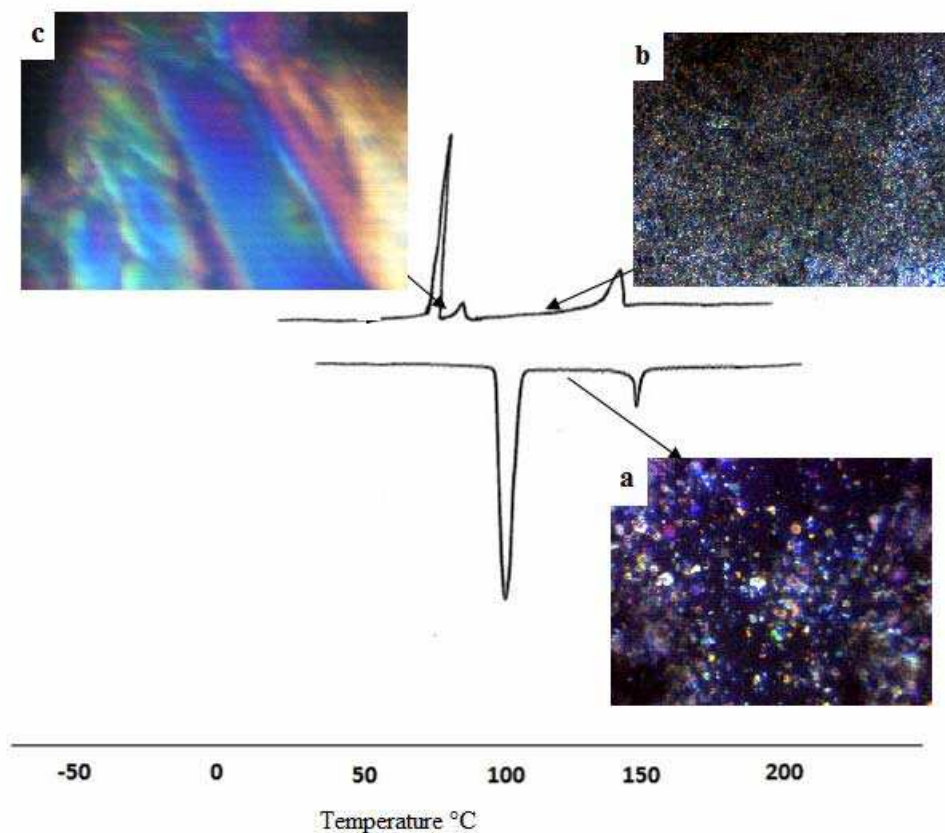


Figure (24): DSC thermograms and the observed PLM images for ABPC-7 on heating; a) 120 °C and on cooling b) 120 °C and c) 80.0 °C.

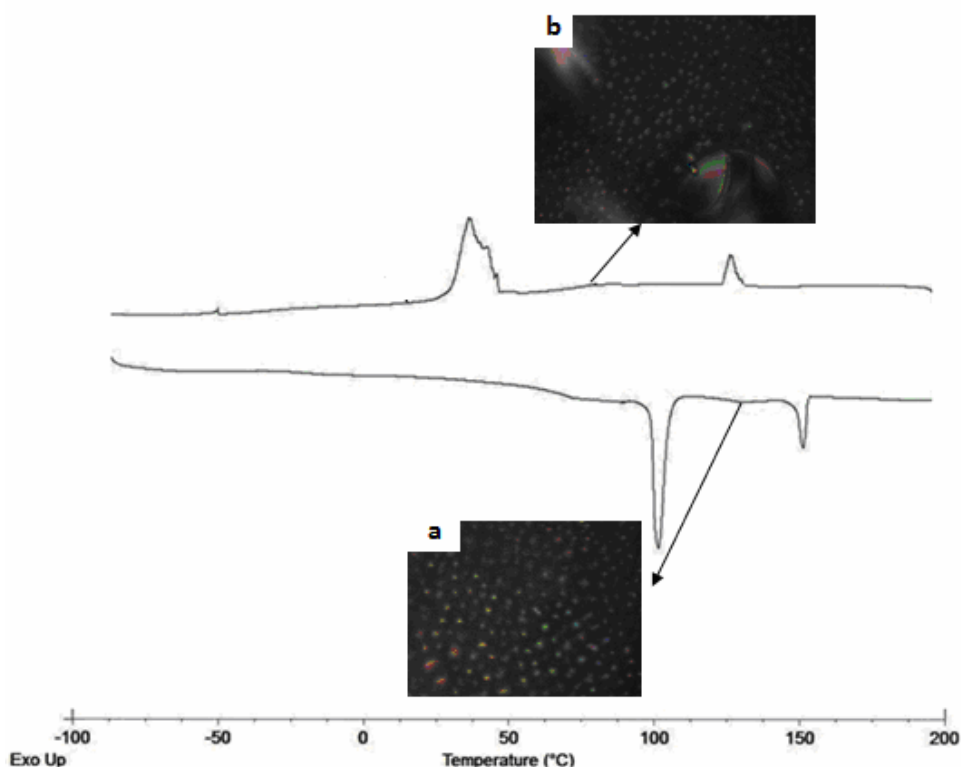


Figure (25): DSC thermograms and the observed PLM images for ABPC-8 on heating; a) 120 °C and on cooling b) 90.0 °C.

Figure 26 presents the DSC curves and the corresponding morphologies of ABPC-10 during heating and cooling. By increasing temperature to 90 °C an endothermic peak with enthalpy of 88.6 J/g appeared and a nematic mesophase, having a range of 40 °C (Figure 26 (a)), was observed before disordering and transferring to the isotropic phase at 130 °C ( $\Delta H = 5.2$  J/g).

On cooling, the thermogram showed the thread-like nematic texture (Figure 26 (b)) that started at 125.5°C, and

transformed to smectic phase (Figure 26 (c)) at 95 °C, and finally solidified at 60 °C.

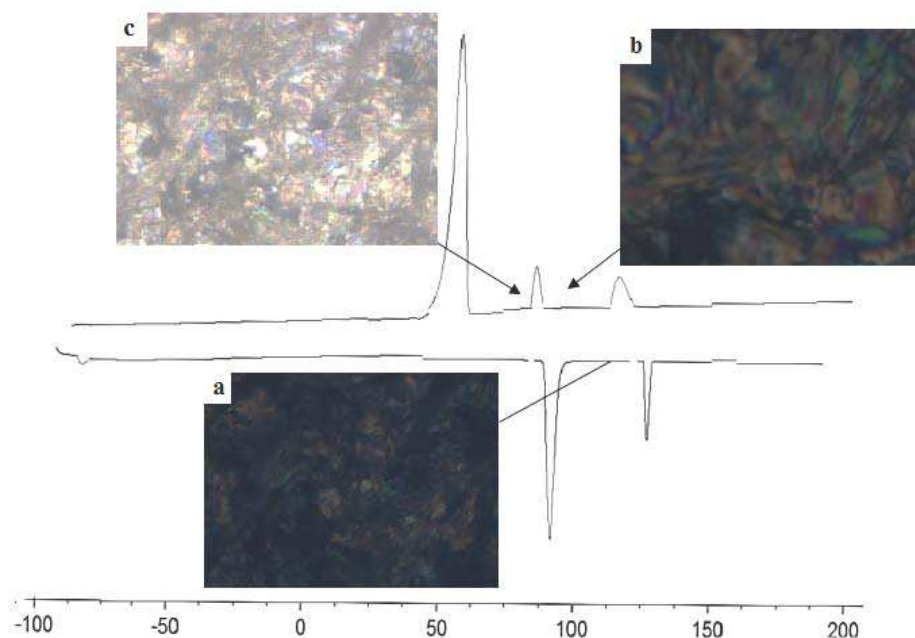


Figure (26): DSC thermograms and the observed PLM images for ABPC-10 on heating; a) 120.0 °C, and on cooling b) 110.0 °C, and c) 80.0 °C.

Figure 27 illustrates the DSC heating and cooling cycles of the sample ABPC-12, and their corresponding PLM images. The endothermic peak appearing at 56.7 °C during the heating cycle is attributed to a transition between two solid transformations, since both phases below and above this temperature are solids. The droplet nematic phase (Figure 27 (a)) appeared on heating in the mesomorphic range from 72 °C to 100 °C and then transformed to isotropic phase. On cooling, the thermogram showed the isotropic-smectic and smectic-smectic phase transformations, in

the ranges from 97.9 °C to 71.7 °C and 71.7 °C to 42.4 °C, respectively before solidification.

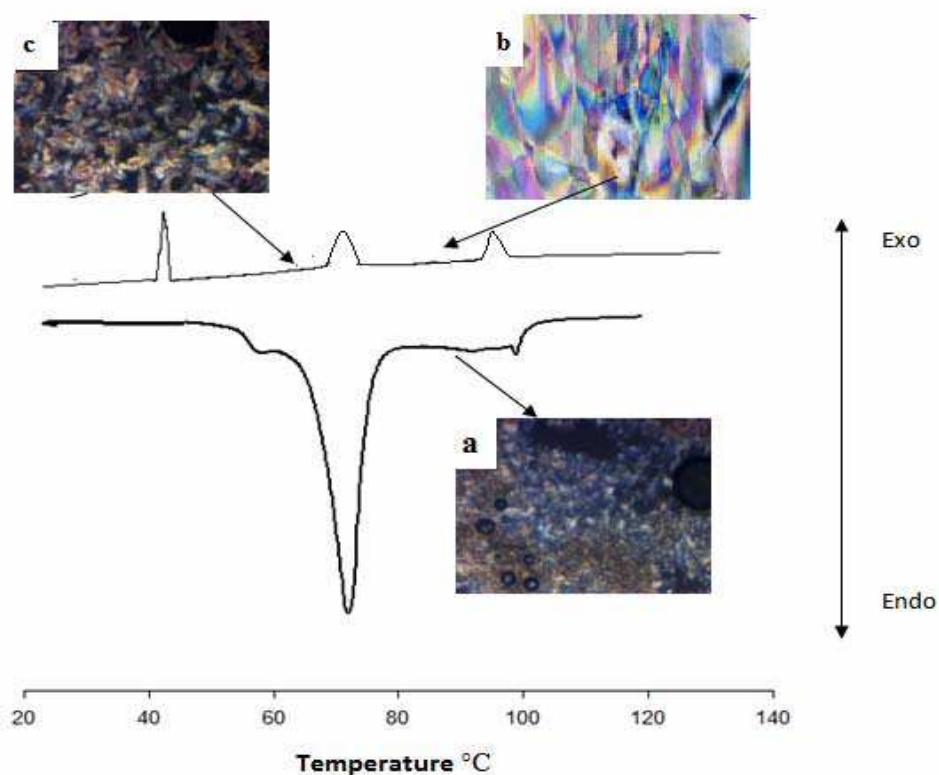


Figure (27): DSC thermograms and the observed PLM images for ABPC-12 on heating; a) 85.0 °C, and on cooling b) 85.0 °C and c) 65.0 °C.

Figure 28 shows the phase transformation of ABPC-14 and its corresponding morphologies (PLM images) upon heating and cooling. The endothermic peak at 62 °C (70.5 J/g) is attributed to the change of solid crystalline state to schlieren nematic phase as

shown in Figure 28 (a) and the mesomorphic range is 38°C from 62 °C to 100°C. On cooling, the transformation from isotropic to thread-like nematic transition appeared at 99.0 °C (Figure 28 (b)) in a narrow range (9 °C) followed by the smectic phase at 90.3 °C (Figure 28 (c)). The enthalpy of isotropic-nematic transition was 4.3 J/g and the nematic-smectic was 2.1 J/g.

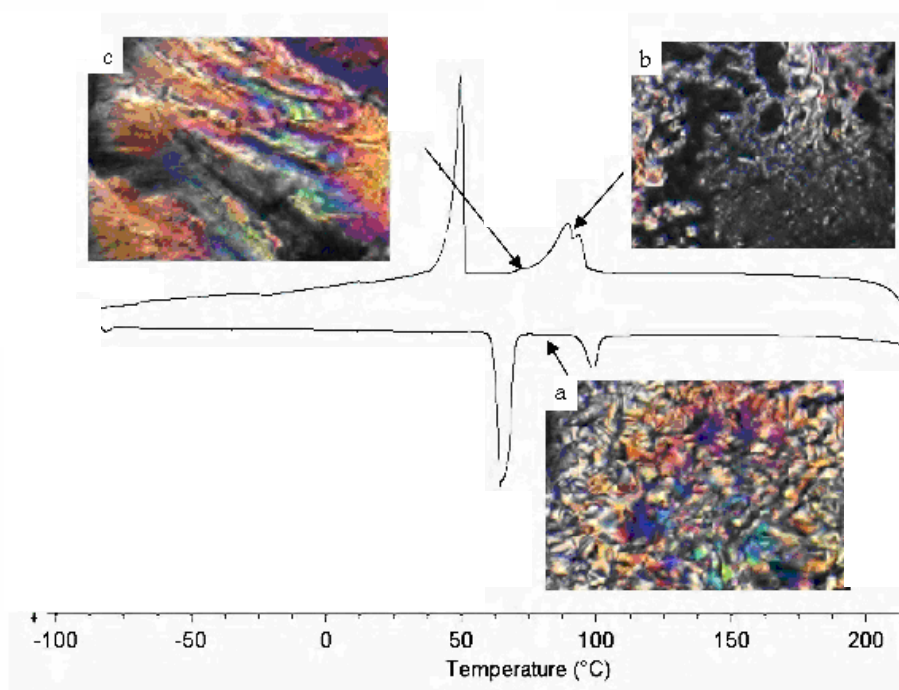


Figure (28): DSC thermograms and the observed PLM images for ABPC-14 on heating; a) 70.0 °C, and on cooling b) 90.0 °C and c) 60.0 °C.

From the previous results, we can observed that all the ester derivatives showed one phase upon heating and two phases upon cooling, respectively, except ABPC-8 where a remarkable

characteristics was observed. Upon cooling the transformation from the isotropic to the crystalline solid was performed through one phase.

#### **3.3.4. Lyotropic liquid crystalline properties of ABPC-*n*.**

Many studies have been conducted on the lyotropic behavior of HPC and its derivatives (Werboj and Gray 1976; Huang *et al.* 2007) and showed that HPC and most of its derivatives form cholesteric liquid crystal solutions when dissolved in various organic solvents, as disclosed first by Werboj and Gray (1976). In this study the textures and birefringence of HPC and its derivatives (ABPC-*n*) in DMA solutions were observed using PLM and refractometer.

##### **- Determination of critical concentration.**

The critical concentration (C.C.) is the most important characteristic of lyotropic liquid crystalline materials. The C.C. was estimated by measuring the refractive indices (*n*) of HPC and ABPC-*n* solutions in DMA with several concentrations (20, 30, 40, 50 and 60 wt %). The C.C. can be determined by plotting the mean refractive index versus concentration as shown in Figures 29.

It is known that the solution is isotropic below the critical concentration and anisotropic above that concentration. A strong birefringence starts to appear at this concentration. The results showed that the C.Cs. were found to be close to each other in the

range from 42 % to 46 %. This birefringence is confirmed by PLM images, 60 wt % for the derivatives bearing even number of carbon atoms in the side chain. Figure 30 shows the lyotropic textures of ABPC-n solutions in DMA at 60 wt %. Among the examined concentrations, it was found that solutions of concentrations lower than the critical one is isotropic whereas solutions of higher concentrations than the critical one possess liquid crystalline properties, i.e. the mesophase begins to appear.

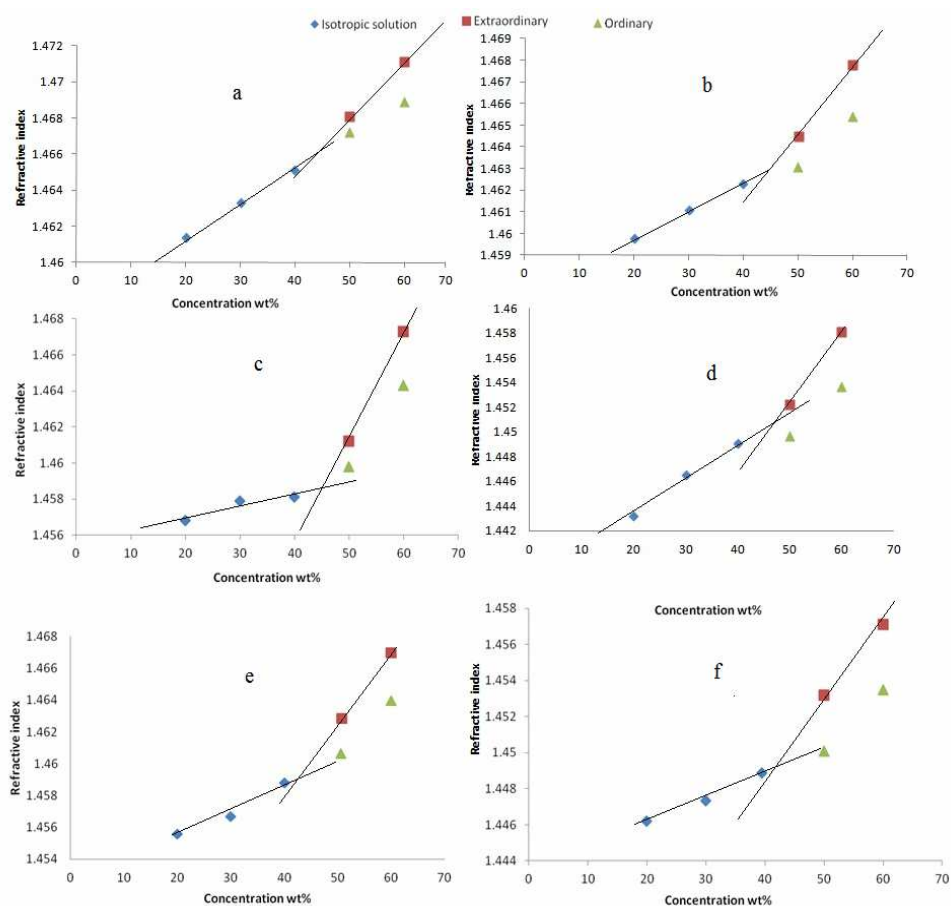


Figure (29): Plot of the mean refractive index vs. concentration for a) ABPC-2, b) ABPC-4, c) ABPC-8, d) ABPC-10, e) ABPC-12 and f) ABPC-14.

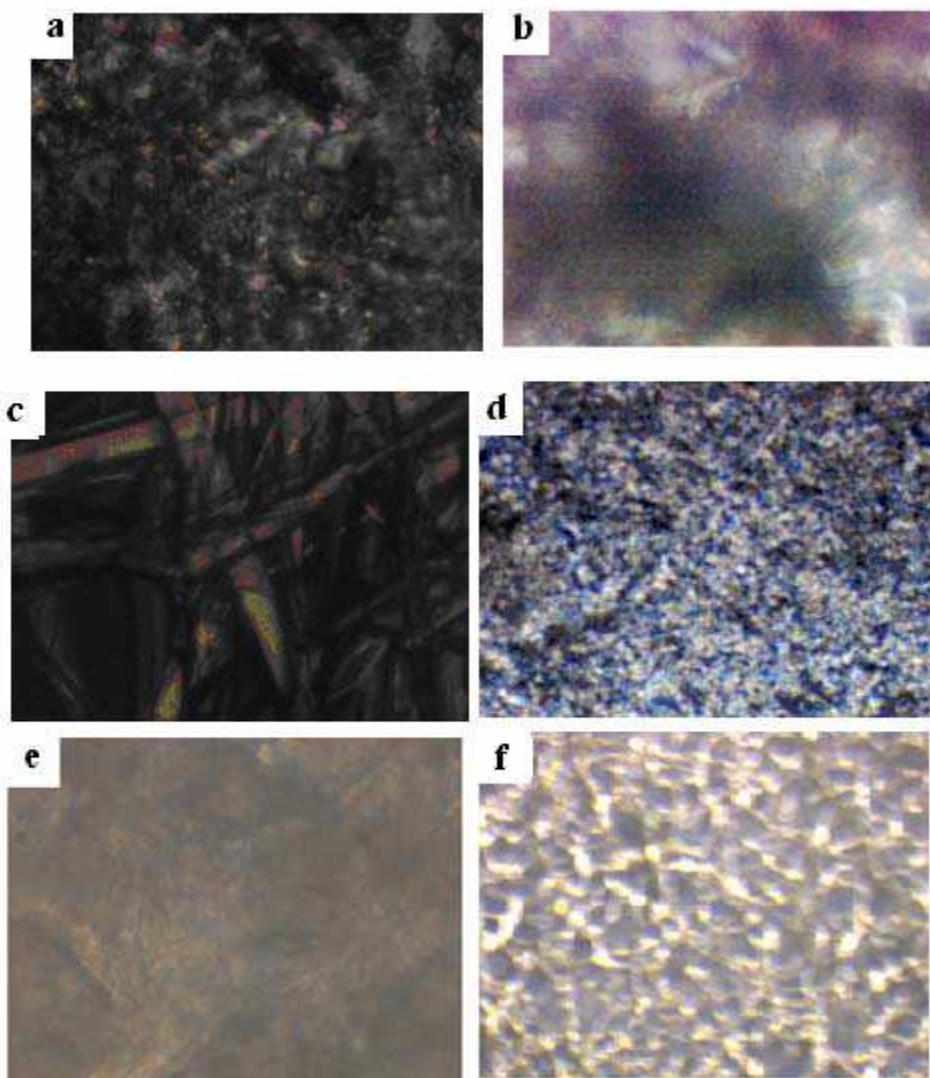


Figure (30): PLM images of a) ABPC-2, b) ABPC-4, c) ABPC-8, d) ABPC-10, e) ABPC-12 and f) ABPC-14 in 60 wt % DMA at room temperature.

Table 15 presents the extraordinary refractive index ( $n_e$ ), ordinary refractive index ( $n_o$ ), birefringence ( $\Delta n = n_e - n_o$ ), average refractive index ( $n$ ), and the critical concentration. Figure 31 illustrates the dependence of birefringence ( $\Delta n$ ) on chain length. From the Figure and Table, one can observe that on increasing the length of alkoxy group, the birefringence of ABPC- $n$  decreases and the average refractive index is independent on the chain length. It is notable that the derivatives with alkoxy group of odd number carbon atoms (ABPC-1, 3, and 7) do not show birefringence thus obeying the odd-even effect and hence are not included in the figure and table. This phenomenon was previously studied by Mali 2010 who stated the same conclusion.

Also, the results show that increasing the alkoxy chain length results in decreasing the C. C. Steric hindrance makes the macromolecular chain more unfolded and rigid in solution; hence, it can form liquid crystals more easily (Caiqi *et al.* 2003).

Table (15): Optical Properties of ABPC-*n* (values calculated for solutions of 60 wt %).

ABPC- <i>n</i>	$n_e$	$n_o$	Birefringence $\Delta n \times 10^3$	$N$	Critical Conc. (wt %)
HPC	1.4585	1.4524	6.1	1.4565	46
ABPC-2	1.4524	1.44329	9.11	1.4494	44
ABPC-4	1.4651	1.4579	7.2	1.4627	44
ABPC-8	1.4598	1.4557	4.1	1.4584	43
ABPC-10	1.4671	1.4641	3	1.4653	43
ABPC-12	1.4531	1.4509	2.2	1.4524	42
ABPC-14	1.4577	1.4562	1.5	1.4567	42

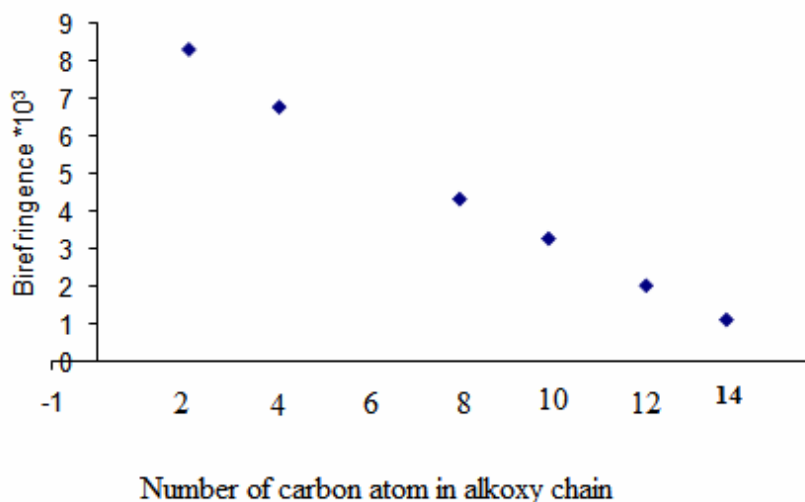


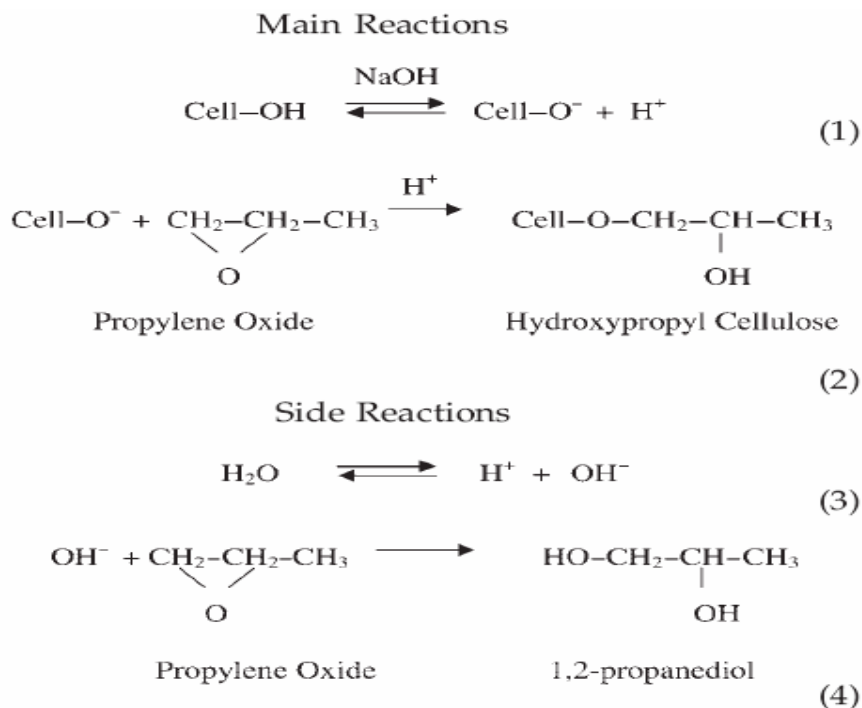
Figure (31): Dependence of the birefringence on the number of the methylene groups of ABPC-*n*.

### 3.4. Hydroxypropylation of dissolving bagasse pulp.

It is known that the degree of substitution of cellulose and its derivatives plays an important role in determining the structure-property behavior. In the previous part, the LC behavior of the esters bearing different numbers of carbon atoms in the side chain prepared by derivatization of fully substituted HPC was reported. Selected alkoxybenzoic acids in the previous part were chosen to esterify the partially substituted HPC and their properties are compared with their analogues having different DSs.

Heterogeneous etherification of dissolving bagasse pulp with propylene oxide was performed. HPC with DS 1.87 was

obtained. An illustrative scheme of this reaction is presented in scheme 2 (Ritu *et al.* 2009).



Scheme 2: Hydroxypropylation of cellulose and the side reactions.

### 3.4.1. FT-IR spectra of bagasse pulp and derivatized product.

The FT-IR spectra of the dissolving bagasse pulp (cellulose) and the HPC<sub>B</sub> (prepared from dissolving pulp) are shown in Figure 32 (A and B respectively). The spectra showed the typical absorption bands of cellulose backbone ( $\nu_{\text{OH}}$  3390  $\text{cm}^{-1}$ ,  $\nu_{\text{CH}}$  2892  $\text{cm}^{-1}$ , and 1420  $\text{cm}^{-1}$ , and  $\nu_{\text{COC}}$  1070  $\text{cm}^{-1}$  (Bellamy, 1975; Klemm *et al.* 1998). HPC<sub>B</sub> showed the same characteristics bands of cellulose in addition to the double absorption bands in

the range between 2800 and 3000  $\text{cm}^{-1}$  assigned for the -CH stretching vibration of the methylene groups of HPC.

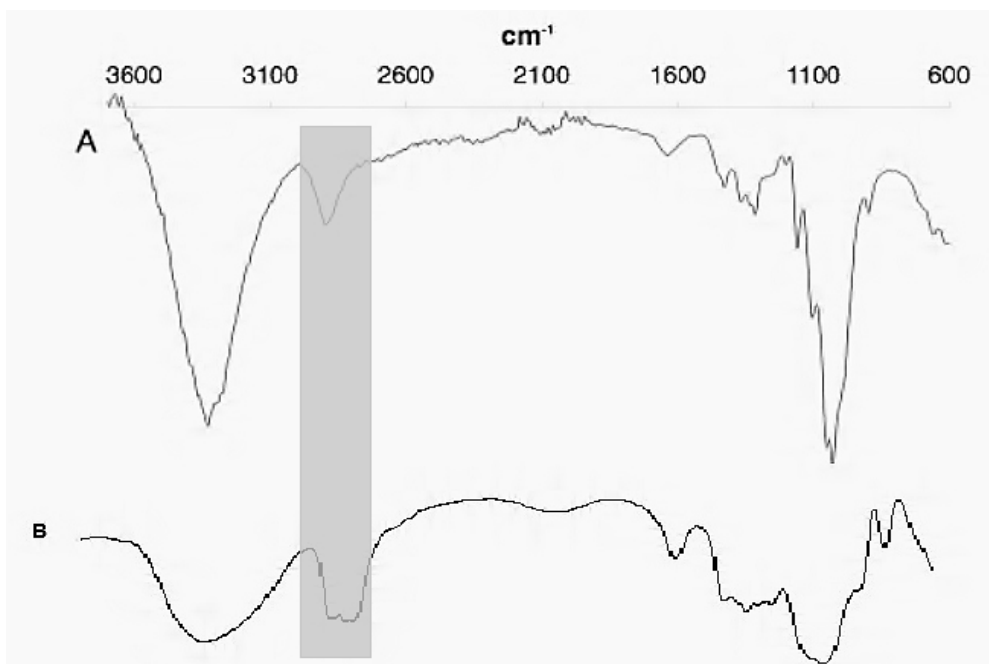


Figure (32): FTIR spectra of (A) bagasse pulp (cellulose) and (B) its hydroxypropyl derivative ( $\text{HPC}_B$ ).

### 3.4.2. $^1\text{H}$ NMR analysis.

Figure 33 shows a typical  $^1\text{H}$  NMR spectrum of  $\text{HPC}_B$  in which a strong peak at 1.0 ppm is assigned to the methyl protons, whereas the broad peak in the range 2.8 to 4.7 ppm is due to the protons of glucose units.  $^1\text{H}$  NMR spectroscopy was employed for determination of the DS of  $\text{HPC}_B$  (Ritcey *et al.* 1988). The DS was calculated and found to be 1.87.

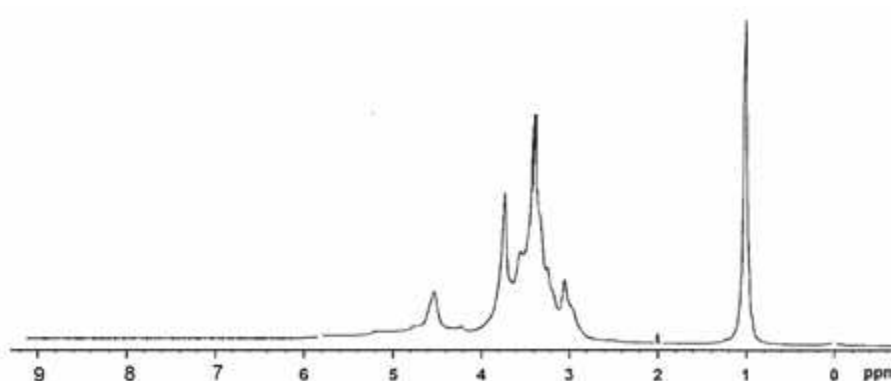


Figure (33):  $^1\text{H}$  NMR spectra of  $\text{HPC}_B$ .

### 3.4.3. Thermal characterization of $\text{HPC}_B$ .

DSC curves (heating and cooling) for  $\text{HPC}_B$  are shown in Figure 34. The thermogram of HPC reveals that glass transition temperature is at 25 °C and mesophase formation at 145 °C. On heating, the endothermic peak is detected at 220 °C (7.6 J/g) corresponds to the transition from the cholestric liquid crystal phase to the isotropic phase. On cooling, a small endothermic peak at 208 °C (3.6 J/g) corresponds to the transition from the isotropic phase to the liquid crystalline phase. Figure 34 (a) shows the typical PLM photomicrograph of the  $\text{HPC}_B$  at 180 °C.

The fully substituted HPC reveals the  $T_g$  and  $T_c$  are at 15 °C and 195 °C, respectively. One can deduce that the  $T_g$  decreases with increasing the hydroxypropyl content, i. e. introducing hydroxypropyl groups may reduce the interactions of the unsubstituted hydroxyls of the cellulose chain to the extent that

the polymer becomes much more amorphous, thus lowering  $T_g$ . This explains the different behavior of the samples with different degrees of substitution,  $HPC_B$  with a smaller number of hydroxypropyl groups have higher  $T_g$  and thermal stability than  $HPC_P$  (with higher DS) (Kararli *et al.* 1990).

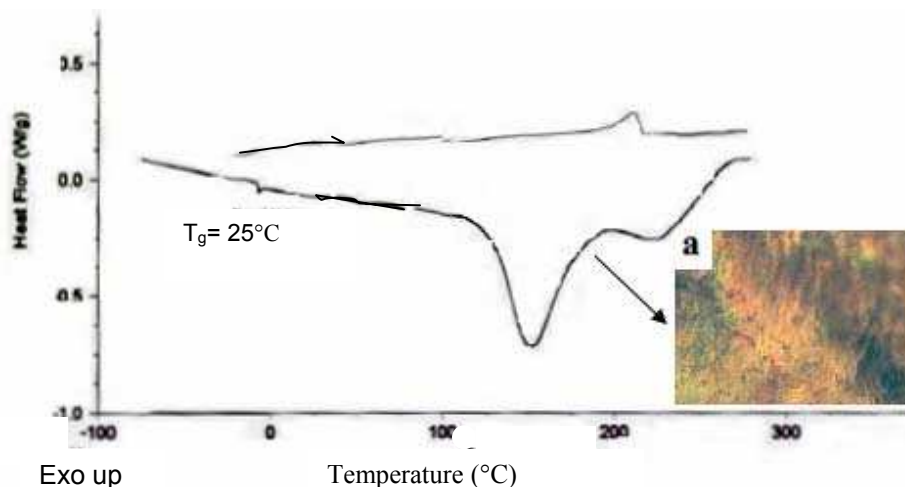


Figure (34): DSC heating/cooling curves of  $HPC_B$ , and PLM image (a) of  $HPC_B$  at 180°C.

#### 3.4.4. The Lyotropic liquid crystal phase of $HPC_B$ .

PLM was used to characterize the liquid crystal phase of the  $HPC_B$ . The birefringence was studied for  $HPC_B$  solutions (20, 30, 40, 50, and 60 wt %) in DMA. The C. C. was estimated from the refractive indices of solutions in DMA, and determined from the plot of the refractive index versus concentration (see Figure 41). It was found to be 48 wt %, whereas it was 46 for the HPC of DS 3.

Figure 35 shows the texture obtained from HPC<sub>B</sub> solutions in DMA with 60 wt % concentration. The solution shows strong birefringence and iridescent color which is typical for cholestric liquid crystals. The picture taken for a 50 wt % solution also shows birefringence.

In related study reported by Dong *et al.* (1996), it was stated that an inverse relation between the solubility and C. C. was found where the high solubility leads to formation of mesophase at lower C.C. while relatively lower solubility leads to the formation of the mesophase at higher C.C.



Figure (35): PLM image of HPC<sub>B</sub> solution in DMSO (60 wt %) at room temperature.

### 3.5. Characterization of n-alkoxybenzoyloxypropyl cellulose (ABPC-*m*).

The FT-IR and  $^1\text{H}$  NMR spectroscopies were used to confirm the structure of the synthesized compounds. FT-IR spectra of modified  $\text{HPC}_\text{B}$  are shown in Figure 36 (b, c and d). The unmodified HPC shows a broad peak from 3100-3600 due to -OH stretching vibrations. The remaining peaks in the spectra at around  $3400\text{ cm}^{-1}$ , were attributed to stretching vibrations of the associated -OH groups, showing that the  $\text{HPC}_\text{B}$  was not completely substituted. Comparison between the FT-IR spectra of ABPC-*m* with that of unmodified HPC showed a new peak at around  $1750\text{ cm}^{-1}$ , which is assigned to the carbonyl groups. Also, the occurrence of new absorptions in the range of  $650\text{-}800\text{ cm}^{-1}$ , associated with bending vibrations of the aromatic ring (Ar) confirms the esterification reaction in ABPC-*m*. Moreover, the peaks observed at around  $1250\text{ cm}^{-1}$  are assigned to C-O stretching vibrations of the ester groups.

In the  $^1\text{H}$  NMR spectra of the synthesized derivatives (Figure 37 (b, c and d)), the common signals at around 6.9 and 7.9 ppm, due to aromatic protons, are detected for all ABPC-*m* derivatives. For ABPC-2 the resonance peak observed at 3.9 and 1.33 ppm are due to methylene and methyl groups in the alkoxy chain, respectively. ABPC- 10 and 12 showed similar absorption around 0.95 ppm for the terminal  $-\text{CH}_3$  groups whereas the

protons of the CH<sub>2</sub> groups in alkoxy chain appear at the range 1.1-1.8 ppm.

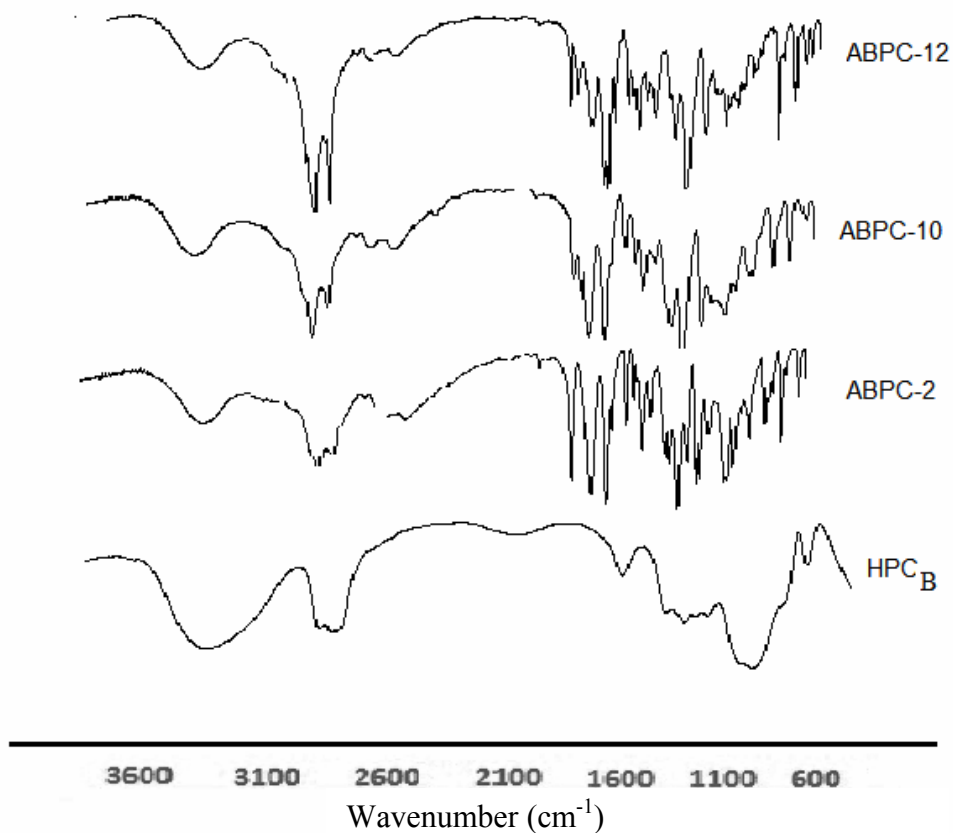


Figure (36): FTIR spectra of HPC, ABPC-2, ABPC-10 and ABPC-12.

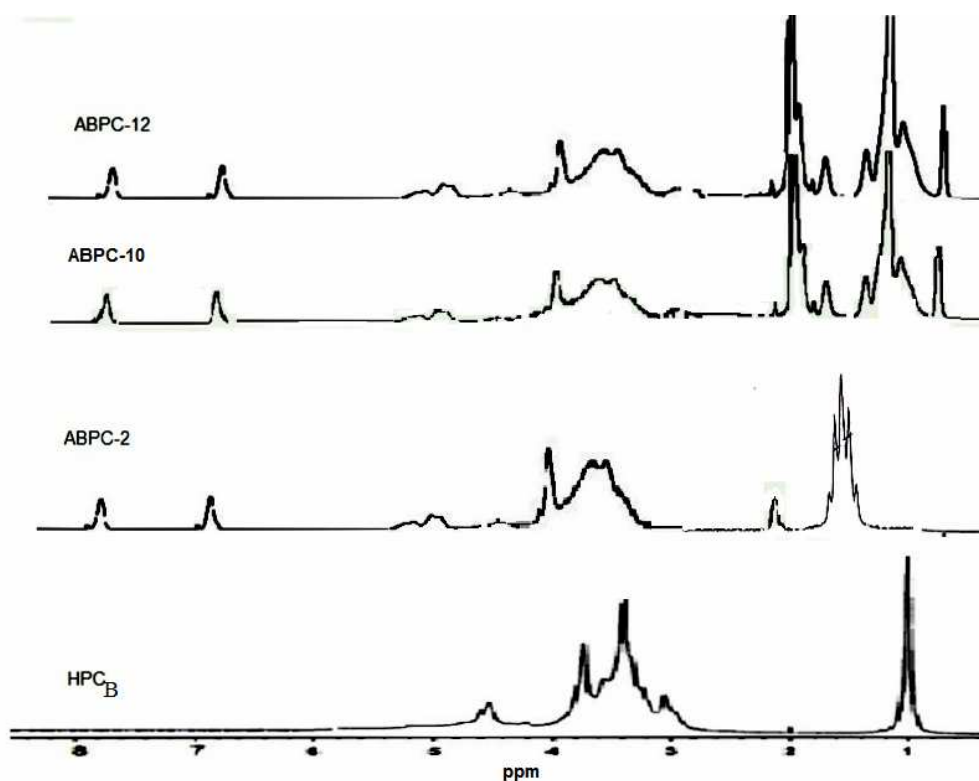


Figure (37):  $^1\text{H}$  NMR spectra of  $\text{HPC}_\text{B}$ , ABPC-2, ABPC-10 and ABPC-12.

### 3.5.1. Thermotropic phase behavior of n-alkoxybenzoyloxypropyl cellulose (ABPC-*m*).

Figure 38 illustrates the DSC curves of ABPC-2, ABPC-10 and ABPC-12 upon heating. The glass transition ( $T_g$ ), melting ( $T_m$ ), and clearing temperatures ( $T_c$ ) and their corresponding enthalpies ( $\Delta H$ ) are listed in Table 16.

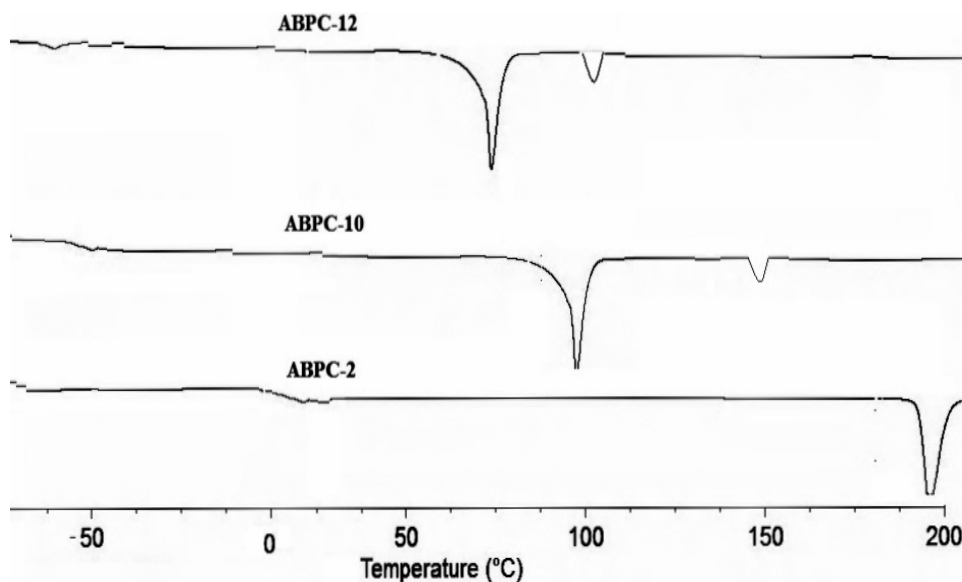


Figure (38): DSC heating curves of ABPC-2, ABPC-10 and ABPC-12

Increasing the length of the alkoxy chains results in a decrease in glass transition ( $T_g$ ), melting ( $T_m$ ), clearing temperatures ( $T_c$ ) and their corresponding enthalpies ( $\Delta H$ ). The mesomorphic range ( $T_c - T_m$ ) of the liquid crystal phase becomes narrower with an increase in the alkoxy chain length. Regarding all thermal parameters ( $T_g$ ,  $T_c$ , and  $T_c - T_m$ ), it is clearly predicted that not only the backbones but also the side chains are involved in the formation of the LC phases and phase transitions. The results showed that ABPC- 2 did not show any thermotropic mesophase. Nevertheless they still exhibit lyotropic LC. On the other hand, the samples ABPC-10 and 12 showed both lyotropic and thermotropic liquid crystal behavior, as detected by both DSC and the PLM.

Table (16): Thermal properties of ABPC-*m* (HPC<sub>B</sub> prepared from dissolving bagasse pulp).

Derivative	DS	T <sub>g</sub> (°C)	T <sub>m</sub> (°C)	ΔH <sub>m</sub> (J/g)	T <sub>c</sub> (°C)	ΔH <sub>c</sub> (J/g)	ΔT(°C) T <sub>c</sub> -T <sub>m</sub>
HPC <sub>B</sub>	1.87 <sup>a</sup>	25	145	162.6	220	3.2	75
ABPC-2	1.5 <sup>b</sup>	-5	190	166.7	-	-	-
ABPC-10	1.3 <sup>b</sup>	-51	95	115.3	150	7.6	55
ABPC-12	1.2 <sup>b</sup>	-62	75	92	110	4.5	35

<sup>a</sup> number of hydroxypropyl groups per anhydroglucose unit

<sup>b</sup> number of ester groups per hydroxyl propyl glucose unit

Figure 39 illustrates the DSC heating and cooling cycles of the sample ABPC-10 and its corresponding morphologies upon heating and cooling. The endothermic peak at 95 °C is attributed to the change of crystal structure from crystalline to nematic phase (Figure 39 (a)). The enthalpy calculated from this peak was 58.5 J.g<sup>-1</sup>. On further heating the nematic mesophases are transformed to the isotropic phase at 150 °C. On cooling, it can be seen that the nematic phase (Figure 39 (b)) grew from isotropic at 149 °C. The endothermic peak at 149 °C possess  $\Delta H = 6.4 \text{ Jg}^{-1}$ . Further cooling results in appearance of the smectic mesophases at 110 °C (Figure 39 (c)) with enthalpy 4.2 Jg<sup>-1</sup>. The change to crystalline phases on cooling was found to be at 40 °C.

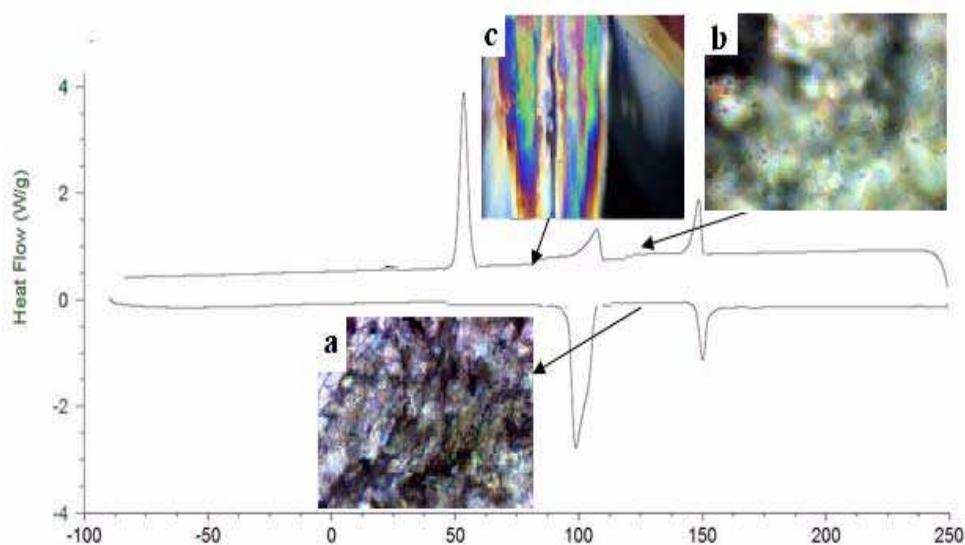


Figure (39): DSC thermograms and the observed PLM images for ABPC-10 on heating; a) 125.0 °C, and on cooling b) 120.0 °C and c) 75.0 °C.

Figure 40 presents the DSC curves and the corresponding morphologies for ABPC-12 during heating and cooling cycles. On heating, it could be seen that ABPC-12 showed a cholestric mesophase between 75 °C and 110 °C. An endothermic peak with enthalpy of 92 J/g, appeared and a cholestric mesophase (Figure 40 (a)) was observed before the phase is disordered and transferred to isotropic phase at 110 °C, with  $\Delta H = 2.1$  J/g.

On cooling, the isotropic phase, to nematic transition was observed at 109.5 °C, which was only 0.5 °C lower than the clearing temperature measured on heating, with  $\Delta H = 2$  J/g (Figure 40 (b)). The nematic structure appeared at 109.5 °C and when the temperature was lowered to 78 °C. The nematic structure changed to the smectic phase upon cooling down to 78 °C with enthalpy 4.2 J/g (Figure 40 (c)).

The more order crystallization structure formed at 50 °C. In comparison with the heating process, the crystallization temperature decreased by about 25 °C on cooling whereas the corresponding enthalpy was  $\Delta H = 55.6$  J/g. (The enthalpy decreased by about 37 J/g).

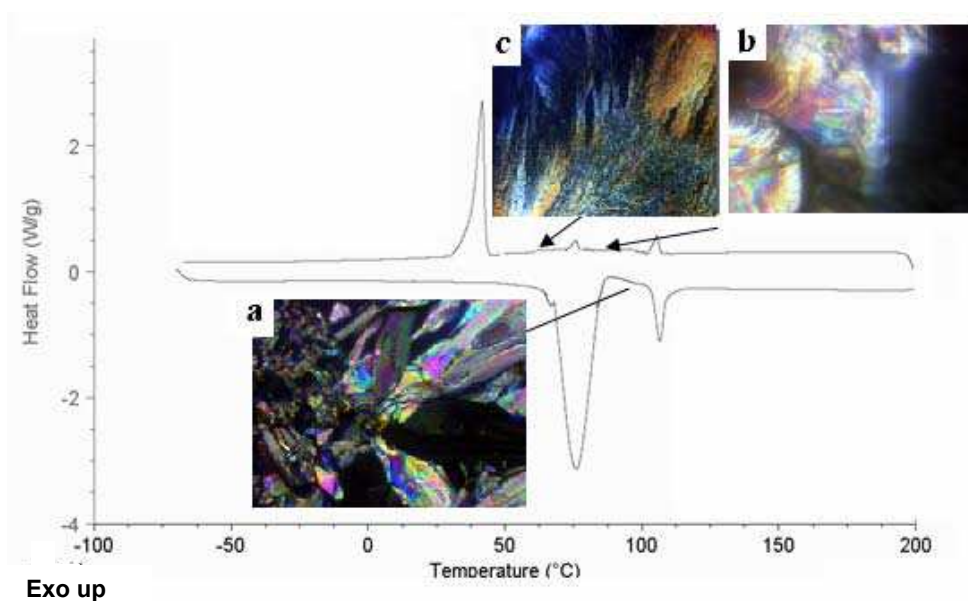


Figure (40): DSC thermograms and the observed PLM images for ABPC-12 on heating; a) 100.0 °C, and on cooling b) 95.0 °C and c) 70.

### 3.5.2. Lyotropic liquid crystalline properties of ABPC-*m*.

#### *Determination of critical concentration.*

The critical concentration can be estimated by refractive indices ( $n$ ) measurement of series of HPC and ABPC-*m* solutions in DMA with various concentrations (20, 30, 40, 50 and 60 wt %). An Abbe refractometer was used for measuring the two principal refractive indices  $n_e$  (Extraordinary) and  $n_o$  (Ordinary) at 25 °C. Figure 41 shows the plot of the refractive index versus concentration of the ABPC-*m*.

Table 17 represents the extraordinary refractive index ( $n_e$ ), ordinary refractive index ( $n_o$ ), birefringence ( $\Delta n = n_e - n_o$ ), average

refractive index ( $n$ ), and the critical concentration of the samples (ABPC- $m$ ). It is clear from the table that when increasing the length of alkoxy groups, the birefringence ( $\Delta n$ ) of ABPC- $m$  decreases and the average refractive index was not varied regularly with the chain length ( $m$ ).

The derivatization with alkoxybenzoic acids furnishes easily soluble samples in common organic solvents. This solubility could be ascribed to the rigidity and unfolding of the macromolecular chains due to the steric hindrance of the substituted long chains. These new characteristics led to easily formation of liquid crystal (Caiqi *et al.* 2003). Below the C.C. isotropic feature at room temperature was shown. This result is also confirmed by PLM; where non-continuous mesophase is formed. At concentrations higher than the critical one, the mesophase becomes continuous and colored. Figure 42 shows the birefringence texture of the derivatives solutions at 60 % concentration.

There is a difference in the solubility between more rigid HPC and less rigid ABPC- $m$ . Therefore, further evidence of the esterification of HPC with 4-alkoxy benzoic acid was noted from the increased solubility of the ester derivatives in organic solvents such as DMA, and tetrahydrofuran (THF).

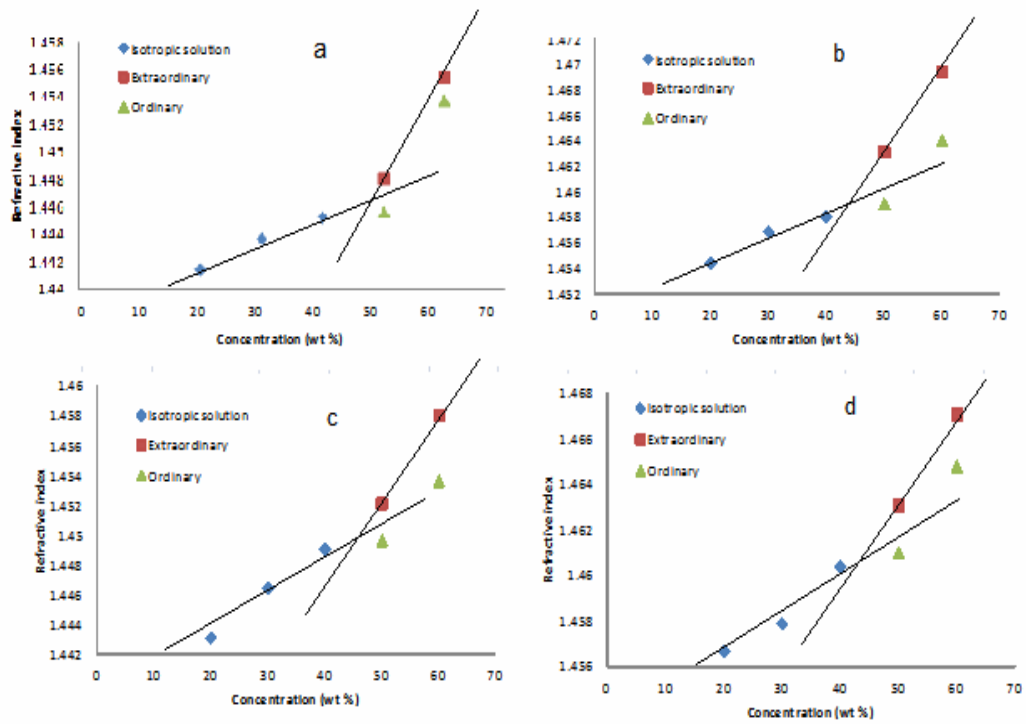


Figure (41): Plot of the mean refractive index vs. concentration for a) HPC<sub>B</sub>, b) ABPC-2, c) ABPC-10 and d) ABPC-12.

Table (17): Optical Properties of ABPC-m (values calculated for solutions of 60%).

Derivatives	$n_e$	$n_o$	Birefringence $\Delta n \times 10^3$	$n$	Critical Conc.(wt%)
HPC <sub>B</sub>	1.4555	1.4508	4.7	1.4523	48
ABPC-2	1.4695	1.4641	5.4	1.4659	47
ABPC-10	1.4581	1.4537	4.4	1.4551	45
ABPC-12	1.4671	1.4648	2.3	1.4655	45

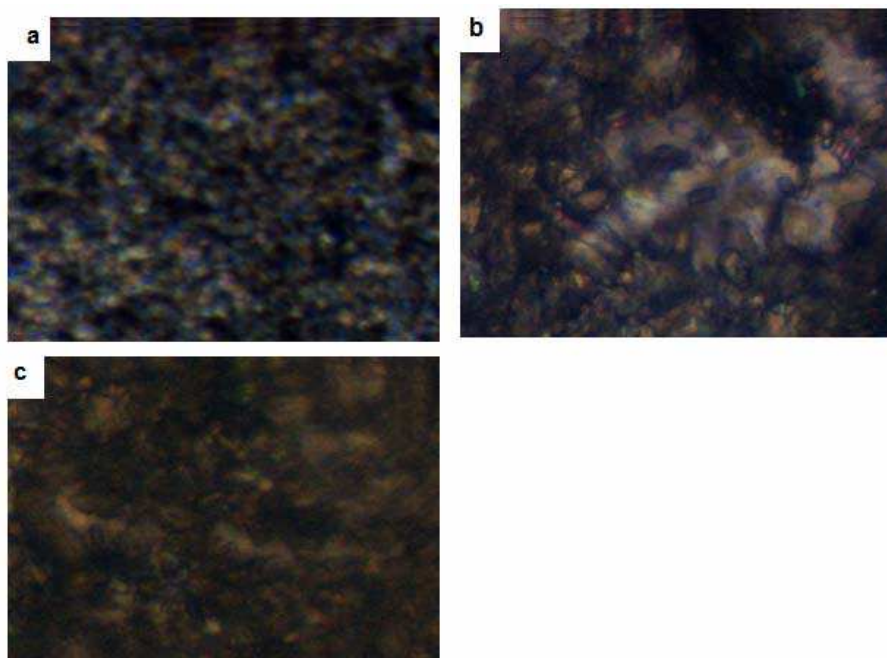


Figure (42): PLM images of a) ABPC-2, b) ABPC-10 and c) ABPC-12 in 60 wt % DMA at room temperature.

## **Summary**

Accumulation of agriculture wastes, such as bagasse, and development of alternatives to petrochemical-based polymer have received more attention in the last two decades due to increasing the population and increasing concern to the environmental safety. This study is a trial to contribute in resolving these problems through two main approaches. The first is related to the natural binder-based paper composites and the second is concerned with preparation and characterization of advanced cellulosic derivatives having liquid crystalline properties.

Regarding the natural binder-based paper composites, modification of soy protein isolate (SPI) was conducted via denaturation, addition of acrylamide and changing pH aiming to enhance certain new range of properties and makes SPI more useful and acceptable in versified applications. Preliminary experiments were carried out to determine the optimum SPI concentration which furnishes paper sheets of practical mechanical and physical properties. SPI concentrations 0.5, 2.5, and 5 wt %, based on dry pulp, were used and 2.5 % was found to be the optimum one. To increase the adhesion properties of SPI acrylamide was used as an additional modifier in 1.5, 2.5 and 5%. The nucleophilic addition of acrylamide to the protein chains in presence of alkali enhances

the solubility of SPI and increases its adhesive properties. The additional effect of acrylamide on SPI was pronounced, where the mechanical and physical properties were improved. Since the net charge on SPI can be changed by varying the pH of the aqueous medium, so correlating the mechanical and physical properties of paper sheets with the pH of SPI was studied. The pH was varied from 3, 5, 7 and 10, where it was reported that pH 5 is the isoelectric point (IEP) of SPI, and at this pH the number of positive and negative charges is almost identical. Recently, it was reported that at this pH adsorption of protein on different surfaces was enhanced and the present results confirmed this finding. An extra benefit of SPI was found by acting as a retention aid to kaolin to enhance the physical properties of paper sheets. The maximum retention value of kaolin is increased from 21 to 37.2 % upon using 2.5 % denatured SPI.

The second approach in this work is concerned with the preparation and characterization of a series of 4-alkoxybenzoyloxypropyl cellulose (ABPC-*n*) derivatives. These derivatives were synthesized via the esterification of the purchased hydroxypropyl cellulose (HPC) of DS 3 with 4-alkoxybenzoic acid bearing 1, 2, 3, 4, 7, 8, 10, 12 and 14 carbon atoms in the alkoxy chain. On the other hand dissolving bagasse pulp was prepared from Egyptian bagasse pulp and

characterized. Hydroxypropylation was then conducted on the obtained cellulose and partially substituted HPC<sub>B</sub> was obtained. Finally, esterification of the latter product with 4-alkoxybenzoic acids, bearing 2, 10 and 12 carbon atoms in the alkoxy chain was performed and the derivatives were denoted as (ABPC-*m*). The molecular structure of the partially substituted HPC and both esters (ABPC-*n* and ABPC-*m*) confirmed by Fourier transform infrared (FT-IR) and <sup>1</sup>H NMR spectroscopy. Also the liquid crystalline (LC) phases and transition behavior were investigated using polarized light microscopy (PLM) and differential scanning calorimetry (DSC) respectively. To investigate the lyotropic property, solutions of various concentrations of samples were dissolved in DMA, (20, 30, 40, 50 and 60 wt %) and the critical concentration was determined by measuring the refractive index of the solutions and by plotting the refractive indices versus mentioned concentrations. For ABPC-*n*, it was found that the glass transition ( $T_g$ ) and clearing ( $T_c$ ) temperatures and the mesomorphic range ( $T_m-T_c$ ) decreases with increasing the alkoxy chain length. This series of ABPC-*n* polymers exhibit characteristic features of cholesteric LC phases between their glass transition and isotropization temperatures. Also the lower samples, ABPC-1, 2, 3 and 4, did not show any thermotropic mesophase. Nevertheless, they still exhibit lyotropic phase. On

the other hand, the samples ABPC-7, 8, 12 and 14 exhibit both lyotropic and thermotropic liquid crystal behavior, as detected by both DSC and the PLM.

Derivatization of HPC<sub>B</sub> prepared from dissolving bagasse pulp, was carried out and the glass transition ( $T_g$ ) and clearing ( $T_c$ ) temperatures have the same trend with increasing of the alkoxy chain length. The behavior of the ABPC-*n* and ABPC-*m* revealed that both the backbone of cellulose and the length of the alkoxy chain of the acid have affected the formation of the liquid crystalline phase.

## Résumé

L'accumulation de déchets agricoles tels que la bagasse et le développement d'alternatives aux polymères issus de la pétrochimie ont reçu une attention croissante au cours des deux dernières décennies, due à l'augmentation de la population et à la préoccupation croissante pour la préservation de l'environnement. Cette étude tente de résoudre ces problèmes à l'aide de deux approches principales. La première est liée à des composites à base de papier et de liant naturel et la seconde est associée à la préparation et à la caractérisation de dérivés cellulosiques présentant des propriétés cristaux liquides .

En ce qui concerne les composites à base de papier et de liant naturel, la modification par dénaturation d'isolat de protéines de soja (SPI), l'ajout d'acrylamide et le changement de pH améliorent certaines propriétés et rendent les SPI plus utiles et acceptables dans diverses applications. Des expériences préliminaires ont été menées pour déterminer la concentration optimale de SPI permettant d'obtenir des propriétés mécaniques et physiques maximales. Des concentrations de 0,5%, 2,5%, et 5% ont été utilisées et 2.5% correspond à la concentration optimale. Pour augmenter les propriétés adhésives du SPI, l'acrylamide a été utilisé comme un

modificateur supplémentaire dans des proportions 1,5%, 2,5% et 5%. L'addition nucléophile de l'acrylamide aux chaînes de protéines en milieu alcalin améliore les propriétés de solubilité du SPI et augmente ses propriétés adhésives. L'effet supplémentaire de l'acrylamide sur le SPI est prononcé sur les propriétés mécaniques et physiques. Comme la charge nette du SPI peut être modifiée en faisant varier le pH du milieu aqueux, la corrélation entre les propriétés mécaniques et physiques des feuilles de papier et le pH du SPI a été étudiée. Les pH utilisés ont été 3, 5, 7 et 10, où le pH 5 est le point isoélectrique (IEP) du SPI. A ce pH, le nombre de charges positives et négatives est pratiquement identique. Récemment, il a été signalé que'à ce pH l'adsorption de protéines sur différentes surfaces est amélioré et les résultats confirment cette constatation. Un avantage supplémentaire du SPI est d'agir comme un promoteur de rétention du kaolin pour améliorer les propriétés physiques des feuilles de papier. La valeur de rétention maximale du kaolin a augmenté de 21 à 37,2% avec 2,5% de SPI dénaturé.

La seconde approche a consisté à préparer et caractériser une série de dérivés celluloses 4 - alkyoxybenzoyloxypropyl (ABPC-n). Ces dérivés ont été synthétisés par estérification d'hydroxypropylcellulose

(HPC) avec un DS 3 par l'acide 4-alkoxybenzoic portant 1, 2, 3, 4, 7, 8, 10, 12 et 14 atomes de carbone dans la chaîne latérale. D'autre part, de la pâte de bagasse a été préparée et caractérisée à partir de bagasse égyptienne. L'hydroxypropylation a ensuite été menée sur la cellulose obtenue et de l'HPC partiellement substituée a été obtenue. En outre, l'estérification de ce dernier avec des acides 4-alkoxybenzoic portant 2, 10 et 12 atomes de carbone dans la chaîne latérale a été réalisée et les dérivés ont été désignés (ABPC-m). La structure moléculaire du HPC partiellement substitué et des deux esters (ABPC-n et ABPC-m) a été confirmée par spectroscopies infrarouge à transformée de Fourier (FT-IR) et  $^1\text{H}$  RMN. Les phases cristalline (LC) et les transitions de phases ont été étudiées par microscopie en lumière polarisée (PLM) et calorimétrie différentielle à balayage (DSC), respectivement. Pour étudier les propriétés lyotropiques, différentes concentrations de ces échantillons ont été dissous dans le diméthylacétamide (DMA) (20, 30, 40, 50 et 60% en poids) et la concentration critique a été déterminée par réfractométrie en mesurant l'indice de réfraction des solutions dans le DMA et en traçant l'évolution des indices de réfraction en fonction des concentrations. Pour ABPC-n, nous avons observé que les

températures de transition vitreuse ( $T_g$ ) et de compensation ( $T_c$ ) diminuent avec la longueur de la chaîne alkoxy et que la gamme mésomorphe ( $T_m-T_c$ ) diminue avec la longueur de la chaîne alkoxy. Cette série de polymères ABPC-n présente les caractéristiques de phases LC cholestériques entre la transition vitreuse et la température d'isotropisation. Les échantillons ABPC-1, 2, 3, 4 ne présentent pas de mésophase thermotrope. Néanmoins, ils se comportent comme des LC lyotropes. De plus, les échantillons ABPC-7, 8 et 12 montrent un comportement de cristal liquide lyotrope et thermotrope.

La dérivatisation du HPC préparé à partir de la pâte de bagasse a été réalisée et les températures de transition vitreuse ( $T_g$ ) et de compensation ( $T_c$ ) ont montré la même tendance avec l'augmentation de la longueur de la chaîne alkoxy. Le comportement de ABPC-n et ABPC-m révèle que la formation de la phase cristal liquide est affectée à la fois par la chaîne principale de la cellulose et les chaînes alkoxy de l'acide.

## References

- Abrantes, S., Amaral, M. E., Costa, A. P., Duarte, A. P. “Cynara cardunculus L. alkaline pulps: Alternative fibres for paper and paperboard production,” *Bioresour. Technol* 98, (2007) 2873.
- Agriculture Economic and Statistics Institute. Ministry of Agriculture, Agric., Economics, Part 1. Publ. By Agric. Res. Center, Egypt (2009).
- Aguiar, C. M. Hidrólise enzimática de resíduos lignocelulósicos utilizando celulases produzidas pelo fungo *Aspergillus Níger*. Dissertação de Mestrado, Universidade Estadual do Oeste do Paraná – UNIOESTE, Toledo, PR, Brazil (2010).
- Alinec, B., Lebreton, R., and St. Amour, S., "Using cationic starch in filled papers". *J. Tappi*, Vol. 73, 3, (1990) 191.
- Antunes, A., Amaral, E., and Belgacem, M. N. “Cynara cardunculus L.: Chemical composition and soda-anthraquinone cookingc” *Ind. Crop. Prod.* 12, (2000) 85.
- Atalla, R. H., "Celluloses". In *Comprehensive Natural Products Chemistry*, Vol. 3, (1999) 529.
- Babkov, L. M.; Gorshkov, O. V.; Golovina, N. A.; Puchkovskay, G. A.; Khakimov, I. N. Phase transitions, conformational lability, and intermolecular interactions in alkoxyacyanobiphenyls *J. Struct. Chem.* 36, (1995), 739.

- Balsler K, Hoppe L, Eicher T, Wandel M, Astheimer H. J, Steinmeier H, Allen J. M. "Cellulose esters". In: Gerhartz W, Stephen YY, Thomas CF, Pfefferkorn R, James F (eds) Ullmann's encyclopedia of industrial chemistry. Wiley, New York (1986).
- Barba, C., De la Rosa, A., Vidal, T., Colom, J. F., Farriol, X., and Montane, D. "TCF bleached pulps from *Miscanthus sinensis* by the impregnation rapid steam pulping (IRSP) process," *J. Wood Chem. Technol.* 22(4), (2002) 249.
- Barndt L. "Cellulose ethers". In: Gerhartz W, Stephen YY, Thomas CF, Pfefferkorn R, James F (eds) Ullmann's encyclopedia of industrial chemistry. Wiley, New York (1986).
- Barnes, A. C., *The sugar cane. The world crop series.* Leonard Hill books second edition (1980).
- Bellamy, L. J. "The infrared spectra of complex molecules" (3rd ed.). London: Chapman and Hall. (1975).
- Bhadani, S. N., Tseng, D. L., and Gray, D. G. "Lyotropic and thermotropic phase formation from fractions of a semiflexible cellulosic polymer," *Macromol. Chem.* 184, (1983) 1727.
- Bicho, P., Gee, W., Yuen, B., Mahajan, S., McRae, M., and Watson, P. "Characterization of Canadian agricultural residues and their pulps". Proceedings of the TAPPI Pulping Conference; October 31–November 4, 1999; Orlando, FL, TAPPI Press, Atlanta, GA, 2 (1988) 829.

- **Boopathy, R. "Use of post-harvest sugarcane residue in coastal reclamation: A feasibility study," Sugar cane International. Jan/Feb, (2004) 9.**
- **Bryan R. F. and Paul H. "An X-Ray Study of the p-n-Alkoxybenzoic Acids. Part V. Crystal Structures of the Nematogenic Acids Having Three and Five Alkyl-Chain Carbon Atoms". (1980) 259.**
- **Bryan, R. F.; Hartley, P.; Miller, R. W.; Shen, M. S. "An X-Ray Study of the p-n-Alkoxybenzoic Acids. Part VI. Isotypic Crystal Structures of Four Smectogenic Acids Having Seven, Eight, Nine, and Ten Alkyl Chain Carbon Atoms" Mol. Cryst. Liq. Cryst. 1980, 62, 281.**
- **Caiqi W., Yuping D., Huimin T. "Study on lyotropic liquid-crystalline properties of trimethylsilyl hydroxypropylcellulose". Carbohydrate Research 338 (2003) 535.**
- **Casey J. P, "Pulp and Paper Chemistry and Chemical Technology ", Wiley Interscience, New York (1961).**
- **Casey, J. P, "Pulp and Paper Chemistry and Chemical Technology" Wiley Interscience, New York (1982).**
- **Charlet, G., and Gray, D. G. "Solid cholesteric films cast from aqueous (hydroxypropyl) cellulose," *Macromolecules* 20, (1987) 33.**

- **Chen, C. R. and H. S. Ramaswamy.** “Rheology of Tapioca Starch.” *Food Research International*. 32 (1999) 319.
- **Chen, J., Yu, J., and Zhan, H.** "Study on mechanisms of kraft and AS-AQ pulping of bamboo". *Cellul. Chem. Technol.*, 21(6) (1987) 651.
- **Chia, C. H., Zakaria, S., Nguyen, K. L., and Abdullah, M.** “Utilisation of unbleached kenaf fibers for the preparation of magnetic paper,” *Ind. Crop. Prod.* 28(3), (2008) 333.
- **Cladis, P. E.** "Nematic and smectic A phases of N-p-cyanobenzylidene-p-noctyloxyaniline in tubes." *Philosophical Magazine* 29(3) (1974) 641.
- **Cladis, P. E. and M. Kleman** "Nonsingular disclinations of strength  $S = + 1$  in nematics." *Journal de Physique (Paris)* 33(5-6) (1972) 591.
- **Collings P. J.,** "Liquid crystals", 1 edn., Princeton Universty Press, Princeton, New Jersey, USA, 1990.
- **Cordeiro, N., Belgacem, M. N., Torres, I. C., and Mourad, J. C. V. P.** “Chemical composition and pulping of banana pseudo-stems,” *Ind. Crop. Prod.* 19, (2004) 147.
- **De Souza Lima, M. M., Borsali, R., Rodlike,** "Cellulose Microcrystals: Structure, Properties, and Applications". *Macromolecular Rapid Communications*, 25 (7), (2004) 771.
- **Deniz, I., Kirci, H., and Ates, S.** "Optimization of wheat straw *Triticum drum* Kraft pulping". *Ind. Crops Prod.*, 19(3) (2004) 237.

- Doherty, W., Halley, P., Edey, L., Rogers, D., Cardona, F., Park, Y., and Woo, T. "Studies on polymers and composites from lignin and fiber derived from sugarcane, *Polym. Adv. Technol.* 18(8) (2007) 673.
- Dong Yanming and Zhang Shiyong "Studies on critical concentration of liquid crystalline ethylcellulose" *Chinese Journal of polymer science* vol 14 (2) (1996) 134.
- Dutt, D., Upadhyaya, J. S., Tyagi, C. H., Kumar, A., and Lal, M. "Studies on *Ipomea carnea* and *Cannabis sativa* as an alternative pulp blend for softwood: An optimization of kraft delignification process," *Ind. Crop. Prod.* 28 (2008) 128.
- Ebeling, K., "A Critical Review of Current Theories for the Refining of Chemical Pulps", *International Symposium on Fundamental Concepts of Refining.* Institute of Paper Chemistry, Appleton, USA. (1980) 1.
- Edgar, K. J., Buchanan, C. M, Debenham, P. A. R., Seiler, B. D., Shelton, M. C., Tindall, D. "Advances in cellulose ester performance and application". *Prog. Polym. Sci.*, 26, (2001) 1605.
- Endres, J. G. *Soy protein products: characteristics, nutritional aspects, and utilization*, Revised and expanded edition, AOCS Press, ISBN 1-893997-27-8, Champaign (2001).
- Eugenio, M. E., Alaejos, J., Diaz, M. J., Lopez, F., and Vidal, T. "Evaluation of Holm oak (*Quercus*

- Ilex) wood as alternative source for cellulose pulp,”**  
**Cellul. Chem. Technol. 40(1-2), (2006) 53.**
- **FAO. (2009). Faostat-forestry. Available from: www.fao.org. Accessed date: November 9, 2009.**
  - **Fardous Mobarak, Nabila A El-Shinnawy, Aisha A.A. Soliman and Ahmed A El-Gendy, ” Effect of Some Chemical Treatments of Upgraded Egyptian Kaolin on Its Retention by Bagasse Pulp” of Journal of Scientific & Industrial Research. 57(1997) 316.**
  - **Fayolle, B., C. Noel, and J. Billard. "Investigation of polymer mesophases by optical microscopy." Journal de Physique, Colloque(3) (1979) 485.**
  - **Feeney, R. E., Whitaker, J. R. "Food proteins: improvement through chemical and enzymatic modification". Adv. Chem. Ser 160, ACS, Washington DC, (1977) 3.**
  - **Feeney, R. E., Whitaker, J. R., In: Altschul, A. M., Wilcke, H. L. (Eds.), "Chemical and Enzymatic Modification of Plant Proteins in New Protein Foods". Academic Press, New york, (1985) 181.**
  - **Fengel, D., and Wegener, G. "Hydrolysis of Polysaccharides with Trifluoroacetic Acid and Its Application to Rapid Wood and Pulp Analysis." Hydrolysis of Cellulose: Mechanism of Enzymatic and Acid Catalysis ed. J. Brown, R.D., and Jurasek, L. Vol. 181: ACS. (1979) 145.**

- Fengel, D., and Wegener, G. "Wood- Chemistry, Ultrastructure, Reactions." Walter de Gruyter & Co. Berlin. p6 (1983).
- Finkelmann, H. Liquid crystal polymers. Thermotropic Liquid Crystals. G. W. Gray, John Wiley & Sons. 22 (1987) 149.
- Fiserova, M., Gigac, J., Majtnerova, A., and Szeiffova, G. "Evaluation of annual plants (Amaranthus caudatus L., Atriplex hortensis L., Helianthus tuberosus L.) For pulp production," Cellul. Chem. Technol. 40(6), (2006) 405.
- Franz G., Sheldon R. A., in: B. Elvers, S. Hawkins, G. Schulz (Eds.), Ullmann's Encyclopedia of Industrial Chemistry, Vol. A (18), 5th Edition, VCH, Weinheim, (1991) 261.
- French, A. D.; Bertoniere, N. R.; Brown, R. M.; Chanzy, H.; Gray, D.; Hattori, K.; Glasser, W., "Cellulose. In Kirk-Othmer Encyclopedia of Chemical Technology". (5th Edition), Vol. 5, (2004) 360.
- Fukumasa, M. Kato T., Uryu T., Frechet, J.M.J. The Simplest Structure of the Hydrogen-Bonded Mesogen Built from 4-Alkoxybenzoic Acid and 4-Alkylpyridine Chem. Lett. 1 (1993) 65.
- Ghorpade V. M., H. Li, A. Gennadios and M. A. Hanna. "Chemically Modified Soy Protein Films." Transactions of the ASAE. 38 (1995) 1805.

- Goldemberg, J. "The Brazilian biofuels industry. *Biotechnology for Biofuels*". Vol.1, No.6, (May 2008), pp. 1-7, ISSN (2008) 1754.
- Gominho, J., Fernandez J., and Pereira H. "Cynara cardunculus L.: A new fibre crop for pulp and paper production," *Ind. Crop. Prod.* 13, (2001)1.
- Gray, D. G. "Liquid crystalline cellulose derivatives," *J. Appl. Polym. Sci., Appl. Polym. Symp.* 37, (1983) 179.
- Gümuüşkaya, E. and Usta, M. "Crystalline structure properties of bleached and unbleached wheat straw (*Triticumaestevum* L.) soda–oxygen pulp". *Turk. J. Agric. For.*, 26(5) (2002) 247.
- Halpern, M. G., "Paper Manufacture". Printed in United States, (1975).
- Hamad W. "On the development and applications of cellulosic nanofibrillar and nanocrystalline materials". *Can J Chem Eng.*; 84 (2006) 513.
- Hans, K. and H. Rolf. *Handbook of Liquid Crystals.* (1980).
- Heinze, T. and Koschella, A. "Solvents applied in the field of cellulose chemistry: A mini review". *Polímeros*, 15(2) (2005) 84.
- Heinze, T. and Liebert, T. "Unconventional methods in cellulose functionalization". *Prog. Polym. Sci.*, 26, (2001) 1689.
- Heinze, T. and Petzold, K. "Cellulose chemistry: Novel products and synthesis paths". In M. N. Belgacem and A. Gandini (Eds.), *Monomers,*

- polymers and composites from renewable resources. Amsterdam: Elsevier (2008) 343.
- Hou, H. Q., Reuning, A., Wendorff, J. H., and Greiner, A. "Tuning of the pitch height of thermotropic cellulose esters," *Macromol Chem Phys.* 201, (2000) 2050.
  - <http://pslc.ws/macrogcss/starch.html>. "Starch." The Macrogalleria. University of Southern Mississippi; Department of Polymer Science.
  - Huang W. N. and Sun X. Z. "Adhesive properties of soy protein modified by urea and guanidine hydrochloride". *J Am Oil Chem Soc.*77 (1) (2000)101.
  - Huang, B., Ge, J. J., Li, Y. H., and Hou, H. Q. "Aliphatic acid esters of (2-hydroxypropyl) cellulose. Effect of side chain length on properties of cholesteric liquid crystals," *Polymer*, 48, (2007) 264.
  - Huang, J. and Zhu D. "Preparation and characteristics of PDLC (polymerdispersed liquid crystal) display material." *Zhongshan Daxue Xuebao, Ziran Kexueban* 29(2) (1990)125.
  - Hurter, A. M. "Utilization of annual plants and agricultural residues for the production of pulp and paper". *Proceeding of TAPPI Pulping Conference 1988; October 30–November 2, 1988; New Orleans, LA, Book 1, TAPPI Press, Atlanta, GA, (1988)139.*
  - Jacobs, R. S., Pan, W. L., Fuller, W. S., and MsKean, W. T. "Genetic and environmental influences on the chemical composition of Washington State wheat straw". *Proceedings of the TAPPI Pulping*

- Conference; October 31–November 4, 1999; Orlando, FL, TAPPI Press, Atlanta, GA, 2 (1999) 839.
- Jimenez, L., and Lopez, F. “Characterization of Spanish agricultural residues with a view to obtaining cellulose pulp,” *Tappi J.* 73(8) (1990) 173.
  - Jiménez, L., Lopez, F., and Alaejos, J. “Materias primas alternativas para pastas de papel. Tipos, características, procesosy situación actual,” *Ingeniería Química* 435(4) (2006) 76.
  - Jiménez, L., Lopez, F., and Martinez, C. “Paper from sorghum stalks,” *Holzforschung* 47, (1993) 529.
  - Jiménez, L., Rodriguez, A., Perez, A, Moral, A., and Serrano, L. “Alternative raw materials and pulping process using clean technologies,” *Ind. Crop. Prod.* 28(1) (2008)11.
  - Jiménez, L., Sanchez, I., and Lopez F. “Olive wood as a raw material for paper manufacture,” *Tappi J.* 11, (1992) 89.
  - Joseph Marton, "Surface Chemical Role of Fines in Papermaking Furnish" *Ind. Eng. Chem. Prod. Dev.*, 21 (2) (1982)146.
  - Kalapathy, U., Hettiarachchy, N. S., Rhee, K. C. "Effect on drying methods on molecular properties and functionalities of disulfide bond cleaved by soy proteins. *J. Am. Oil Chem. Soc.* 74, (1997) 195.
  - Kaldor, A.F., Karlgren, C., and Verwest, H. "Kenaf-a fast growing fiber source for papermaking". *Tappi J.*, 73(11) (1990) 205.

- Kato, T.; Kubota, Y.; Nakano, M.; Uryu, T. *Chem. Lett.* 1995, 1127.
- Khristova, P., Kordsachia, O., Patt, R., and Karar, I. "Comparative alkaline pulping of two bamboo species from Sudan," *Cellul. Chem. Technol.* 40(5), (2006) 325.
- Kihara H. , Ryoichi Kishia, Toshiaki Miuraa, Shin Horiuchia, Yuji Okadaa, Kiyoshi Yasea and Hisao Ichijo. "Thermomechanical analysis of a polymer dispersed liquid crystal containing a thermoplastic elastomer." *Liquid Crystals* 28(11) (2001) 1655.
- Kinsella, J. E. "Functional properties of soy proteins". *J. Am. Oil Chem. Soc.* 56, (1979) 242.
- Kissinger, M., Fix, J., and Rees, W. E. "Wood and non-wood pulp production: Comparative ecological footprinting on the Canadian prairies". *Ecological Economics*, 62(3-4) (2007) 552.
- Klemm, D., Heublein, B., Fink, H.-P., Bohn, A. "Cellulose fascinating biopolymer and sustainable raw material". *Angew. Chem. Int. Ed.*, 44(22) (2005) 3358.
- Klemm, D., Philipp, B., Heinze, T., Heinze, U., Wagenknecht, W. "Comprehensive cellulose chemistry: Fundamentals and analytical methods". (1st ed., vol. 1). Weinheim: Wiley-VCH (1998).
- Klemm, D., Schmauder, H.-P., Heinze, T. Cellulose . In E.J. Vandamme, S.D. Baets and A. Steinbüchel (Eds.), *Biopolymers* (1st ed., vol. 6, 275. Weinheim: Wiley-VCH (2002).

- Koivunen, K., Niskanen, I., Peiponen, K. E., and Paulapuro, H. "Novel nanostructured PCC fillers" *J. Mater. Sci.* 44(2) (2009) 477.
- Kontturi, E.; Tammelin, T.; Osterberg, M., "Cellulose--model films and the fundamental approach". *Chem. Soc. Rev.* 35 (12), (2006) 1287.
- Krässig, H. A. "Cellulose: Structure, accessibility and reactivity" (1st ed). Amsterdam: Gordon and Breach Science Publishers (1993).
- Lambuth A. L. "Soybean glues". In: Skeist, I. (Ed.), *Handbook of Adhesives*, 2nd ed. Van Nostrand, New York, (1977) 172.
- Leadbetter, A. J. "Structural classification of liquid crystals. Thermotropic Liquid Crystals". G. W. Gray, John Wiley & Sons. 22 (1987) 1.
- Lenorad, J., Coughlin, "Hand Book of Pulp and Paper Technology "Printed in United States, (1984).
- Liebert, T. "Cellulose solvents – Remarkable history, bright future". In T. Liebert, T. Heinze and K.J. Edgar (Eds.), *ACS symposium series - Cellulose solvents: analysis, shaping, and chemical modification* (vol. 1033, 3-54). Washington, D.C.: American Chemical Society (2010).
- Liesbet J., Bart G., Igor D., and Koen B. " Influence of the Chain Length on the Thermal Behavior of Lanthanide(III) 4-Alkoxybenzoates" *Chem. Mater.*, 15, (2003) 212.

- López, F., García, J.C., Pérez, A., García, M.M., Feria, M.J., and Tapias, R. "Leucaena diversifolia a new raw material for paper production by sodaethanol pulping process". *Chem. Eng. Res. Des.* 88 (2010) 1.
- Lovinger, A. J., Amundson, K. R and and Davis, D. D. "Morphological investigation of UVcurable polymer-dispersed liquid-crystal (PDLC) materials." *Chemistry Materials* 6(10) (1994) 1726.
- Magagnini, P., Paci M., Poli, G. Tonti, S. M. Narducci, P. "Polymer-dispersed liquid-crystal polymers (PDLCPs). Morphology of the LCP droplets." *Polymer Engineering and Science* 39(10) (1999) 1891.
- Maher, S. L., in TAPPI 1985 Adv. Topics in Wet End Chem. Sem., Tappi Notes, Atlanta, GA, 21(1985).
- Mali K. S., Lava K, Binnemans K., De Feyter S. "Hydrogen bonding versus van der Waals interactions: competitive influence of noncovalent interactions on 2D self-assembly at the liquid-solid interface". *Chemistry*. 16(48) (2010) 14447.
- Manuel A.V. Ribeiro da Silva, Ana I.M.C. Lobo Ferreira, Fabrice M. Maciel. "Experimental standard molar enthalpies of formation of some 4-alkoxybenzoic acids. " *J. Chem. Thermodynamics* 42 (2010) 220.
- Market opportunity summary, February. "Soy-based wood adhesive". (2000).

- Md Yasir S. B., Sutton K. H., Newberry M. P., Andrews N. R. Gerrard. J. A. "The impact of Maillard cross-linking on soyproteins and tofu texture" *Food Chemistry*, 104 (2007)1502.
- Meier, G., Sackmann E., Grabmaier J. G. *Applications of Liquid Crystals*. Berlin, Springer-Verlag. (1975).
- Minna B., "Modification of cellulosic fibers by carboxymethyl cellulose effects on fiber and sheet properties". Dissertation for the degree of Doctor of Science, Helsinki University of Technology Department of Forest Products Technology, Espoo, (2007), pp. 2, 7-17, 25.
- Mo X., Hu, J., Sun X. S. and Ratto J. A. "Compression and tensile strength of low density straw–protein particle board". *Ind. Crops Prod.* 14, (2001) 1.
- Mobarak F. M., M.Sc. Thesis, " Utilization of Black Liquor Silica in Papermaking, and its Comparison with Fillers and Pigments" Cairo University (1968).
- Mollaahmad, M. A. "Sustainable fillers for paper" Master Thesis of Lulea University of Technology, Lulea, Sweden (2008).
- Moore, W. E. and Janson, D. B. "Producing for the chemical analysis of wood and wood products. Forest product laboratory, U. S. Department of Agriculture Wisconsin(1967).
- Morais, L. C., and Campana Filho, S. P. "Carboximetilação de Polpas de Bagaço de Cana-de-

- Açúcar e Caracterização dos Materiais Absorventes Obtidos. Polimeros: Cienciae Tecnologia, 99 (1999) 46.**
- **Moure, A.; Sineiro, J.; Domínguez, H. & Parajó, J. C. (2006). Functionality of oilseed protein products: A review, Food Res. Int., Vol. 39, No. 9, 945-963, ISSN: 0963-9969.**
  - **Nagano, T., Tamaki E. and Funami T. “Influence of Guar Gum on Granule Morphologies and Rheological Properties of Maize Starch.” Carbohydrate Polymers. 72 (2008) 95.**
  - **Navaee-Ardeh, S., Mohammadi-Rovshandeh, J., and Pourjoozi, M. Influence of rice straw cooking conditions in the soda–ethanol-water pulping on the mechanical properties of produced paper sheets. Bioresour. Technol. 92(1) (2004) 65.**
  - **Nevell T. P., Zeronian S. H. "Cellulose chemistry and its applications". Ellis Horwood, Chichester York (1985).**
  - **Nelida G. Maria B. R., Jose L. S., and Maria R. "Hydrogen-Bonded Banana Liquid Crystals". Angew. Chem. Int. Ed. 2004, 43, 5235 –5238**
  - **Oinonen, H. and Koskivirta, M. "Special challenges of pulp and paper industry in Asian populated countries, like Indian sub-continent and China". Proceedings of the Paperex 99-4th International Conference on Pulp and Paper Industry: Emerging Technologies in the Pulp and Paper Industry; December 14–16, 1999; New Delhi, India, (1999) 49.**
  - **O'Sullivan, A. C., "Cellulose: the structure slowly unravels". Cellulose 4 (3), (1997) 173.**

- Page, D. H., “The Beating of Chemical Pulps. The Action and the Effects”, in *Papermaking Raw Materials: Transactions of the Ninth Fundamental Research Symp. Vol. 1*, Baker, C. F. and Punton, V. W. Mechanical Engineering Publications Ltd. London, U. K. (1989) 1.
- Park, S. K.; Hettiarachchy, N. S.; Ju, Z. Y. & Gennadios, A. Formation and properties of soy protein films and coatings, In: *Protein-based films and coatings*, Gennadios, A. (Ed.), pp123-138, CRC Press, ISBN: 978-1587-16107-0, Boca Raton (2002).
- Patricia Nordell, *Wet-Strength Development of Paper, Modification of cellulose fibers by adsorption of a natural biopolymer*, Master’s Thesis, Lulea University of Technology, Department of Applied Physics and Mechanical Engineering, (2006) 9.
- Pavel, D., J. Ball. "Overview of liquid crystals and liquid crystalline polymers." *Memoriile Sectiilor Stiintifice - Academia Romana* 22 (2002) 177.
- Petri Myllytie, "Interactions of polymers with fibrillar structure of cellulose fibers: a new approach to bonding and strength in paper" *Doctoral Thesis*, Espoo, 28 (2009) 10.
- Pinkert, A., Marsh, K. N., Pang, s., Staiger, M. P. "Ionic liquids and their interaction with cellulose". *Chem. Rev.*, 109(12) (2009) 6712.
- Poudyal, S. "High yield semichemical pulping of sabai grass and rice straw for corrugating medium and container board". [M. Sc. thesis]. *Pulp and Paper Technology Program, School of Environment, Resources and Development, Asian Institute of Technology. Pathumtani, Thailand*, (1999) 44.

- Priestley, E. B. "Liquid crystal mesophases. Introduction to Liquid Crystals". E. B. Priestley, Peter J. Wojtowicz and P. Sheng. London, Plenum Press (1974) 1.
- Puppo M. C., Añón M. C. "Rheological properties of acidic soybean protein gels: Salt addition effect". *Food Hydrocolloids*, 13 (1999) 167.
- Qiang G., Sheldon Q. Shi, Jianzhang Li, Kaiwen Liang, Xiumei Zhang. "Sobean meal-based adhesive" *BioResources* 7(1) (2011) 946.
- Reichel, F." The Chemistry of Papermaking and its Environmental Significance" (Ludwigshafen, Fed. Rep. Ger.) *Wochenbl Papierfabr.* ,118 (8), (1990) 328.
- Renkema J. M. S. and Vliet van, T. "Concentration dependence of dynamic moduli of heat-induced soy protein gels" *Food Hydrocolloids* 18 (2004) 483.
- Rezayati-Charani, P., Mohammadi-Rovshandeh, J., Hashemi, S. J., and Kazemi-Najafi, S. "Influence of dimethyl formamide pulping of bagasse on pulp properties". *Bioresour. Technol.*, 97(18) (2006) 2435.
- Ritcey, A. M., Holme, K. R., and Gray D. G. "Cholesteric properties of cellulose acetate and triacetate in trifluoroacetic acid," *Macromolecules* 21, (1988) 2914.
- Ritu Sharma. V. K. Varshney, Ghanshyam S. Chauhan, Sanjay Naithani, P. L. Soni "Hydroxypropylation of Cellulose Isolated from Bamboo (*Dendrocalamus strictus*) with Respect to

- Hydroxypropoxyl Content and Rheological Behavior of the Hydroxypropyl Cellulose". *Journal of Applied Polymer Science*, 113, (2009) 2450.**
- **Roberts J. C, "Paper Chemistry 2nd edition", Chapman and Hall, Blackie Academic and Professional as imprint of Wester cleddens Road, Glasgow G642 NZ, (1996).**
  - **Rodrigues Filho, G., da Cruz, S. F., Pasquini, D., Cerqueira, D. A., Prado, V. S., and Assuncao, R. M. N. "Water flux through cellulose triacetate films produced from heterogeneous acetylation of sugar cane bagasse". *Journal of Membrane Science*, 177, (2000) 225.**
  - **Rodríguez, A., Moral, A., Serrano, L., Labidi, J., and Jiménez, L. Rice straw pulp obtained by using various methods. *Bioresour. Technol.*, 99(8) (2008). 2881.**
  - **Rousu, P., Rousu, P., and Anttila, J. Sustainable pulp production from agricultural waste. *Resour. Conserv. Recycl.*, 35(1) (2002) 85.**

- Rowell R. M. "Handbook of wood chemistry and wood composites". Boca Raton: CRC Press; (2004).
- Rowell, R. M. and Cook, C. "Types and amounts of nonwood fiber available in the U.S. Tappi North America Nonwood Fiber Symposium"; August 31-September 2, 1998; Chicago, Illinois, (1998) 43.
- Russell, G. M., B. J. A. Paterson, et al. "Thermal characterization of polymerdispersed liquid crystals by differential scanning calorimetry." *Chemistry of Materials* 7(11) (1995) 2185.
- Rutt, J. S., Takahashi, Y., and Karasz, F. E. "Phase behavior of thermotropic liquid crystalline/conducting polymer blends," *Polymer Bulletin*, 27, (1991) 261.
- Salmela, M., Alén, R., and Vu, M.T.H. Description of kraft cooking and oxygen– alkali delignification of bamboo by pulp and dissolving material analysis. *Ind. Crops Prod.* 28(1) (2008) 47.
- Salmon, S.; Hudson, S. M., "Crystal morphology, biosynthesis, and physical assembly of cellulose, chitin, and chitosan". *Journal of Macromolecular Science, Reviews in Macromolecular Chemistry and Physics* C37 (2), (1997) 199.
- Sarwar, M. J., Nasima, C. D. A, and Russe, M. "Alkaline sulfite-anthraquinonemethanol (ASAM) pulping of corn stalks,." *Cellul. Chem. Technol.* 40(7), (2006) 531.
- Schick, C. and G. W. H. Hohne. "On temperature calibration of power compensation DSC in cooling mode." *Thermochimica Acta* 187 (1991) 351.

- Scott, W. E. "Principles of Wet-End Chemistry." TAPPI Press. Atlanta, GA. p.11 (1996).
- Seth, R. S., Page, D. H., "Fracture resistance: a failure criterion for paper". Tappi 589, (1975)112.
- Shatalov, A. A. and Pereira, H. "Influence of stem morphology on pulp and paper properties of *Arundo donax* L. reed". Ind. Crops Prod. 15(1) (2002) 77.
- Shatalov, A. A., Quilho, T., and Pereira, H. "Arundo donax L. reed: New perspectives for pulping and bleaching. 1. Raw material characterization," Tappi J. 84(1), (2001) 96.
- Shimamura, K., White, J. L., and Fellers, J. F. "Hydroxypropylcellulose, a thermotropic liquid crystal: Characteristics and structure development in continuous extrusion and melt spinning," Appl. Polym. Sci. 26, (1981) 2165.
- Silvy, J. Romatier, G. Chiodi, R. "Méthodes pratiques de contrôle du raffinage", Revue ATIP 22 (1) (1968) 31.
- Singh, H. "Modification of Food Proteins by Covalent Cross-linking." Trends in Food Science and Technology. 2 (1991) 196.

- Song, X.Z., Li, J.X. Zhang S.W., Study on the effects of a deformation gradient on recrystallization in a material containing precipitates *Liq. Cryst.* 30 (2003) 1123.
- Sturcova, A.; His, I.; Apperley, D. C.; Sugiyama, J.; Jarvis, M. C., Structural Details of Crystalline Cellulose from Higher Plants. *Biomacromolecules*, 5 (4), (2004) 1333.
- Sun, R., Fang, J., Tomkinson, J., Geng, Z. and Liu, J. "Fractional Isolation, Physico-Chemical Characterization and Homogeneous Esterification of Hemicelluloses from Fast-Growing Poplar Wood". *Carbohydrate Polymers*, vol. 44, (2001) 29.
- Svenningsen, N., Visvanathan, C., Malinen, R., and Patankar, M. Cleaner product in the pulp and paper industry: Technology fact sheets. Asian Institute of Technology and the United Nations Environment Programme (UNEP). Pathumtani, Thailand, p. 1-35 (1999).
- Tay Sok Li, Guo Qin Xu, Conrad O. Perera. "Aggregation profile of 11S, 7S and 2S coagulated with GDL". *Food Chemistry* 91 (2005) 457.
- Tiefenbacher, K. F. "Starch-based Foam Materials: Use and Degradation Properties." *Pure Applied Chemistry*. 30 (1997) 727.
- Torrezan R., Whye P. T., Alan E. B., Richard A. F., Marcelo C. "Effects of high pressure on functional properties of soy protein" *Food Chemistry* 104 (2007) 140.

- Tseng, S. L. Laivins, G. V, and Gray, D. G. “The propanoate ester of (2-hydroxypropyl) cellulose: A thermotropic cholesteric polymer that reflects visible light at ambient temperatures,” *Macromolecules* 15, (1982) 1262.
- Viera, R. G. P., Meireles, C. S., Assuncao, R. M. N. de, Rodrigues Filho, G. "Production and characterization of methylcellulose from sugar cane bagasse". In *Proceedings of 5th International Symposium on Natural Polymers and Composites, 8th Brazilian Symposium on the Chemistry of Lignins and the other Wood Components* (pp. 1–3). Sao Pedro-SP, Brazil (2004).
- Walsh, M. *Miscanthus handbook. Miscanthus Productivity Network (AIRCT92-0294)*. Hyperion Energy Systems Ltd, Cork, Ireland, (1998) 225.
- Waranyou S. *The Environmentally Benign Pulping Proces of Non-Wood Fibers*. *J. Sci. Technol.* 17(2) (2010)105.
- Werbowyj, R. S., and Gray, D. G. “Liquid crystalline structure in aqueous hydroxypropyl cellulose solutions,” *Liq. Cryst.* 34, (1976) 97.
- Yamagishi T., Fukuda T., Miyamoto T., and Watanabe J. “Thermotropic cellulose derivatives with flexible substituents. II. Effect of substituents on thermal properties,” *Polym. Bull.* 20(4), (1988) 373.
- Yamagishi, T., Fukuda, T., Miyamoto, T., and Watanabe, J. “Thermotropic cellulose derivatives with flexible substituents. I. Preparation of tri-O-(b-methoxyethoxy) ethyl cellulose and its cholesteric

- mesophase properties,” *Mol. Cryst. Liq. Cryst*, **172**, (1989) 17.
- Yamagishi, T., Fukuda, T., Miyamoto, T., Ichizuka, T., and Watanabe, J. “Thermotropic cellulose derivatives with flexible substituents. IV. Temperature dependence of cholesteric pitches exhibiting a cholesteric sense inversion,” *Liq. Cryst.* **7**(2), (1990) 155.
  - Yamagishi, T., Fukuda, T., Miyamoto, T., Yakoh, Y., Takashina, Y., and Watanabe, J. “Thermotropic cellulose derivatives with flexible substituents. IV. Columnar liquid crystals from ester-type derivatives of cellulose,” *Liq. Cryst.* **10**(4), (1991) 467.
  - Yamamoto, Y. “Engineered ‘Green’ Composites using Kenaf and Bamboo Fibers with Modified Soy Protein Resin.” Cornell University. 2006.
  - Yehia Fahmy, Nahla A. El-Wakil, Ahmed A. El-Gendy, Ragab E. Abou-Zeid M.A. Youssef. "Plant proteins as binders in cellulosic paper composites". *International Journal of Biological Macromolecules*, **47** (2010) 82.
  - Zomers, F. H. A., Gosselink, R. J. A., Van Dam, J. E. G., and Tjeerdsma, B. F. "Organosolv pulping and testpaper characterization of fiber hemp". *Tappi J.*, **78** (5) (1995) 149.
  - Zugenmaier, P. In: *Handbook of Liquid Crystals*, D. Demus, J. Goodby, G. W. Gray, H. W. Spiess, and V. Vill (eds.), Wiley-VCH, Weinheim, Vol. 3, (1989) 453.

### الملخص العربي

يعتبر السليلوز من المواد الطبيعية الأكثر وفرة على سطح الأرض حيث يمكن استخدامه كمادة أولية في أغراض عدة مثل صناعة الورق والكرتون بالإضافة إلى تحضير مشتقات سليلوزيه بعد فصله بصورة نقية . يوجد عدة مصادر لإستخلاص السليلوز مثل الأخشاب الطبيعية وأيضاً المصادر اللجنوسليلوزية التي يمكن استخدامها كبديل للأخشاب الطبيعية في البلاد التي تفتقر الغابات. في جمهورية مصر العربية يتم إنتاج أكثر من 33 مليون طن في مخلفات المحاصيل يشكل منها مصاص القصب 3 مليون. ويعتبر مصاص القصب من أهم المواد الأولية التي تستخدم لاستخلاص اللب الذي يمكن استخدامه في صناعة الورق والمشتقات السليلوزية.

تهدف هذه الدراسة إلى استخدام لب مصاص القصب لتحضير ورق معالج بالبروتينات الطبيعيه المتجدده والمتاحة وذلك تكلفتة مقبولة بدلاً من المواد البتروكيمياويه . حيث تم استخدامبروتين الصويا بعد تحويله باليوريا وهيدروكسيد الصوديوم واستخدامه بنسب مختلفه كإضافات للورق للوصول إلى أفضل نسبه لاستخدامها في باقى التجارب العمليه .

وحيث أن بروتين الصوبا يعتبر من ال (polyelectrolytes) حيث يتميز بوجود شحنات سالبة وموجبة على المجموعات المميزه له. وتعتبر الشحنة النهائية للبروتين من العوامل الهامة التي تحدد الخواص النهائية للبروتين ويعبر عنها الاس الهيدروجينى . وبناءً على ذلك تم دراسة الخواص الميكانيكية والفيزيائية للورق بعد ملئه ببروتين الصويا المحضر عند الاس هيدروجينى 3,5,7,10 وأظهرت النتائج تقارب خواص الورق المحضر عند الرقم الهيدروجينى 7,5 حيث تحسنت الخواص الميكانيكية ولم تتغير الخواص الفيزيائية تغيراً ملحوظاً . لذلك تم اضافة الكاولين كمادة مائه لتحسين الخواص الفيزيائية والاستفاده من الشحنة الموجبه

الموجوده على البروتين لاستخدامه كمادة تزيد نسبة استبقاء الكاولين بالإضافة إلى دورها الأساسي في تحسين الخواص الميكانيكية .

كما تهدف إلى اتجاه آخر وهو استخدام لب مصاص القصب المحلى بعد استخلاص السليلوز منه بصورة نقيه في تحضير مشتقات سليلوزيه لها خواص البلورات السائلة والتي يمكن استخدامها في عدة تطبيقات مثل شاشات LCD حيث أن صفاتها تتغير بتغير المؤثرات الخارجية.

تم تحضير عينات من *alkoxybenzoyloxypropyl cellulose* عن طريق تفاعل الاسترة للمشتق السليلوزي HPC ذو درجة استبدال 3 مع احماض 4-*alkoxybenzoic acids* ذو سلسله جانبيه تتغير فيها عدد ذرات الكربون من 2 إلى 14 ذرة. وتم تحديد درجة الاستبدال للمشتق الناتج بواسطة  $^1\text{H NMR}$  كما تم توصيف المشتقات الناتجه بواسطة PLM, DSC. كما تم تحضير HPC من لب مصاص القصب الإيدابي بعد توصيفه ثم اجراء نفس تفاعل الاسترة عليه بواسطة حمض *alkoxybenzoic acids* مع سلسله جانبيه تحمل ذرات كربون 2,10,12. وفي كلتا الحالتين للمشتقات السليلوزيه تم دراسة الخواص الحرارية بواسطة ال DSC وحساب ال ( $T_g, T_m, T_c$ ) و دراسة ال *phase behavior* بواسطة المجهر الضوئى المستقطب . حيث تم دراسة ال *Lyotropic behavior* للمشتقات المذابة فى DMA بعد تحديد ال *Critical concentration* بواسطة قياس معامل الانكسار بال *refractometer* ودراسة خواص ال *Thermotropic* من درجة حرارة الغرفة حتى يتحول المشتق إلى *Isotropic phase* ثم تبريده مرة أخرى ولوحظ أن المشتقات التى تحتوى على عدد كربونات فردى تعتبر *.Non-mesomorphic*